UCLouvain

École polytechnique de Louvain

Fabrication of magnetic microcarriers for stem cell expansion

Author: **Maddalena Cesaro**
Supervisors: **Karine Glinel, Alain Jonas**
Readers: **Anne des Rieux, Anitha Ajith Kumar, Eleana Somville**
Academic year 2019–2020
Master [120] in Chemical and Materials Engineering
Master in Functionalized Advanced Materials and Engineering (FAME+)

Abstract

The use of microcarriers in dynamic cell culture allowed, in the last years, to increase the cell culture production yields for stem cell expansion. This increase of the production yields is strongly demanded by the crucial need of high numbers of stem cells to be employed in emerging cell therapy strategies in the framework of regenerative medicine. This project focuses on the production of biopolymer-core magnetic MCs obtained by an organic-solvent-free method and provided with a biofunctional coating to enhance cell adhesion. MCs are characterized and employed as cell culture substrates for the expansion of human adipose derived mesenchymal stromal/stem cells (hASCs) in semistatic culture conditions. After optimization of the properties of these MCs in previous studies, the study reported herein represents the first step towards the possible application of these magnetic MCs as cell culture substrate for dynamic cell culture. The employment of magnetic MCs in dynamic cell culture would be innovative and beneficial, leading to a simplification of the cell harvesting procedure and allowing an easy sampling for inline cell characterization.

Acknowledgments

In the first place, I would like to thank my supervisors, Karine Glinel and Alain Jonas, for allowing me to join this project and giving me the opportunity to carry out a master thesis on a topic that I am passionate about. Then, I would like to thank Anitha Ajith Kumar and Eleana Somville, for training me and helping me during the experimental work, and for being supportive, patient and helpful during the writing of the thesis.

Moreover, I would like to thank the members of the BSMA research groups for welcoming me and for having performed some of the analyses reported in this thesis.

Finally, I would like to thank my friends. This master thesis has been written during what was, unequivocally, a peculiar period, due to the CODIV-19 confinement measures. This gave me the opportunity to get closer to new and old friends, without whose support this thesis would have been surely more difficult to write. A special mention goes to Carla, who has been my rock.

Contents

List of Figures

List of Tables

Introduction

Regenerative medicine is a field of medicine that aims to regenerate or substitute a damaged tissue by different strategies employing stem cells. Cell therapy is a branch of regenerative medicine which gained a huge interest in the last years and consists on injecting or transplanting cells which might be differentiated or not. Cell therapy scopes require a consistent amount of cells, in the order of 10^7-10^8 cells for a 70 kg patient [1]. However, this need is not currently supported by the cell expansion techniques for anchorage-dependent cells [2, 3].

The expansion of cells in dynamic culture supported by microcarriers (MCs) was initially developed in the 1970s and is emerging nowadays as the most promising cell expansion technique to produce a large number of cells in a limited volume [4, 5]. MCs are particles with a size of a few hundreds of microns and they have emerged as an interesting substrate for culture of anchorage-dependent cells thanks to their high surface to volume ratio compared to other available culture substrates. Many research groups focused on the optimization of size, features, matrix material, coating, etc. of MCs, in order to successfully culture anchorage-dependent cells with a high production yield and without compromising their clinical grade [6].

The PROSTEM project, from the Université catholique de Louvain, aims to develop innovative biomaterials allowing to improve the yield of production of stem cell in dynamic culture. This project represents the framework for the development of MCs for dynamic culture of human adipose stromal/stem cells. The MCs are made of biocompatible and biodegradable poly(L-lactic acid) (PLLA), fabricated by a solvent-free method and free of animal-derived components. Moreover, a first magnetic version of these MCs has been recently obtained and tested. These MCs were designed to achieve a simplification of the harvesting of cells at the end of the culture and to allow the collection of samples of MCs during the culture for inline characterization.

This thesis is performed within the frame of PROSTEM project and aims to optimize the fabrication of magnetic MCs and study their performance for human adipose stromal/stem cell expansion in static conditions. The main objectives of the thesis are to fabricate the magnetic , characterize their properties, test their performance as substrate for cell culture compared to the non-magnetic and evaluate their eventual cytotoxicity to cells.

The structure of the thesis is the following.
The state of the art is presented in Chapter 1. Initially, the urgent need of developing more efficient cell culture expansion techniques, to address the demand of consistent amounts of stem cells for cell therapy, is stated and contextualized. Afterwards, the main cell expansion techniques currently available are briefly presented, with an special

focus on dynamic cell culture conduced in mechanically stirred bioreactors. Later on, the requirements of for cell expansion are presented and a brief overview of the available on the market is done. Finally, the principles driving cell adhesion are explained and the possible surface modifications to enhance cell adhesion are mentioned.
Chapter 2 briefly presents the scope of the project and the experimental strategy adopted to meet the scope.
Chapter 3 presents the materials used and the experimental procedures followed for the preparation of MCs, for the characterization performed and for the culture of human adipose stromal/stem cells.
Chapter 4 presents the characterization of magnetic and non-magnetic. In this chapter, important features of the magnetic MCs are evaluated, which influence their suitability as cell culture substrate and their magnetic properties.
Chapter 5 aims to evaluate the suitability of magnetic MCs for culture of human adipose stromal/stem cell by studying the cell proliferation. Then, the cytotoxicity of magnetic MCs is evaluated.
Finally, the conclusions of this master thesis are drawn and the possible outlooks are mentioned.

Chapter 1

Literature review

1.1 Regenerative medicine and stem cells

Stem cells are the protagonists in the field of regenerative medicine, which has the scope of creating a functional tissue by replacing or repairing a tissue or an organ damaged due to aging, traumas, or degenerative diseases. In the framework of regenerative medicine, cell therapy, gene therapy and tissue engineering (TE) fields develop, explained herein [2]. Cell therapy, considered as one of the four pillars of modern medicine, is based on the transplantation and injection of stem cells in a tissue to enhance its repairing and regrowth. In order to perform cell therapy, stem cells, after isolation, can be directly transplanted in the patient or they can be expanded *in vitro* and, if needed, can be combined with growth factors for cell differentiation prior to transplanting (routes 1 and 2 in Figure 1.1). The cells can also be combined with therapeutic genes, an approach known as gene therapy (route 2 in Figure 1.1) [2, 7].

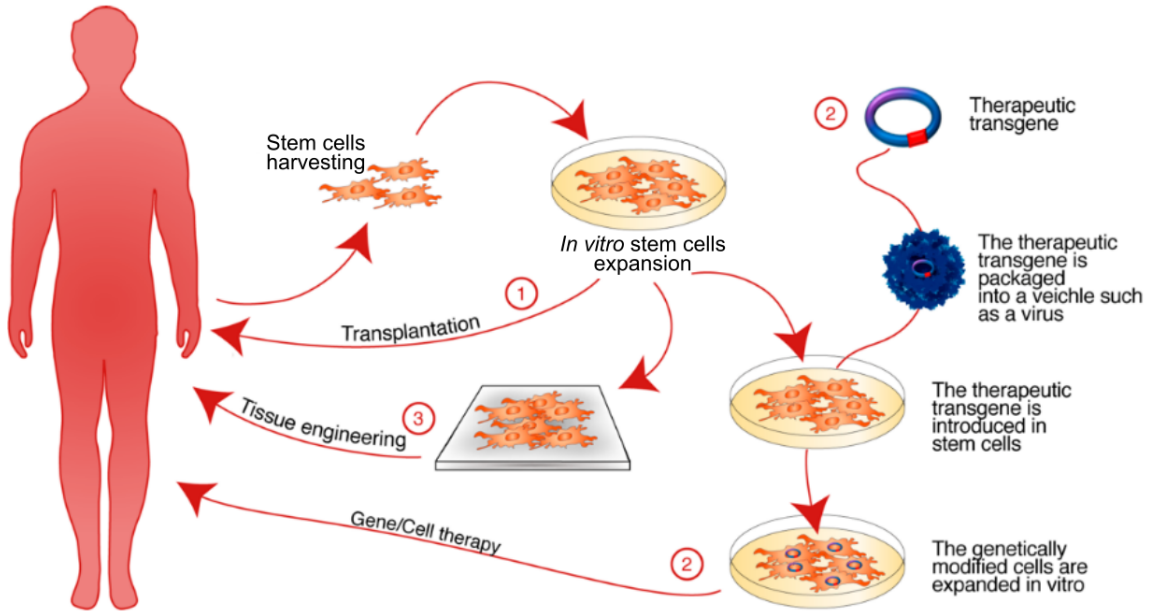

Figure 1.1: Different uses of stem cells in the framework of regenerative medicine. Adapted from [2].

Cell transplantations can be autologous or allogeneic. In the case of autologous cell transplantation, the cells are isolated in small quantities from the patient ex vivo, expanded, then, transplanted back to the patient. On the other hand, allogeneic cells come from a donor. They are usually extensively expanded after the isolation, then transplanted to the patient. The use of autologous cells is advantageous because there is lower risk of infection compared to allogeneic cells and the patient is expected to have no immune response to the transplantation. Therefore, generally, there is no need to use immunosuppressive drugs prior transplantation. Contrarily, in the case of transplantation of allogeneic cells, many risks rise. For instance, the presence of myeloablation[1], the reconstitution of a new immune system, the use of immunosuppressive drugs and graft versus host disease (GvHD) are possible risk factors for complications [8]. Moreover, the use of allogeneic cells might elicit humoral and cellular immune responses *in vivo*, especially if an inflammation is occurring in the transplantation site [9].

However, even if autologous transplantation appears as advantageous, it also faces limitations. First of all, the amount of cells that can be retrieved from the patient is usually small, thus, it is necessary to expand them, which is a time consuming procedure. Another drawback is that the patient, already in precarious health conditions, might be hospitalized for long periods and submitted to demanding procedures that could lead to infection or loss of function of the interested tissue [2]. Differently, in allogeneic transplantation, many patients can benefit of the donation of one single donor, which can also be selected for having optimal features for a specific therapeutic application. Moreover, time consuming procedures, as cell expansion, are less problematic in the use of allogeneic cells, since the cells can be isolated, expanded, stored for several months if necessary and used when needed [2, 10]. Currently, between the two methods, the use of allogeneic cells attracts more clinical and commercial interest [5].

On the other hand, tissue engineering consists in designing artificial organs made of autogenous or allogeneic stem cells loaded on a scaffold and engineered ad hoc for the specific patient. For this scope, the cells, after isolation and expansion ex vivo, are loaded on a scaffold and then implanted in the patient (route 3 in Figure 1.1). Thanks to the developments performed during the last decades, TE is widening the horizon of organ transplantation [11]. These improvements address the original problem related to the risk of organ rejection by the patient's immune system response, which would be certainly reduced using an engineered tissue made of autologous cells of the patient. TE approaches represent an alternative to classic transplants, procedures which inevitably face difficulties related to donors availability and compatibility with the patient.

For some of the therapies just mentioned, medium and low doses of cells are sufficient, on the order of magnitude of 10^6-10^7 cells per patient, but for several more extensive approaches, larger amounts of cells are required, at a scale of 10^8-10^{10} cells per patient (assuming a weight of the patient of $\approx$ 70 kg) [1, 3, 12, 13]. Taking into account also the increasing demand of therapies, highly efficient cell production methods have been developed allowing to produce high amount of cells without compromising their quality and clinical grade [14].

In the next sections, stem cells are presented considering their properties and their

[1]Suppression of the ability of bone marrow to produce blood cells.

classification in different types, as well as the bioreactor technologies allowing their expansion.

1.2 Definition and classification of stem cells

Stem cells have the unique properties of self-renewal and pluri/multi-potency, unlike all other kinds of cells. Self-renewal consists in the ability of proliferation while maintaining the stem cell reservoir in the undifferentiated state. On the other hand, pluri/multi-potency is the capacity to differentiate towards different cell lineages. These two fascinating properties are the consequence of a specific cell division mechanism displayed by stem cells, called asymmetric division, consisting in generation from the stem cells of two daughter cells: one identical to the mother and one with committed characteristics. The latter one can transform in a specific progenitor cell able to differentiate following a specific linage (Figure 1.2, left side) [15]. Nevertheless, stem cells can also perform symmetric division generating two daughter cells identical to the mother, that afterwards can transform in progenitor cells (Figure 1.2, right side).

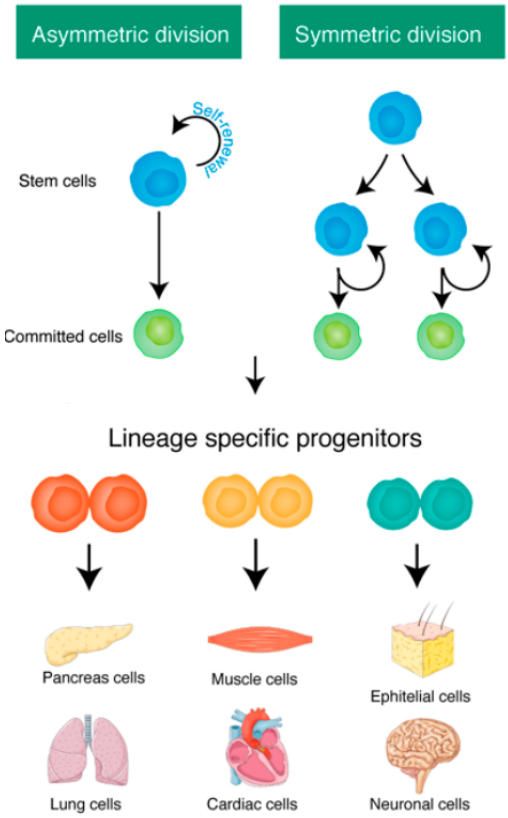

Figure 1.2: Asymmetric and symmetric divisions of stem cells lead to committed cells that generate lineage specific progenitors, able to differentiate into different cell types [2].

The properties of self-renewal and multi/pluripotency, combined with their immunocompatibility and with the ability to secrete biochemical agents promoting positive resolution of inflammations and stimulating the tissue renewal, makes stem cells interesting for medical therapies [2, 11].

Two kinds of stem cells can be classified depending on their source: embryonic stem cells (ES), which are retrieved from embryos in the early stages of their development, and adult stem cells, that come from several tissues of an adult organism [2, 10]. A third kind of stem cells is worth mentioning: induced-pluripotent stem cells (iPSCs), which are adult cells genetically "reprogrammed" to assume a stem cell-like state [16].

1.2.1 Embryonic stem cells (ES)

ES are found in embryos at their early stage of development (5-7 days), a tissue of origin scarcely available [2, 10]. Due to their origin, the use of human embryonic stem cells (hES) for biomedical applications raises ethical questions and is frowned upon by the public opinion mostly in Europe and USA [17]. Having distinctive properties such as self-renewal, pluripotency and genomic stability, they generated great interest in the early 21st century in different fields such as regenerative medicine and immunotherapy. In spite of that, their use for biomedical applications can be problematic due to the possibility of forming a teratoma[2] and the difficulty in obtaining clinical grade quality cells [10].

1.2.2 Induced-pluripotent stem cells (iPSCs)

iPSCs cells have been isolated for the first time in 2006 when they were produced starting from terminally differentiated somatic cells. The somatic cells were engineered with genes to regress to their pluripotent state, acquiring the abilities of self-renewal and pluripotency [18]. Thanks to significant advances in the protocols to engineer iPSCs, these cells can now be generated with different cocktails of genes and starting from different types of somatic cells [2]. Nowadays, different procedures allow the production of liver, pancreas, gut (intestinal, stomach, and colon), lung and thyroid cells. However, a major limitation is the impossibility to generate fully functional cells in most of the mentioned cases. Thus, the application of these cells for regenerative medicine scopes is still not contemplated [19]. The variability of differentiation of iPSCs still represents a major challenge, as well as the understanding of the genetic mechanisms driving it. Moreover, many consistent obstacles are present from the clinical point of view: more numerous clinical and *in vitro* studies will be needed to reach a full understanding of the biological phenomenons occurring when these cells are implanted *in vivo* [19, 20].

1.2.3 Adult stem cells

The tissues of an adult organism are continuously renewed following a natural life cycle, where new cells substitute the dying ones. This task is addressed by the stem cells, present in small quantities all over our organism, and also by other kinds of cells. Types of adult stem cells include endothelial, neuronal, mammary, hematopoietic, intestinal and mesenchymal stem cells (MSCs) (Figure 1.3). However, depending on their location, certain types are easier to access and to isolate than others.

Mesenchymal stem cells (MSCs)

The first kind of adult stem cells to be isolated were MSCs, initially from the bone marrow and later from skeletal muscle and adipose tissues. Lately, another important source

[2]Tumor of the embryonic tissues.

emerged, which is fetal tissues, such as the placenta, amniotic fluid, Wharton jelly and umbilical cord blood, leading to the isolation of fetal MSCs [3, 10].
Thanks to their multilineage differentiation capacity, immunomodulation, and regenerative abilities, MSCs gained the interest of the scientific community and became quickly the most clinically studied type of cells for cell therapy applications [2].

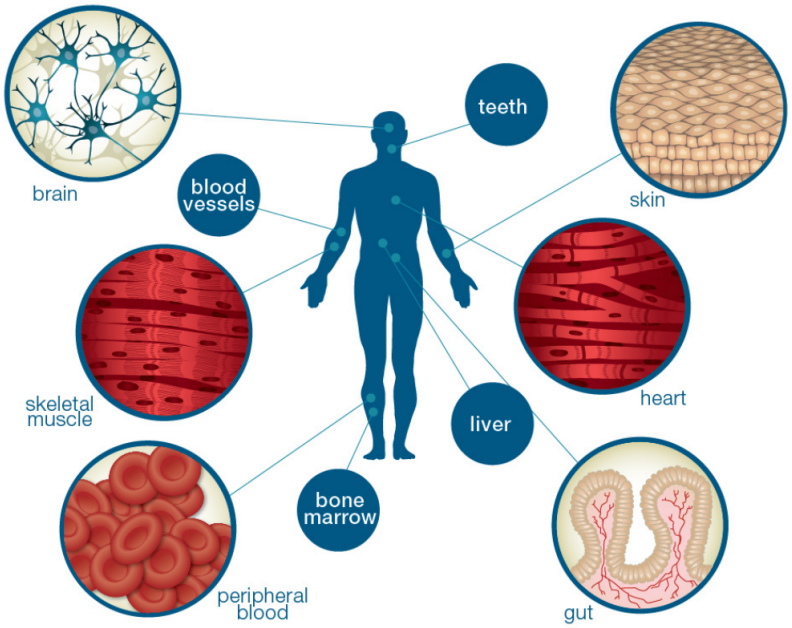

Figure 1.3: Different sources of adult stem cells [21].

It is worth citing how the definition of mesenchymal stem cell is controversial by itself. Indeed, several names and classifications had been delineated over the years, such as "marrow stromal cells", "multipotent stromal cells", "mesodermal stem cells" and "mesenchymal stromal cells" [10]. Currently, according to the International Society for Cell Therapy (ISCT), the minimal criteria for defining MSCs consists in: plastic adhesion (*i.e.* their propensity to adhere and proliferate on a tissue culture flask surface), expression of a panel of cell surface markers and ability to differentiate along the adipogenic, chondrogenic and osteogenic lineages *in vitro* [22].

Usually, MSCs are as well able to differentiate along the myogenic, tendogenic and marrow stroma lineages and to secrete immunoregulatory chemical agents, useful in order to regenerate injured tissues [23]. As a matter of fact, in the last decades, several therapies involving the use of MSCs have been clinically tested: exclusively in 2018, 600 clinical trials of MSCs have been reported [3]. Despite great scepticism caused by the novelty of the methods and several inconclusive clinical trials, recent studies reported successful clinical outcomes [3, 23]. Some, among the several applications, are worth mentioning.
MSCs can be used for immunomodulatory therapies as acute graft-versus-host disease (GVHD) and Crohn's disease and, after being properly differentiated towards the adequate lineages, for bone, cartilage and myocardium regeneration [10]. Another important use is the one of hematopoietic stem cells extracted from the bone marrow (BM). These cells are responsible for blood cell renewal (hematopoiesis) and they are useful for the production of blood and blood products with enhanced safety. These products are mainly needed for blood transfusion and treatment of leukemia [11]. MSCs are also used as gene therapy

targets, to aid the immune system in its response to transformation or infection with virus, in therapy against autoimmune disorders, in tissue repair therapies, or for biosensor applications [11].

Historically, the bone marrow-derived mesenchymal stem cells (BMSCs) represented the most studied end evaluated for clinical application source of MSCs. Nevertheless, bone marrow is extracted through a painful and expensive procedure and BMSCs isolation leads to particularly low yields (0.002%) [7, 24]. In order to find other kinds of stem cells that meet the requirements of easy harvesting and high yields, as well as good renewal and potency, stem cells coming from other tissues have been evaluated.

Adipose derived stem cells (ASCs)

Adipose derived stem cells (ASCs), or simply adipose stem cells (ASCs), can differentiate into multiple lineages as adipocytes, fibroblasts, osteoblasts, chondrocytes, myocytes, neurocyte, endothelial cells and tenocyte [7, 25], depicted in Figure 1.4. ASCs are MSCs, but they have the capability to differentiate also towards non-mesenchymal cell lineages as myogenic, neuronal and endhothelial [2].

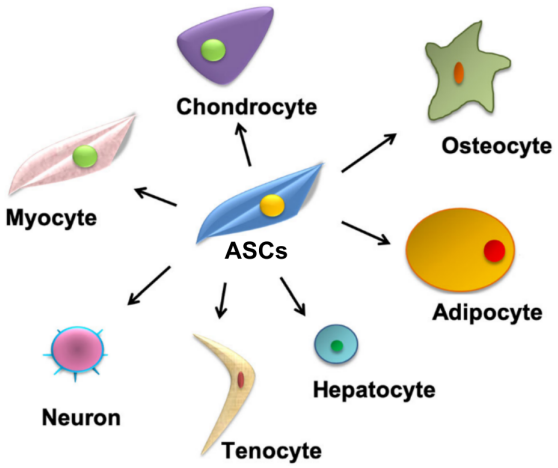

Figure 1.4: Differentiation potential of ASCs [25].

ASC secretome[3] contains biological components having the capacity of cytoprotection[4] and activation of reparative mechanism. Moreover, ASCs exhibit striking immunomodulatory and immunoprivileged features, attractive characteristics for the treatment of diseases where minimal immune rejection is necessary [26].

ASCs are extracted by purification of adipose tissues, which is retrieved by adipose tissue biopsy or by liposuction or lisoaspiration (plastic surgery). Adipose depots contain a heterogeneous population composed of stromal vascular fraction (SVF) cells, mature adipocytes, lymphocytes and macrophages, vascular and stromal cells [25]. After being extracted, the adipose tissues, are washed and digested by incubation at 37°C with collagenase. The digestion product is centrifuged and the SVF cell pellets, separated by the byproducts, can be isolated and cultured. The SVF isolation procedure is schematized

[3]Set of proteins expressed by an organism and secreted into the extracellular space.
[4]Protection of the cell from harmful agents.

in Figure 1.5. ASCs can be extracted from the SVF through further processing and they constitute around 2-10% of the former [10].
The extraction of adipose tissues from lisoaspirate is the most common method and, also, the one that allows to obtain the higher amount of adipose tissue. This is possible due to the increasing frequency with which this procedure is performed in more economically developed countries. In the US, 400,000 liposuction procedures are performed every year and each operation can yield from 10 mL to more than 3L of adipose tissue [24]. The extraction of adipose tissues by lisoaspirate is a non-painful and non-invasive procedure: it does not require total anesthesia in most of the cases and does not cause post-operative discomfort.

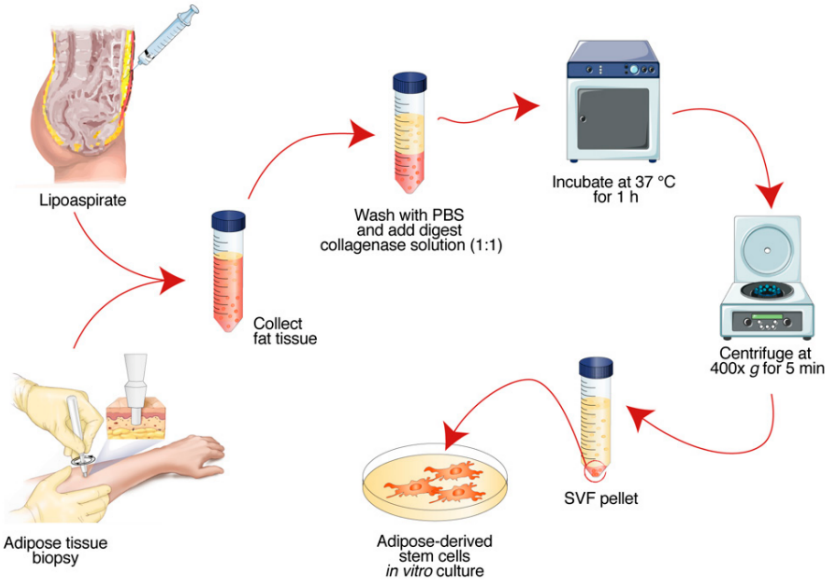

Figure 1.5: Main steps for harvesting ASCs from lipoaspirate or biopsy of subcutaneous adipose tissue [2].

One limitation concerning the use of ASCs is the batch-to-batch variability, which is caused by two main factors: donor-dependent heterogeneity and intra-individual heterogeneity. Donor-dependent heterogeneity comprehends factors as donor age, body mass index (BMI) and diseases. According to several studies, donor aging seamed to negatively influence the self-renewal ability of the cells [27]. Nevertheless, the correlation between the donor's age and the harvesting yields is still widely discussed [7, 28]. Concerning intra-individual heterogeneity, the harvesting site is the main factor influencing the variability: the adipose tissues obtained by lisoaspiration can come from different sources as subcutaneous gluteal fat, subcutaneous abdominal, visceral abdominal and, thus, different extraction sites might present different yields of ASCs [2, 7].

Concerning the biomedical applications, ASCs, as well as SVF, can be injected in damaged or inflamed parts of the body in order to enhance the regeneration of the tissue, to act as a filler or to promote a positive resolution of the inflammation [26]. Clinical trials showed successful results concerning the use of ASCs for: bone and cartilage repair, ischaemic diseases, soft tissue augmentation and reconstructive surgery[7].
Moreover, it is worth citing that also human adipose tissue derivatives are promising for soft tissue regeneration applications. Indeed, as the adipose tissue is in majority composed by

adipocytes, it can be used for autologous fat grafting (AFG) for the treatment of soft tissue defects. Extracellular matrix (ECM) components can be obtained by decellularization of the adipose tissue and, subsequently, used for a wide range of options. Among them, are: providing binding sites for cell surface receptors, modulating the structural properties of tissue, participating in immunological responses and being all the former properties of the ECM, meeting the requirement of maintaining the homeostasis[5] of a tissue [25].
ASCs and adipose tissue derivatives are thus efficient and safe for clinical applications, however, in order to achieve their use in routine medical procedures, some obstacles have to be overcome. These are the lack of a regulatory framework on the harvesting and culture, lack of definition of a clinical grade and lack of efficient and optimized expansion procedure [7].
In conclusion, the advantages related to the harvesting of ASCs combined with their wide multi-lineages differentiation properties and *in vitro* biological properties, make the ASCs a competitive candidate when compared to other stem cell sources and types.

1.3 Cell expansion techniques

Cell culture has been historically performed in 2D conditions in planar vessels. Since these technologies face several drawbacks, in the last decades, bioreactor technology evolved to propose designs which were less labor intensive, allowing higher sterility and safety, as well as reaching higher production yields.

The most classic and early developed methodologies for cell culture can be classified as adherent cell culture or suspension cell culture. In adherent cell culture, cells grow on a cell-adhesion substrate, usually in tissue-culture vessels, *i.e.* a vessel whose cell-material affinity has been enhanced through a physical or chemical surface treatment. In suspension cell culture, cells grow clustering in aggregates that are suspended in a continuously agitated medium. Depending on the cell type, one or the other methodology is more suited. Indeed, cell types can be primarily divided in anchorage-dependent cells (ADCs), adapted to be cultured by adherent culture, and non anchorage-dependent (non ADCs), adapted to be cultured by both adherent and suspension culture [29].
The design of innovative bioreactors for culturing ADCs aims to optimize the surface to volume ratio, in order to grow ADCs in high density without implying large culture volumes. These systems also address the major need of producing high amount of cells for therapeutic applications, mentioned in section 1.1 [14] without compromising the quality of the expanded cells.

In this section some of the most common technologies for culturing ADCs are described, going through planar technologies, perfusion-based technologies and mechanically-driven technologies. Advantages, drawbacks and efficiencies are mentioned for the different systems. Finally, more attention is dedicated to stirred bioreactors, since they are more related than the others to the scope of this project.

Planar systems for cell expansion

Planar and static cultures have been extensively used in the last decades. The most used systems are T-flasks made of polystyrene treated with plasma to enhance the cell

[5]Property of a living system of maintaining steady internal, physical, and chemical conditions.

adhesion. The main limitation of static culture performed in T-flasks is the limited area which restricts the number of obtained cells, lowering the method efficiency [11, 30].
Multilayer vessels represent the first significant improvement of planar systems for cell expansion. These systems consist in multilayer stacking of planar vessels where the cells can grow covered by medium.
Each multilayer vessel, having between 8 to 10 layers, can grow approximately 25,000-30,000 cells/cm^2 and a culture conduced in multilayer vessels or similar setups allows to grow up to 10 billion cells in an affordable way [31]. The production can be enhanced even more by increasing the number of layers in each vessel (up to 100 billion cells using 40 layers per bioreactor). Planar and static technologies are suitable for production of small batches of cells that can be sufficient for small clinical trials. In order to grow bigger amounts of cells for more consistent clinical trials, more advanced technologies have to be contemplated [3].

Planar systems are economically reasonable and easy to operate, but they often face several limitations and drawbacks. They do not ensure repeatibility and in-line control, are difficult to monitor and the frequent handling required to feed cultures and acquire data increases the possibility of contamination of the culture [30]. They are also labor-intensive and have a larger footprint due to the use of single-use devices. Moreover, the static nature of these systems can cause gradients in pH, dissolved oxygen, cytokines and metabolites [3, 30]. Planar systems and, in particular, planar multilayer vessels, are still the most common setup for commercial manufacture of cells. However, considering their several drawbacks and the increasing demand of cells for various applications, they will soon become disadvantageous and obsolete [5, 12].
Advanced planar designs have been developed with the idea of reducing the amount of labor and variability by automatizing the procedures. Nevertheless, considering the available marketable technologies, the reached efficiency is not worth the maintenance cost and risk failure [3].

Mechanically-driven bioreactors

In mechanically-driven bioreactors, the cells adhere and grow on the surface of microparticles, commonly defined as microcarriers (MCs), suspended in a medium solution under continuous stirring. MCs appeared in the cell culture field already at the end of the 70s, emerging as a promising substrate for cell growth, having a high surface to volume ratio [4, 14, 32]. They can be made of different materials and usually their size ranges from 100 to 300μm [33]. They also allow an easy scale-up by adding fresh MCs in the system (bead-to-bead cell transfer). This leads to an increase of the production yield of the culture, as more cells grow in a limited volume [6].

The most basic example of mechanically-driven bioreactors are wave mixed bioreactors (displayed in Figure 1.6B), in which cells growing on MCs are placed in a bag filled with culture medium, which at the same time, is swinging [34].

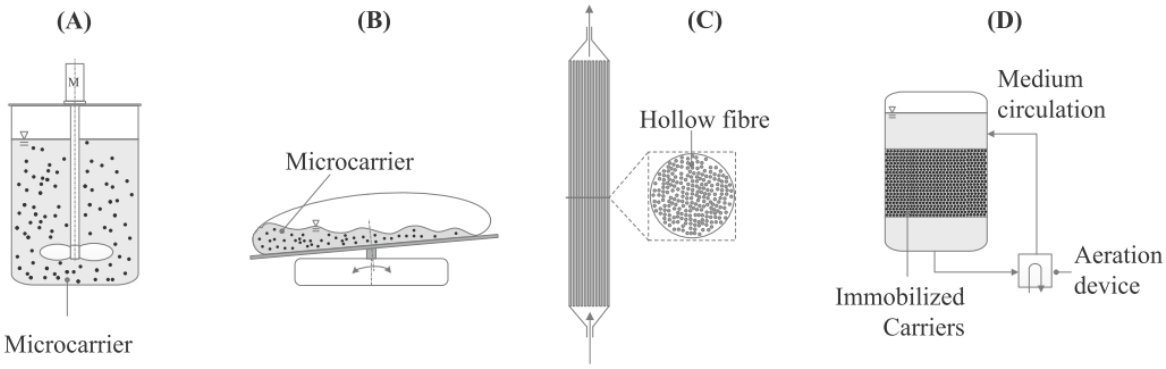

Figure 1.6: Bioreactors for culture of ADCs. A) Stirred bioreactor, B) wave-mixed bioreactors, C) hollow fiber bioreactor, and D) fixed bed bioreactor [5].

Stirred bioreactors are another type of mechanically-driven bioreactors based on MCs (displayed in Figure 1.6A). Their working principle is similar to the wave mixed bioreactors, but MCs with cells adhered on their surface are dispersed in a container filled with medium. The container is equipped with a mechanical or magnetic stirrer allowing to suspend the MCs. Considering stirred bioreactors for the culture of ADCs, some alternatives to the use of MCs have been considered. For instance, cell growth can be supported by cell encapsulation in hydrogel scaffolds or by creation of cell aggregates [35, 36]. However, as ADCs are an anchorage dependent cells, these options are feasible but troublesome, because they do not provide a sufficient support for cell growth, as would do a surface. Moreover, both these options face the drawbacks of low oxygen and nutrient diffusion in the inner part of cell aggregates or particles containing cells, leading to the risk of premature death of the internal cells.

Stirred bioreactors using MCs can yield up to 500 billion cells and are available in different sizes and shapes depending on the final purpose of the culture. Lab-scale bioreactors, as spinner flasks, suitable for smaller amount of cells production for studies or testing, can have small (3-250 mL) or medium (1.5-5 L) volumes. Bioreactors at pilot scale (50-300 L) and production scale (500-2,000 L) are characterized by larger volumes and allow to reach cell numbers suitable for substantial clinical trials [3].

Stirred bioreactors are advantageous because they provide a homogeneous environment for cell growth. Besides, they allow easy sampling, monitoring and control of culture conditions, reducing the risk of contamination [11, 37]. Indeed, a small amount of culture medium can be collected during the culture for further analysis. Parameters such as mass transfer, dissolved oxygen concentration, pH, temperature and metabolite gradients can be regulated easily in real-time [3].

However, the culture in stirred bioreactors can be delicate and influenced by several parameters. One of them is the shear stress caused on cells due to the stirring movement. The shear stress acting on the object in solution, which might be a single cell, an aggregate of cells or a cell-laden MC, becomes not negligible when the Kolomogrov eddy size has the same order of magnitude of the diameter of the object in solution[38]. Too low shear stress might cause clumping of cells while too high shear stress might cause cell death. Also, low agitation rate affects more cells on MCs or in aggregates than single cells in solution.

Another source of shear stress might be the sparking with gas bubbles, usually performed to ensure the adequate oxygen income to the cells [39].
Another drawback of stirred bioreactors is related to the possibility of non homogeneous growth throughout the MCs. Indeed, since the MCs are rarely in contact between them, it might be difficult for cells to migrate from one MC to another one [40]. Another disadvantage in stirred reactors is the tendency of aggregation or sedimentation of the MCs at low stirring speed, *i.e.* low shear stress conditions. In order to avoid MC aggregation due to the formation of cell aggregates on the MC surface, bead to bead transfer of MCs, *i.e.* feeding fresh MCs during the culture, can be performed: it allows the cells to spread on new surface without having to replace the MCs.
Moreover, the detachment of cells from MC surface is not yet optimized: currently the harvesting efficiency is of about 60% [33]. Usually, cells are detached from the surface by enzymatic treatments including trypsin and collagenase. Different alternative strategies have been tested to achieve a more efficient and less traumatic detachment process for cells. Cell detachment can be induced by applying a weak shear stress to cells (mechanical detachment) or by using chemical agents that mimics the action of enzymatic agents, but are less damaging (chemical detachment). Moreover, it has been considered to produce MCs coated with thermo-responsive polymers, which can induce cell detachment by temperature stimulus [3, 41].

Perfusion-based bioreactors

An important class of bioreactors are perfusion-based bioreactors, also called hydraulically driven bioreactors, in which cells are immobilized on MCs or other surfaces and they are continuously perfused with fresh culture medium. Perfusion bioreactors allow to reach up to 100 million cells and their cost is comparable to stirred bioreactors or planar technologies [3]. The main drawback of these systems is that, due to the fact that cells are immobilized in their position, the nutrients and the oxygen might be delivered unevenly throughout the culture [3]. Moreover, perfusion speed must not exceed $3 \cdot 10^{-4}4$ m/s, so that the shear stress applied to the growing cells is minimal.

Packed bed bioreactors (displayed in Figure 1.6D) are one of the most common type of perfusion-based bioreactors in which cells grow on porous structures, such as fixed or packed beds. In these bioreactors, cells grow in three dimensions in the hollow space between the closely packed beds, in a manner that mimics the growth *in vivo* [33, 42, 43]. Packed beds can have different porosity and structure and be made of different materials, such as fused polystyrene pellets that have undergone a surface plasma treatment [40].

Hollow-fiber bioreactors (displayed in Figure 1.6C) are another example of perfusion-based bioreactors where the substrate for cell growth consists of stacked semi-permeable hollow fibers. Cells adhere and grow on the intra-capillary surface of the fibers. The membrane is permeable to nutrients and oxygen and acts as separation between the cell environment and the medium which is continuously perfused [3].
These systems allow real-time control of metabolites, glucose in the culture and consequently kinetics of cell growth. Despite appearing promising, controversial opinions emerged on the efficiency of this type of technology, because they induce problems the cell harvesting process. In these bioreactors, cells grow in a very limited space, which is the extra-capillary space between the fibers, and, when they are treated with enzymatic agent to induce detachment, they tend to remain stuck between the hollow fibers. In order to

overcome this problem, strategies such as increasing the flow rate on the extra-capillary side to augment the enzymatic dissociation were tested [3, 11, 33].

In conclusion, the development of cultures in stirred or perfused bioreactors allows to culture cells in controlled and strictly defined conditions thanks to the homogeneous environment in which the cells are growing and the possibility to monitor and adapt in real time the culture parameters. These advantages make the stirred and perfused cultures, compared to the static culture in vessels, more likely to be successful, large-scale and long-term culture methods. Nevertheless, stirred and perfused bioreactors are delicate systems with several factors to control and drawbacks to overcome [39]. Just to cite a few examples, cell growth and differentiation can be easily influenced by tuning pH, perfusion rate, partial pressure of O_2 (pO_2) or parameters influencing the shear stress to which the cells are subjected. The choice of the bioreactor should depend, therefore, on the type of cells to expand, the amount of cells needed, on whether the cells have to differentiate or not, as well as on practical and economic considerations.

1.4 Microcarriers for cell culture

The advantages that MCs offer as cell culture substrate in dynamic culture, *i.e.* using mechanically driven bioreactors, are easy sampling, easy expansion of the culture by addition of fresh carriers, easy separation of the cell-laden MCs from the culture medium and easy harvesting, in most of the cases. MCs can be also used as growth substrate for fluidized and packed bed bioreactors, although this section is not focused of these uses [6, 37, 44].
In this section, the different materials used to fabricate MCs and the specifications that the MCs have to fulfill are mentioned. Moreover, the current landscape of commercially available MCs is briefly reviewed and some additional applications are mentioned.

1.4.1 Used materials and specifications

There is not one kind of MCs optimal for every culture and application. Several types of MCs are available on the market and various examples based on different designs and fabrication processes have been reported in the literature [45, 46]. The kind of cells to be cultured and expanded as well as their final application, are the main parameters to take into account when defining the specifications of the MCs (e.g. material, porosity, rigidity, degradation and biocompatibility). Regardless of this, some general material specifications can be defined.

The material chosen should be rigid enough to support cell spreading and to resist, during the culture process, collisions between MCs and shear forces caused by the stirring movement in the bioreactor [12, 37]. MC mechanical resistance is of particular importance for long-term cultures. The density of the material should be just above the medium one, thus, between 1.02 and 1.04 g/cm3, in order to allow suspension of the MCs in the medium under gentle stirring [12, 37, 47]. Moreover, MCs should not have a too high sedimentation speed: this parameter depends firstly from the density but also from the size, shape and porosity of the microparticles [37]. Ideally, the chosen material should also withstand the organic acids and proteases usually contained in culture supernatants, be transparent, in order to allow a direct microscopy observation of cells growing and, if

possible, be heat-resistant for autoclave sterilization [12, 37].

The choice of the material is important because it influences parameters such as toxicity, hydrophilicity, hydrophobicity, microporosity, mechanical stability, diffusion of oxygen or medium components, permeability, density and shape of the MCs [37]. The first materials to be adapted for MCs production were synthetic polymer-based such as poly(lactide-co-glycolide) (PLGA), polyhydroxyethylmethacrylate (PHEMA), polyacrylamide, polystyrene (PS) and polyurethane (PU) [6]. Nowadays, both synthetic and natural materials are used for MCs fabrication. Considering the first ones, materials such as organic polymers (PS, polyethylene (PE), polyester, polypropylene(PP), poly(L-lactic acid) (PLLA), PLGA, polycaprolactone (PCL), silicone rubber) and inorganic materials such as glass and silica, have been considered [6, 37, 48–50]. Considering the second ones, polysaccharides such as chitosan, chitin, cellulose (gelatin), hyaluronic acid, dextran, alginate and laminarin have been used [45]. Moreover, hydrogels processed from synthetic or natural polymers have been used [46].

Nowadays, polymers are the most used type of materials for production of MCs. An advantage of synthetic polymers is that their chemical and physical properties are easily tunable and reproducible. Indeed, they can be modified by changing their chemical nature (backbone and side chains), molar mass and molar mass distribution and/or by producing copolymers. Moreover, the crosslinking degree of the polymer (or the absence of crosslinking) strongly influence the mechanical properties of the final material. Generally, a higher crosslinking degree leads to an increase of the stiffness of the material.
However, synthetic polymers, lacking bioadhesive moieties, tend not to show good bioadhesiveness towards cells. Therefore, MCs prepared from synthetic polymers usually require a surface treatment to allow the adhesion of cells. Contrarily, MCs based on natural or semi-natural polymers show a better cell-material interaction, but face the limitations of having less adjustable mechanical properties and, in some cases, are affected by batch-to-batch variability [6]. Anyway, as for synthetic polymers, the mechanical properties of natural polymers can be modified by changing the degree of crosslinking.

Additionally, adhesion proteins (or ECM proteins) can be used as material for MCs fabrication. ECM proteins can have animal origin, human origin or be recombinant proteins (the nature of recombinant proteins is better explained in Section 1.5.3). In the last years, animal-origin proteins were the most used kind of proteins for production of MCs and several commercial MCs are made of these proteins (see Table 1.1 for further specifications). Recently, human-origin proteins and recombinant proteins gained interest because the use of MCs made of these proteins for cell expansion for regenerative medicine and tissue engineering scopes is in accordance with the cGMP criteria (further explained in Section 1.5.3). As in the case of synthetic and natural polymers, ECM proteins can be crosslinked to modify their mechanical properties [51].
An example of source of human-derived proteins is human adipose tissues from which decellularized ECM proteins can be isolated by purification. These proteins have the advantage of being affordable and the MCs made of these proteins are perfectly suitable for *in vivo* applications [25, 41].

The technique used to fabricate the MCs is also very important regarding their final characteristics. It strongly influences the porosity of the microparticles. MCs can be

classified as non-porous, microporous, with pores of diameter $< 1\mu$m, or macroporous, with pores of diameter ranging from 10μm to 400μm. Considering the average size of a cell (10μm), cells grow exclusively on the external surface of non-porous and microporous MCs, while on macroporous MCs, cells can also grow in the internal pores [33, 37, 48].
The size of microporous MCs is usually between 100 μm and 300 μm. For macroporous MCs, it is reasonable to have sizes up to 5 mm and to use materials with density higher than 2.5 g/cm^3, since they have a highly porous structure [6, 37].

Macroporous MCs are advantageous because they allow to produce bigger amounts of cells compared to microporous or non-porous MCs, given the same culture volume and assuming to perform the cultures for equal periods of time. Indeed, cultures performed on macroporous MCs reach higher cell density (number of cells/volume) thanks to the higher surface to volume ratio that these MCs exhibit, compared to less porous ones. For instance, considering a cell culture conducted at industrial level and performed on microporous MCs in a stirred tank, the cell density in the bioreactor can reach about 10^6 cells/mL, while, the same kind of culture performed on macroporous MCs can reach 10^7 cells/mL [37]. Moreover, macroporous MCs offer some degree of protection from the hydrodynamic shear stress for cells growing into the pores [12, 52].
They also exhibit some drawbacks. First, cells are difficult to harvest due to the porous structure. Second, even if small molecules can still diffuse in the porous structure, cells growing in the inner part of the MC might not receive the adequate nutrients and oxygen income to maintain their viability. This latter phenomenon risks to happen when MCs are completely loaded with cells. Such configuration could compromise the homogeneity and quality of the expanded cells [53].

1.4.2 Polymeric MCs fabrication methods

Polymeric MCs are currently one of the most studied and developed kinds of MCs. Several methods have been employed to fabricate polymeric MCs. Some of them are emulsion solvent evaporation, solvent evaporation, spray drying and jet milling [54–57].

The emulsion solvent evaporation method is probably the most used approach to fabricate polymeric MCs. The polymer is initially dissolved in an organic solvent and the solution is referred as "oil". Then a water/oil/water ($W_1/O/W_2$) or oil/water (O/W_2) emulsion is prepared. Finally the solvent (oil) is evaporated by heating the suspension under continuous stirring for several hours [49, 57]. This causes the precipitation of the polymer and the creation of MCs. The MCs obtained by this method have a spherical shape and their porosity can be increased by adding an effervescent salt acting as gas foaming agent [57, 58].

A common drawback of these fabrication strategies is that they employ organic solvents, which can potentially be toxic, and are time consuming and expensive, two factors limiting a potential large scale-up. A simple and organic-solvent-free method for production of polymeric MCs was proposed by Kuterbekov *et al.* [59]. This method consisted in the fabrication of PLLA MCs by spherulitic crystallization of the polymer in its miscible blend with PEG and is the one followed in this project.

1.4.3 Commercial microcarriers

A wide variety of MCs is commercially available currently, most of them adapted to more than one application. Some of the most known MCs are: Cytodex® made of dextran, Cultispher® made of gelatin, HLXII-170® made of PS, Cytoline® made of PS and silica. Considering MCs made of natural polymers and their derived for *n vivo* applications, some available options are: GELI- BEAD®, Ventregel® and CultiSpher®, all made of gelatin, Verax® made of collagen and Cytopore® made of cellulose [6, 13].
Commercially available MCs can differ in the material used for their fabrication, porosity, chemical and mechanical properties, and many other parameters [12]. Concerning the mechanical properties, generally the MCs can be classified as rigid, made of inorganic materials or polymers, or soft, made of hydrogel. Some other common parameters used to classify them are porosity, type of coating and superficial charge. Table 1.1 classifies some of the most commonly used commercial MCs in relation to the mentioned parameters [60].

Microcarrier	Manufacturer	Diameter (μm)	Matrix	Average density (g/cm^3)	Surface coating	Surface charge	Porosity
Collagen ®	SoloHill Eng. Inc.	125-212	Polystyrene	1.02	Type I porcine gelatin	None	Non-porous
Cultispher-G®	Percell- Biolytica	130-380	Type I porcine gelatin	1.04	None	None	Macroporous (porosity: 50% pore size: 10–30μm)
Cytodex 3®	GE Healthcare	141-211	Dextran	1.04	Type I porcine gelatin	None	Non-porous
FACT III®	SoloHill Eng. Inc.	125-212	Polystyrene	1.02	Cationic Type I porcine gelatin	+	Non-porous
SphereCol®	Advanced BioMatrix	125-212	Polystyrene	1.03	Type I human collagen (VitroCol®)	None	Non-porous
ProNectin® F	SoloHill Eng. Inc.	125-212	Polystyrene	1.02	Recombinant fibronectin	None	Non-porous
Cytodex 1®	GE Healthcare	147-248	Dextran	1.03	DEAE	+	Non-porous
Cytopore 1 and 2®	GE Healthcare	200-280	Cotton cellulose	1.03	DEAE	+	Micro/Macroporous (porosity: >90% pore size: 30 μm)
Enhanced Attachment®	Corning	125-212	Polystyrene	1.02	CellBIND®	None	Non-porous
Glass	SoloHill Eng. Inc.	125-212	Polystyrene	1.02	High silica glass	None	Non-porous

Hillex® CT	SoloHill Eng. Inc.	90-212	Polystyrene	1.12	Cationic trimethyl ammonium	+	Non-porous
Hillex®	SoloHill Eng. Inc.	160-180	Dextran	1.11	Cationic trimethyl ammonium	+	Non-porous
MicroHex®	Nunc	Length: 125, Thickness: 25	Polystyrene	1.05	NunclonTM surface	Not specified	Non-porous
Plastic®	SoloHill Eng. Inc.	125-212	Polystyrene	1.02	None	None	Non-porous
Plastic Plus®	SoloHill Eng. Inc.	125-212	Polystyrene	1.02	None	+	Non-porous
PVA	Loughborough University	100-220	PVA	1.03	None	None	Non-porous
Synthemax II®	Corning	125-212	Polystyrene	1.02	Synthemax II®	None	Non-porous

Table 1.1: Selection of commercially available MCs [60]. DEAE: diethylaminoethyl; PVA: poly(vinyl alcohol).

Several scientific publications reviewed numerous commercially available MCs [61–63]. It is worth mentioning one of these studies done by the group of Rafiq *et al.*, in which thirteen commercially available MCs (reported in Table 1.1) have been systematically tested for cell culture with human bone marrow-derived mesenchymal stem cells (hBMSCs) from three different donors [60]. In order to compare the different MCs, they evaluated parameters such as the degree of proliferation, efficiency of expansion in xeno-free processing conditions and efficiency of the harvesting procedure without causing cell damage or effects on cellular immunophenotype or differentiation capacity. They observed that almost all the MCs supported cell growth in static conditions, except for five of them (SphereCol®, Cytopore 1® and 2®, Glass® and Hillex® CT) which were consequently excluded from the tests in dynamic conditions. In dynamic culture (in spinner flask), they observed that for all the MCs, the initial cell adhesion was of about 55% and the cell harvesting was of higher than 95%. They also verified how cells maintained their differentiation ability towards osteogenic, adipogenic and chondrogenic lineages, in accordance with the ISCT criteria[22]. An improved cell growth was observed in dynamic conditions with respect to static ones. In conclusion, they affirmed that SoloHill® Plastic MCs were the most suitable for proliferation hBMSCs in dynamic conditions, being these MCs performing as others MCs but additionally being produced by xeno-free process.

Nevertheless, similar studies reached significantly different conclusions due to the evaluation of the MCs from different parameters and to the use of different culture conditions and cell lineages [61–63]. Two examples are the study by Timmins *et al.*, where the authors concluded that Cultispher S® showed the best cell attachment rate (90%) and cell expansion in fold increase [34], and the study by Schop *et al.*, where the authors concluded that Cytodex 1® showed the highest seeding efficiency and growth [63].
In conclusion, affirming the predominance of one commercially available type of MCs over the other is not accurate considering also that the choice of the MCs strongly depends on the application. Moreover, commercially available MCs have limited tailored properties

such as elastic modulus and special biological cues, which might not be adapted for some specific applications [45].

1.4.4 Other applications

According to the specifications previously explained, microporous and non-porous MCs are optimal for cell expansion because, even if they reach lower cell density compared to the macropourous MCs, they allow an efficient cell harvesting. Nevertheless, cell expansion is not the only purpose behind the use MCs. Firstly, MCs were developed to improve the culture of ADCs *in vitro*, in order to produce biomolecules secreted by cells and use these products to fabricate vaccines, antibodies and pharmaceutics. For this scope, macroporous MCs are more suited. They allow higher cell density and thus productivity, as there is no need to harvest the cells at the end of the process. Additionally, even if the low diffusion of oxygen and nutrients in the inner part of the carrier spoils the cell quality and clinical grade of the cells, these are not restrictive parameters for a successful culture [44, 47].

Concerning the *in vivo* applications, MCs have been evaluated as scaffold for TE scopes or cell replacement, since they grant a highly localized injection compared to cells alone. Other advantages are their non invasive and localized action, that reduces the chances of an immune response from the patient, and the possibility of releasing therapeutic factors in a sustained manner (controlled rate of release) [47]. MCs and similar microstructures, usually identified as microcapsules, are also used for *in vivo* delivery of genes and biomolecules such as nucleic acids and proteins [6, 47]. Considering that these MCs have to be implanted *in vivo* and to fulfill specific functions, they are submitted to stricter regulation than other kinds of MCs [47]. For cell delivery and TE scopes, synthetic and naturally derived polymers and materials have been used, all displaying good biocompatibility and controlled and not harmful degradation process. Synthetic and natural hydrogels gained as well interest due to their good biocompatibility, high water content, and special properties (such as stimuli responsiveness, injectability, etc.) [12, 45, 58].
Some examples of studies focused on the fabrication of MCs for *in vivo* applications can be mentioned. Mocanu *et al.* designed pullulan-matrix MCs for bone tissue engineering [64] and Kankala *et al.* fabricated PLGA-based highly porous MCs (HOPMs) for skeletal myoblasts proliferating and consequent cell delivery *in situ* [65]. Moreover, Kuterbekov *et al.* cultured human adipose stromal/stem cells (hASC) and murine myoblasts on PLLA biocompatible MCs, fabricated by solvent-free method. They achieved hASC osteogenic differentiation and they proposed the application of these MCs for tissue engineering or regenerative medicine scopes.
Broadly speaking, even though MCs have been used in different applications in industry, they have been mainly implemented in research procedures, such as enzyme-free subcultivation, studies of cell structure, function, metabolism, and differentiation [66].

1.5 Cell adhesion on cell culture substrate

The surface of the cell-culture substrate plays a major influence on cell adhesion as it is the only part of the substrate that is in contact with cells. In Table 1.1, it can be noticed that, among the numerous commercially available MCs, several have been surface coated to enhance their bioadhesive properties. In this section, the different surface coatings and

treatments to enhance cell adhesion are presented, also taking into account the composition of the culture medium used.
In first place, to be able to evaluate the different surface coatings and treatments, it is necessary to clarify the main parameters mediating the cell-material interaction and cell adhesion.

1.5.1 Principles of cell adhesion

The adhesion of cells on a substrate is a multistep process involving the adsorption of adhesive protein to the culture surface, the contact between the cells and the surface, the attachment of the cells to the coated surface and, finally, the spreading of the attached cells. The four steps are clearly displayed in Figure 1.7. Adhesive proteins (*e.g.*, fibronectin, vitronectin, laminin) tend to adhere to the substrate, if they are not already present, and cell adhesion is mediated by the interaction between transmembrane adhesion receptors (*e.g.* integrins) present on the cell membrane and adsorbed adhesion proteins. Ca^{2+} and Mg^{2+} ions act as cofactors in the former interaction [41, 67, 68]. During the adhesion process, the transmembrane adhesion receptors, which are still free, diffuse on the cell membrane, in order to create new bonds with the proteins. This leads to a progressive spreading of the cell on the surface and to an increase of the contact area between cell and substrate [37].

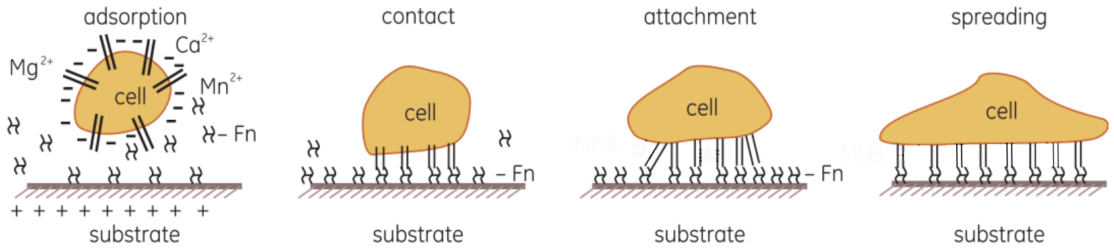

Figure 1.7: Four phases of cell adhesion [37].

The integrin family is the predominant type of transmembrane adhesion receptors that regulate cell adhesion. They consist on heterodimeric glycoproteins composed of α and β subunits. Different integrins bind selectively to specific adhesion proteins: $\alpha_1\beta_1$ binds to collagen, while $\alpha_5\beta_1$ and $\alpha_\nu\beta_3$ bind respectively to fibronectin and vitronectin.

1.5.2 RGD peptide

In 1984 the group of Pierschbacher *et al.* discovered that the domain of fibronectin responsible of cell adherence is a tripeptide sequence composed by Arginine (R), Glycine (G), and Aspartate (D), namely RGD [69]. In the same year, other important discoveries followed concerning the presence of the tripeptide sequence in many other adhesive proteins and of integrins.
RGD is not the only peptide sequence which can mediate cell adhesion by interaction with integrins. In fact, several other sequences have been isolated, such as Tyr-Ile- Gly-Ser-Arg (YIGSR), Arg-Glu-Asp-Val (REDV) and Ile-Lys-Val-Ala-Val (IKVAV) [70, 71].
Nevertheless, the RGD sequence is the sequence which binds to the higher number of integrins. It binds to over 8 out of the 24 integrins constituting the integrin family [70].

An illustration showing the RGD peptide sequence binding to a $\alpha_\nu\beta_3$ integrin is shown in Figure 1.8.

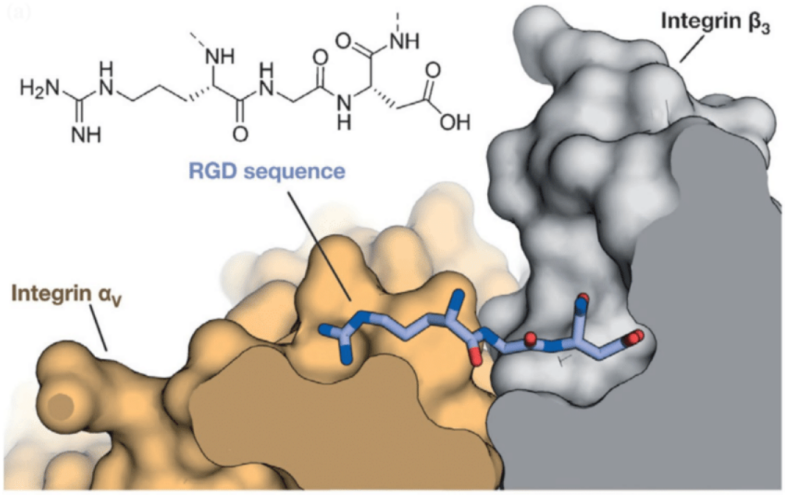

Figure 1.8: Model of recognition of an RGD domain from the α and β subunits of an $\alpha_\nu\beta_3$ integrin [72].

Since its discovery, plenty of research groups investigated and optimized strategies to synthesize and use the RGD sequence as a substitute of ECM adhesion proteins. Soon it was noticed that the RGD sequence performance as mediator of cell adhesion is poorer than the one of ECM adhesion proteins. For example, the hexapeptide GRGDSP, a sequence contained in fibronectin, is about 1000 times less effective for cell attachment than fibronectin itself [70].
This poor performances of the oligopeptide alone (not contained in the adhesion proteins) can be explained considering its interaction with integrins [70].
In most of the cases, the interaction between an adhesion protein and an integrin is not only mediated by the RGD sequence present in the protein. Other peptide sequences, present in the adhesion protein, can interact with auxiliary binding sites of the integrins. Therefore, the interaction is actually a synergy of several interactions, among which the strongest one is performed by the RGD sequence [70]. An illustration of the synergetic interaction between the integrin recognition sites and different domains of an adhesion protein is shown in Figure 1.9.

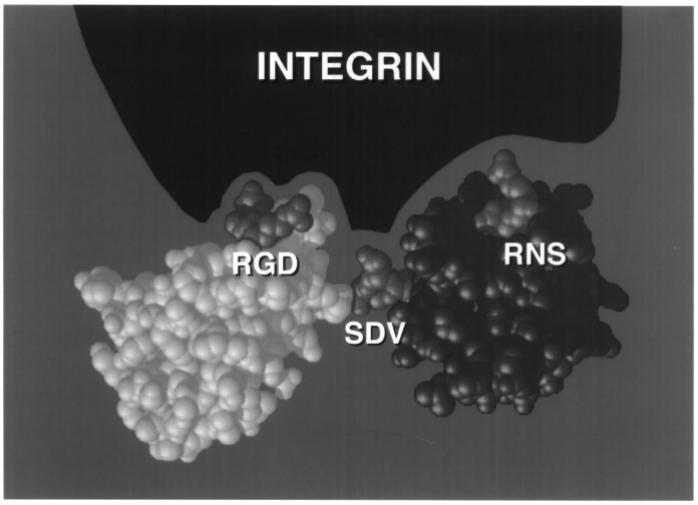

Figure 1.9: A model showing the synergy of the interaction between different recognition sites of an integrin and three domains of the protein in the process of recognition of fibronectin [70]

.

Another reason justifying the poorer interactions of the RGD sequence with integrins compared to the ones of adhesion proteins, is the lack of 3D conformation in the oligopeptide. Indeed, the RGD domain contained in the adhesion proteins has a specific 3D conformation imposed by the ternary structure of the protein, which is clearly not present in the linear oligopeptide alone. In order to mimic the 3D structure typical of RGD domain in adhesion proteins, the peptide sequence has been cycled providing conformational restrain to its structure. This strategy led to successful results, as the cyclic peptide showed enhanced affinities and selectivities for specific integrins [46, 73, 74].

1.5.3 Consideration on cell culture medium formulation

As mentioned in the beginning of this section, cells adhere to substrates thanks to the adsorption of adhesion proteins on the latters. In some cases, the adhesion proteins present on the substrate can be secreted by cells (for instance, diploid fibroblasts) but, in most of the cases, they come from the serum supplement in the medium [37, 41]. It is a common practice in cell culture, to use animal-derived sera such as fetal bovine serum (FBS), also called fetal calf serum, because they contain adhesion proteins. For example, a culture medium supplemented with 10% (v/v) fetal bovine serum contains approximately 2–3 μg fibronectin/mL. When serum-free or low-serum media are used, addition of fibronectin (1–50 μg/mL) can be performed, usually of animal origin [37, 75].

In the last years, the trend of using animal-derived components for cell culture changed drastically, given the criteria established by cGMP[6] of using xeno-free culture medium for culture of clinical grade stem cells [41]. Indeed, animal-derived products are not well-defined, show batch-to-batch variability, their use involves ethical aspects and leads to the risk of transmitting xenogeneic infectious agents [75]. To answer to this new need several options emerged.

[6]Current Good Manufacturing Practice regulations enforced by the FDA.

Humanized culture media

A first alternative to animal-derived formulations are humanized culture media, *i.e.* culture media including supplements of human origin. Some tested alternatives are: thrombin-activated platelet rich plasma, human albumin serum, umbilical cord blood serum, pooled human platelet lysate (hPL) and autologous or allogeneic human serum (auto-HS or allo-HS, respectively). Several studies testing these alternative culture media reported culture efficiencies comparable to the ones in FBS medium [13, 75–78].
Being novel, these options still face some shortcomings. For example, the use of allo-HS is not feasible for medium/large-scale cell expansion, as huge quantities of donors would be needed; hPL affects negatively the exhibited immunosuppressive potential of MSCs and, more generally, all these supplements might transmit human diseases by known or unknown viruses [13, 79].

Serum/xeno-free media

Another school of thought is represented by serum/xeno-free medium (SF/XF), *i.e.* medium formulations not containing serum of human or animal origin. Two kinds of SF/XF media are currently available: chemically undefined and chemically defined SF/XF media [80]. The first ones consist of a wide array of growth factors, proteins and hormones directly derived and purified from human serum. The second ones consist of well defined and characterized components which are not of animal or human origin (animal origin free (AOF)). Thus, chemically defined SF/XF media are composed of growth factors and proteins, which are recombinant versions of the ones present in serum. Recombinant proteins and biomolecules are obtained by introduction of recombinant genetic material in a host organism such as yeast, cells or bacteria.
An example of commercially available chemically undefined SF/XF medium is MesenCult™-XF (STEMCELL™ Technologies), while two examples of chemically defined SF/XF media are MSCGM-CD ™ (Lonza) and MSC Nutristem XF®(Biological Industries) [13].

SF/XF media gained a huge interest in the last decade and, even though multiple studies have been performed to optimize these formulations, their performances are still not comparable to conventional medium formulations that contain animal-derived components. Usually, when a SF/XF medium is chosen for dynamic cell culture, it is then combined with MCs coated with animal-derived ECM, in order to even out the poor performances of the medium. Nonetheless, these combinations are not in accordance with the cGMP criteria. Therefore, several research groups tried to perform a totally xeno-free and serum-free dynamic cell culture and some of them achieved successful results. Santos *et al.* used PS MCs coated with xeno-free proprietary cell adhesive substrate (CELLstart™, Life Technologies) in MesenPRO® RS/ StemPro® MSC SFM XenoFree medium to culture ASCs and BMSCs [81]. The authors chose xeno-free MCs and used a medium being a combination of xeno-free and low-serum media. Another example is the study by De Soure *et al.* in which the authors chose to use Plastic® MCs for the culture of BMSCs in StemPro® MSC SFM Xenofree culture medium. Therefore, the authors succeeded in performing a totally xeno-free culture [13].
In conclusion, given that the culture medium functionalizes the substrate surface to a certain level, the choice of the culture medium fro dynamic cell culture and the one of the MCs should not be independent.

1.5.4 Physical and chemical parameters influencing cell adhesion

The chemical nature of surface plays a fundamental role in cell adhesion. The hydrophilicity/ hydrophobicity of the surface and the chemical groups exposed influence the adhesion of specific proteins to the surface and consequently, adhesion of cells to the surface [41]. Chemical modification of the surface can be performed in order to enhance cell adhesion by creating electrostatic interactions between cells and surface and/or enhancing the hydrophilicity/hydrophobicity of the surface as is explained in the following sections [41]. Besides the chemical nature of the surface, its physical properties are also relevant regarding cell adhesion. Stiffness and elastic modulus, as well as curvature, topography and roughness of the substrate play an important role in cell attachment. These features depend on the material used and on the fabrication method of substrate and/or coating [41]. Among the several chemical and physical properties of the surface, the most relevant ones are charge, roughness, elastic modulus and stiffness [41].

Surface charge

Cells of all vertebrate species possess an unevenly distributed negative surface charge. Therefore, a positively charged surface represents a suitable surface for cell adhesion. It was found that the optimal amount of positive charge is between 1 and 2 millieq/g of dry material and it has been proved that some positively charged MCs can reach about 90% efficiency of attached cells within 1 h [82, 83]. The surface charge is an advantageous feature because it affects cell attachment by enhancing the adhesion proteins adsorption and, therefore, increases integrin binding [41]. Nevertheless, successful cultures are also reported on neutral and negatively charged substrates [37, 67].

Surface elastic modulus and stiffness

Elastic modulus and stiffness of the surface play a role in cell adhesion but are mostly important concerning cell differentiation. For instance, a stiffer substrate enhances the osteogenic differentiation while a softer substrate enhances the adipogenic and chondrogenic differentiation [14].
A substrate with adequate elastic modulus and stiffness should be carefully chosen whenever cell differentiation is not desired. If it is not possible to choose a material with the adequate specifications, several options of surface coatings are available to tune or modify the elastic modulus and the stiffness, as it is explained in the next sections.

Surface topography

Several studies investigated cell adhesion, proliferation and differentiation related to surface roughness. Primavalova *et al.* observed that poly(D-lactide) (PDLA) MCs with smooth surface supported cell growth better than PLLA MCs with higher roughness (Figure 1.10 B1 and B2) [84]. Contrarily, Patntirapong *et al.* developed a method to enhance surface roughness of substrates made of poly(butylene succinate)/b-tricalcium phosphate (PBSu/TCP) composites by hydrolysis with sodium hydroxide (NaOH) solution. The authors tested the substrates for culture of hMSCs and observed a higher cell adhesion and proliferation on treated substrates compared to non-treated ones (Figure 1.10 A1 and A2). In conclusion, enhanced surface roughness does not always lead to higher cell adhesion.

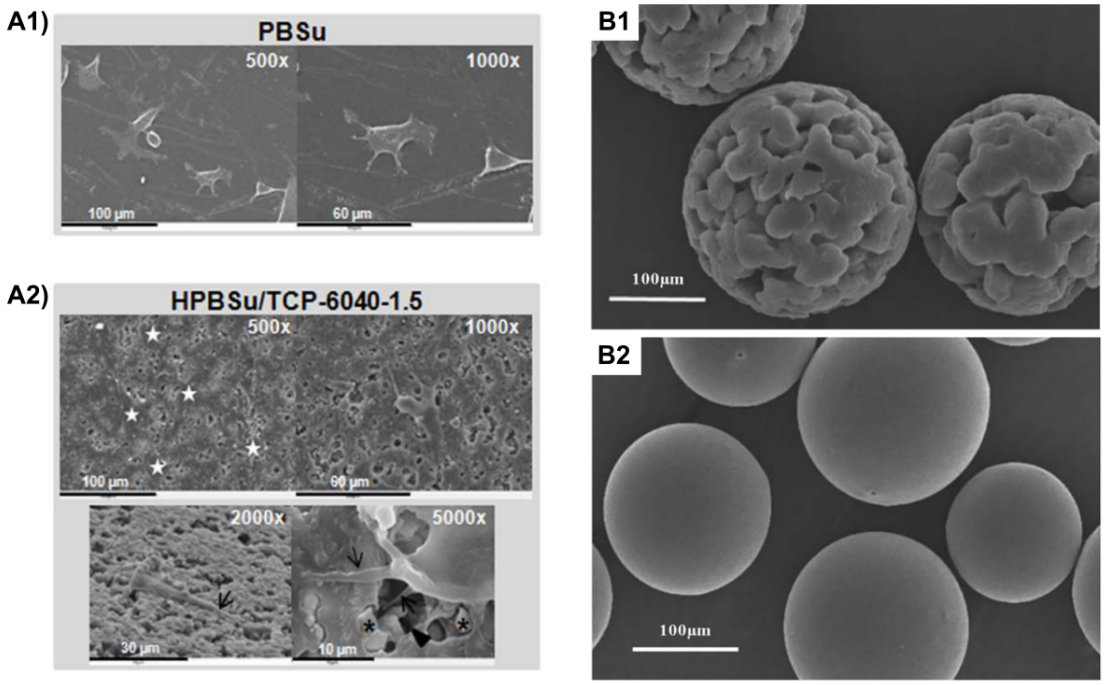

Figure 1.10: Effect of surface roughness on cell adhesion. SEM images of hMSCs adhering on a substrate made of PBSu/TCP composite (A1) and on a substrate made of PBSu/TCP composite treated with NaOH (A2) [85]. SEM images of PLLA MCs (B1) and PDLA MCs (B2) [84].

1.5.5 Surface modification

Common surface coatings

Common surface coating techniques aim to change the chemical nature, elastic modulus, stiffness and mechanical properties of the substrate. These techniques often consist in the use of organic molecules to coat the surface.

The first example is the use of polymers. Polymers can be immobilized on the surface following two strategies: grafting-to and grafting-from. In the first case, polymerization starts from a functional group present on the surface, while in the second case, the polymer is grafted to the surface. The grafting-from strategy is preferred to the grafting-to one because it allows an easier control of the grafting density on the surface and the grafted polymers and facilitates the creation of quality polymer brushes, which are often desired [86]. However, the grafting-from approach is limited to synthetic polymers, while the grafting-to approach is, generally, suited for both the grafting of synthetic and natural polymers. For instance, polylysine, which is generally obtained from natural sources but can also be synthesized, is commonly employed for surface coating of cell culture substrates and it is immobilized on the surface by grafting-to approach [41].

Another common technique is the formation of self-assembled monolayers (SAMs). The formation of SAMs on a surface consists in the spontaneous self-assembling of organic molecules and, then, their grafting to the substrate by covalent bonding. The employed molecules are alkyl thiols and alkyl silanes. The inter-chain interactions occurring between the alkyl chains of these molecules are driving the self-assembly of the layer. Alkyl thiols

are suited to functionalize gold substrates while alkyl silanes are suited to functionalize silicon, silica and polymers. The covalent bonds forms between the head group of the alkane molecules and the substrate. If necessary, the substrate can be surface treated in order to expose the adequate surface groups (usually hydroxyl groups) to bond the head groups of the alkane molecules. These coatings are widely used and allow an easy further functionalization of the coating by adding functional groups to the tail of the organic molecules [87].

Hydrogel coatings are also very common. They are made of synthetic or naturally-derived polymers which, in most of the cases, are also biocompatible. Some examples of used synthetic polymers are PEG and PHEMA. Some hydrogels have the advantages of having easily tunable mechanical properties and degradability. Dias *et al.* developed a PEG-based hydrogel coating deposited on PS MCs and they demonstrated that the elastic modulus of this coating can be tuned as a function of parameters such as the chemical nature of the polymer and crosslinking strategy. This study was developed with the idea of proposing a customizable coating for MCs, an option that is not currently possible with commercially available MCs [46]. A further improvement of this study, and in general of PEG-based hydrogel coatings, is the additional functionalization of the hydrogel by "click" chemistry with adhesion ligands or growth factors.

Finally, a last technique that is worth mentioning is the Layer-by-Layer deposition, which is further explained in Section 1.6 [88].

Coating bearing amino groups

The easiest way to obtain a surface exposing amino groups (-NH_2) is by surface chemical treatment. Alternatively, polymers can be employed. Polymers bearing amino groups, as side chains or ending groups, can be deposited on or grafted to the surface. One example of polymer used for this scope is polylysine. Another option is to functionalize a previously deposited polymer film with amino groups by chemical reaction [41]. Clearly, the hydrophobic or hydrophilic nature of these polymers is a non-negligible factor, as it might influence cell adhesion and proliferation. Several MCs exposing amino groups on their surface are available on the market (DE-52® and DE-53®, Hillex II-170® and Cytodex 1® 2®) [12, 41, 89].
An advantage of surface modifications with amino groups is that they can be manufactured in a cost-effective manner. Moreover, the final surface complies with cGMP conditions. In spite of their good advantages, the performances of amino-group-modified surfaces are not comparable to the ones of ECM-coated surfaces (explained in Section 1.5.5) as they lack the adhesive molecules responsible for proper cell attachment. This problematic limits the application of MCs having a surface modified with amino groups for cultures in serum-free media, a condition requested for regenerative medicine applications [41].

Coating bearing carboxyl groups

Carboxyl groups (-COOH) are another common functional group used to promote cell adhesion as they increase the surface hydrophilicity. There are different methods to conduce this modification. Arifin *et al.* treated PS MCs by means of an ultra-violet (UV) exposition to enhance carboxyl group concentration on the surface, while Samsudin *et al.* combined UV irradiation with exposure to ozone to treat PCL MCs [90, 91]. However,

surface modifications with carboxyl groups are less efficient than other methods to enhance cell attachment, thus, they usually have to be combined with other strategies [92].
Often, this kind of surface modification is used to introduce functional groups on the surface in order to further fuctionalize it [49]. Among several strategies, a common one is to use the combination of reagents EDC/NHS[7], which allow the immobilization of polymers or proteins on the surface by formation of covalent bonds with the carboxyl groups [49]. In the previously mentioned study, Samsudin *et al.* additionally demonstrated that the higher presence of carboxyl groups on the surface of the modified PCL enhanced the immobilization of gelatin by EDAC/NHS strategy.

Coating based on ECM proteins

Conventionally, ECM proteins derived from animal tissues have been used to coat MCs, as it is performed for the commercially available MCs: CGEN 102-L® (Thermo Scientific), Collagen®, Cytodex-3® and Fact III® (see Table 1.1 for specifications) [41]. Moreover, it is a common practice in cell culture to dip the cell-culture substrate, in this case the MCs, in serum before use (usually FBS), in order to allow the adsorption of adhesion proteins on the surface, thus, enhance cell adhesion on the substrate [93]. This strategy is especially used when MCs not coated with ECM proteins are used or when serum-free or low-serum media are used for culture.

Nevertheless, the use of animal-derived ECM to produce the coating deposited onto MCs or to fabricate the MC core is not in accordance with the cGMP directives and can be costly due to the origin of the tissues and the extraction process. Accordingly, alternative routes have been evaluated involving the fields of chemical synthesis and biotechnology [41].

Coatings made of human-derived recombinant proteins or human-derived recombinant proteins combined with synthetic polymers represent two more affordable options in accordance with the cGMP regulation. A study by Varani *et al.* tested the performances of PS MCs coated with polylysine combined with Pronectin® F (a recombinant human protein). They observed a good adhesion and spreading of Madin-Darby Canine Kidney (MDCK) cells which were used for the study [94].

Another option in accordance with the cGMP criteria is the treatment of MCs by humanized derived serum. The substrate is dipped in such a serum in order to obtain a selective adsorption of human adhesion proteins, instead of using FBS for the same scope [93]. Shetty *et al.* tested the performances of substrates dipped in human umbilical cord blood serum while Bernardo *et al.* tested the treatment by platelet lysate with the same goal [77, 78]. Both studies reported successful results concerning cell adhesion: the performances of the human-serum coatings are comparable to the ones obtained with FBS coating.

Use of RGD peptide sequence

The use of RGD moiety for surface functionalization or coating is most often used in TE approaches; strategies mentioned herein are used for functionalization of scaffolds to be

[7](1-ethyl-3-(3-dimethylaminopropyl) carbodiimide hydrochloride/N-hydroxysuccinimide.

implanted in the body more than for cell culture substrates. In the TE field, surface functionalization with RGD is a more adopted strategy than coating based on ECM proteins because the introduction of animal-derived components or human derived components of allogenic origin in the patient's body might be harmful [71]. It is worth mentioning that other peptide sequences showing similar performances to RGD such as YIGSR, REDV, and IKVAV, have been immobilized on various model substrates [74, 95, 96]. The RGD sequence can either be grafted or incorporated in the coating.

Grafting and incorporation of RGD sequence

Grafting of RGD moieties consists in attaching the RGD peptide sequence to the substrate by creating a covalent bond between a functional group on the surface and the RGD group. In order to create this bond, the -NH_2 and -COOH groups of RGD can be exploited or alternately, RGD can be functionalized with another chemical group before the grafting [12, 71, 87]. Long molecules such as oligomers are often used as spacer, *i.e.* a molecule connecting the substrate and the grafted biomolecule, for a better accessibility of RGD groups towards cells.

One example of grafting of RGD moiety, is the study of Chen *et al.* where the authors immobilized RGD sequences onto MCs. As first step, the authors surface treated the MCs to obtain a surface bearing carboxyl groups. Then, the EDC/NHS strategy (mentioned in Section 1.5.5 for grafting polymers or proteins to the surface) was used to create chemical bonds between the COOH groups and peptide sequences containing the RGD moiety (GRGDSPK peptide sequences)[49]. This covalent bond consists of an amide bond between the COOH groups and the NH_2 groups exhibited by the peptide sequences. The enhanced cell adhesion of human chondrosarcoma line OUMS-27 cells on RGD-modified PLLA MCs is showed in Figure 1.11.

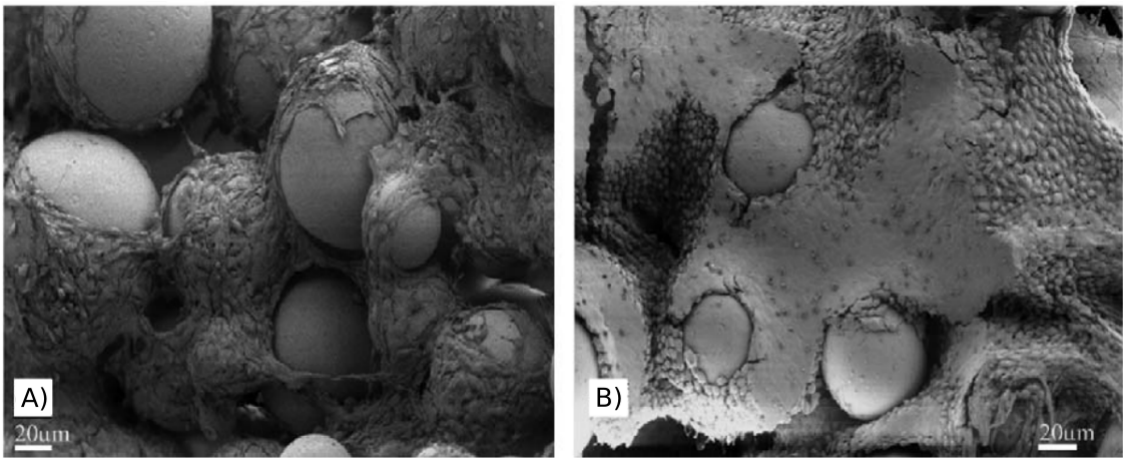

Figure 1.11: From the study Chen *et al.*, SEM observation of MCs after 14 days of culture: A)PLLA MCs and B) PLLA with GRGDSPK surface modification [49]

If the substrate does not expose functional groups to directly immobilize the RGD derivative, other strategies such as incorporation of RGD sequences in a polymeric coating can be used[71]. The RGD sequence can be incorporated in a polymeric coating by being a part of the polymer. For example, by being a monomer species or a side chain of the polymer, or by being immobilized onto a preexisting film by physical, chemical, photochemical or

ionic crosslinking [46, 71]. Also in this case, spacer groups can be used to connect RGD moieties to the backbone of the polymer in order to allow a better accessibility of RGD groups towards cells.
For instance, Hern *et al.* fabricated a hydrogel coating for tissue culture polystyrene made of a co-polymer containing RGD sequences. The coating was directly fabricated onto the tissue culture polystyrene by photopolymerization. The employed co-polymer was poly (PEG) diacrylate. The authors achieved the incorporation of the RGD peptide sequences in the polymer structure by adding acrylate moieties at both ends of the tripeptides, to enable their polymerization. The authors concluded that the hydrogels containing higher percentages of RGD peptide allowed better human foreskin fibroblasts (HFFs) attachment [97].

Advantages, drawbacks and important parameters

The use of RGD groups to functionalize the surface of cell-culture substrates allows to mimic the performances of adhesion proteins by using a totally synthetic approach. The advantages of using RGD sequences compared to ECM proteins, are that their production is usually more affordable, they respect the cGMP regulation and they are relatively more stable during immobilization [71].
Nevertheless, their lack of 3D conformation makes them more difficult to recognize from the transmembrane receptors with respect to adhesive proteins. Therefore, it is often necessary to deposit a higher concentration RGD than ECM proteins on the surface. The high peptide density might enhance the cell attachment but can also have the side effect of impeding cell migration [71].

Several parameters can influence the performances of the functional layers presenting RGD groups or similar peptide sequences. Some of the most important ones are the receptor-peptide affinity, the peptide density on the surface and their spatial distribution. A study by Neff *et al.* observed that the maximum proliferation of fibroblasts on RGD-modified PS was obtained for a surface having a concentration of RGD groups of 33 pmol/cm^2 [98]. In this and other studies, it was also observed that the cell migration diminished by both increasing and decreasing the peptide density. This suggested that there might be an optimal peptide density for a given combination of type of cells and type of substrate.
Another important parameter influencing the interaction between RGD sequences and integrins is the spacer. The function of the spacer is to allow the immobilized RGD sequence to move in the biological environment without experiencing steric impediment and, consequently, to facilitate the interaction with integrins [71, 99]. A study by Hern *et al.* showed that cells preferred to adhere onto a RGD-modified surface with a PEG spacer at low peptide density (0.01 pmol/cm^2) rather than to a RGD-modified surface without the spacer but with higher peptide density (1 pmol/cm^2) [97].
In conclusion, some general principles can be drawn concerning the influence on cell adhesion of parameters, as the length of the spacer and the peptide density on the surface. However, these trends might strongly vary depending on the specific cell types or intrinsic properties of the substrate [71].

1.6 Layer-by-layer surface coating

LbL is a coating technique consisting in depositing oppositely charged species on a substrate. Usually, Lbl is performed using polycations and polyanions as charged species. In that

specific case, the LbL process leads to the formation of a polyelectrolytes multilayer (PEM). LbL technique is a versatile, easy and inexpensive tool that allows to easily coat any surface with a robust and stable film [100]. This technique gained interest thanks to the work of Decher *et.al* in 1997, emerging as a competitive coating technique in the field of organic coatings on solid surfaces.

1.6.1 Working principle

The deposition process, depicted in Figure 1.12, consists in the alternative dipping in aqueous solution of polycation and polyanion, leading to an alternate adsorption of the two species on the charged surface (a positively charged surface in Figure 1.12). After each deposition step, the surface undergoes a charge reversal which causes the repulsion of equally charged molecules, limiting the adsorption to a single layer and resulting in a self-regulation of the adsorption [88]. Between each deposition, the substrate is washed in an aqueous solution in order to remove the non-attached macromolecules.

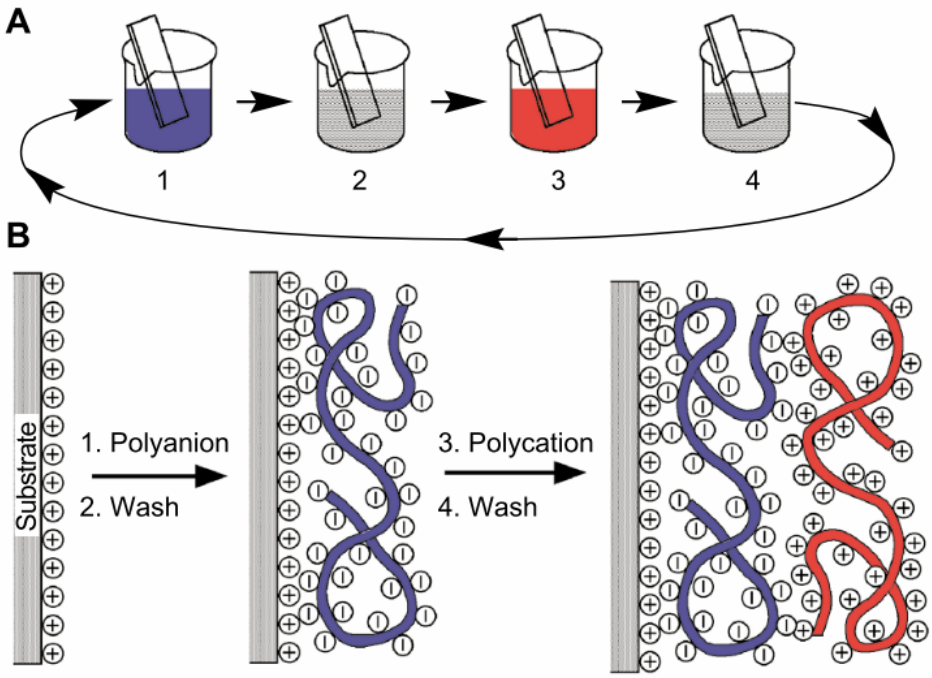

Figure 1.12: A) Schematic drawing of the LBL deposition technique to modify substrate surface. Dipping procedure: 1. the substrate is dipped in a polyanion solution, 2. rinsed in an aqueous solution, 3. dipped in a polycation solution and 4. rinsed in an aqueous solution. B) Schematic drawing of the deposition of a polyanion chain on the surface followed by the polycation deposition [88].

Even though the final film is usually compact, eventually a post-crosslinking reaction can be performed to create covalent bonds between the two polyelectrolyte species leading to enhanced stability [88, 101, 102].
In most of the cases, the driving force for the LbL deposition is the electrostatic attraction between the two chains of polyelectrolytes. Nevertheless, deposition driven by other interactions, such as hydrogen bonding, is also possible [88, 100].

1.6.2 Advantages, drawbacks and important parameters

The LbL coating process can be conducted in mild conditions: low temperature, entirely in aqueous solutions (no exposure to harmful organic solvents) and usually, in mild pH condition [100]. The use of mild preparation conditions is particularly advantageous when biomolecules, enzymes or cells are incorporated in the LBL assembly. These components are sensible to harsh chemical conditions (which might lead to their denaturation) and might have limited solubility in non-aqueous solutions [100].

LbL can be performed on any kind of substrate presenting any kind of roughness and shape (*e.g.*, planar, porous, colloidal particles, cylindrical structures, etc.) and on objects of any size [88, 100]. Moreover, LbL can be done with several types of building blocks other than charged macromolecules. Some examples are clays, dyes, colloids, nucleic acids, proteins, enzymes and viruses. Moreover, different types of organic charged macromolecules can be used such as synthetic polyelectrolytes, polypeptides, proteins, enzymes, etc. These entities can either be used as building blocks, if they display a charge, or they can be incorporated or loaded in the film adding new functionalities to the latter [100, 103–105]. Nonetheless, LbL assembly performed by on dip coating also presents some drawbacks. This technique is time consuming and significant volumes of polyelectrolyte solutions are needed for each deposition, especially when coating with numerous layers are performed. Consequently, to overcome these limitations, alternative deposition procedures to the dip-coating have been evaluated, such as spin- and spray-assisted LbL assembly approaches [100].

The properties of the deposited film such as thickness, stiffness, chemical composition, structure, roughness, hydrophilicity/hydrophobicity, and swelling/shrinking behavior can be tuned playing with different processing parameters. These parameters are the chosen adsorbed species (their charge density, chemical composition and structure), the composition of the aqueous solution (chemical nature, pH, ionic strength) and external parameters (temperature, adsorption time and number of deposited layers) [100].
Concerning the different parameters playing a role on the deposition process, the pH of the polyelectrolyte solutions might be one of the most relevant. Nevertheless, its influence on the system is still widely debated [100].
The study performed by Rubner *et al.* showed how the pH strongly influences the thickness of an LbL coating composed of two weak polyelectrolytes [106]. The two polyelectrolytes are poly(acrylic acid) (PAA) and poly(allylamine hydrochloride) (PAH), having a pK_a of 5.0 and 9.0, respectively. The two chemical structures are reported in Figure 1.13a and 1.13b. At pH close to neutral (6.0-7.5) both polyelectrolytes are fully charged and ionized, and very thin layers are obtained for both polyelectrolytes (3-5 Å), as can be seen in Figure 1.13c. In this case, the interaction between the two species drive them to adhere to the substrate and one to the other assuming an almost extended conformation and having good interactions. Contrarily, at lower pH (2.5-5.5), PAH chains are ionized while PAA are not, as the carboxylic groups are protonated. Therefore, the number of electrostatic bonds between the two polyelectrolytes drastically reduces. Thick layers are obtained for both polyelectrolytes (80 Å for PAH and 45 Å for PAA at pH 5.0) due to the loop-like conformation adopted by the two electrolytes (Figure 1.13c). In the same way, at higher pH (8.5-9.5), a high thickness of polyelectrolyte layers is also observed. In this case, the charge density of PAH is lower due to the deprotonation of the ammonium groups, while PAA stays ionized.

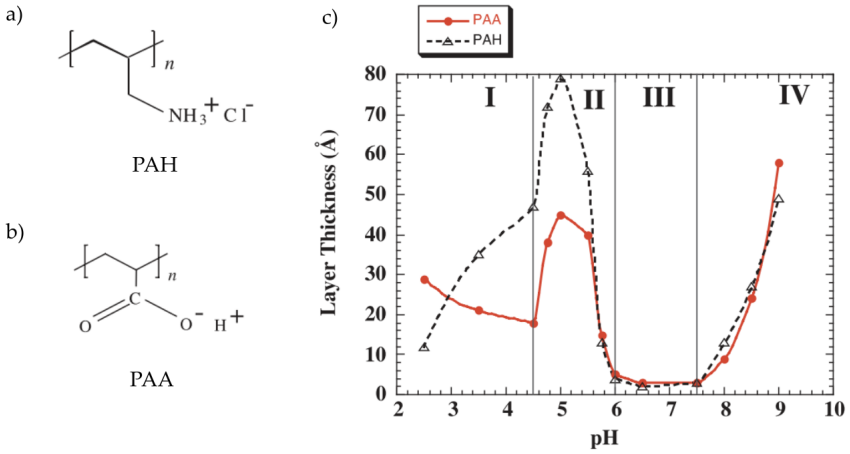

Figure 1.13: Influence of the pH on the thickness of PAH and PAA layers forming (PAH/PAA) LbL film a) Chemical structure of PAH and b) chemical structure of PAA. c) Thickness of PAH and PAA layers depending on the pH [106].

Two main trends have been outlined concerning the deposition phenomenon: the film thickness can grow either linearly or exponentially depending on the nature of polyelectrolyte chains and the conditions used for their LbL deposition [100].

1.6.3 Post-functionalization of PEM films for application as cell culture substrates

LbL coating is not frequently used to coat cell substrates and it is particularly rare to find studies reporting applications in which MCs have been coated by this deposition technique. Despite, a few studies proved that the performance of cell culture substrates coated by LbL deposition are comparable to the ones of currently used cell culture substrates, without inducing cytotoxic[8] effects [107, 108].

A first important consideration is that a PEM film meant to be employed as a cell culture substrate has to be stable in culture medium and in physiological conditions (*i.e.* a medium at $\approx$ 0.15 M NaCl and pH between 5 and 7.4) in order to not dissociate during the culture [109]. PEM films produced for this scope have been fabricated with synthetic polymers and also with polysaccharides and polyaminoacids.
However, it was observed that PEM films consisting of polyaminoacids and polysaccharides tend to be softer than PEM films consisting of synthetic polymers, probably due to their high hydration and low elastic modulus. The softness of these substrates discourages cell attachment and proliferation on the surface. Moreover, a softer PEM tends to be unstable in physiological conditions and might be particularly subjected and damaged by the shear stress forces applied by cells during culture.

Several methods have been employed to enhance the mechanical properties of PEM films made of these polymers in view of enhancing cell adhesion. Covalent crosslinking of the film is the most common approach and leads to a stiffening of the PEM due to the creation of covalent bonds between the different layers constituting the film. The type of crosslinking

[8]Property of a material or chemical specie of being toxic to cells.

reaction employed depends on the chemical nature of the polyelectrolytes [109]. Other options to enhance the mechanical properties of the PEM are to incorporate NPs in the film or to deposit the PEM incorporating one or multiple layers of a different polyelectrolyte species. For instance, Vodouhe *et al.* enhanced the mechanical properties and, consequently, cell adhesion of a PLLA/hyaluronic acid (HA) film, initially non-adhesive, by the addition of a single layer of polystyrene sulfonate (PSS) in the PEM [110].

Other than by the mechanical properties of the substrate, cell adhesion depends on the chemical nature of the substrate and on the presence on the surface of adhesion proteins or peptide sequences that can be recognized by the cell integrins. Thus, the PEM can be biofunctionalized to expose peptide sequences mediating the cell recognition as RGD. This can be performed by employing the EDC/NHs strategy already mentioned in Section 1.5.5. Alternatively, ECM proteins can be incorporated as building blocks of the PEM or adsorbed or grafted to PEM. For instance, the group of Costa *et al.* prepared a biomimetic smart coating using chitosan and recombinant elastin-like recombinamer (ELR), a recombinant protein containing the cell attachment sequence RGD [111]. This elegant strategy allowed the obtainment of a surface coating with tunable properties and strong cell adhesion in a few easy steps. The authors demonstrated that the hydrophilicity of the film can be strongly influenced by changing the coating procedure parameters and they tested the substrate for SaOs-2 cell line culture, obtaining successful results.

1.6.4 Other applications

PEM coatings find applications in disparate fields such as biosensors, biotechnology, gas separation, bioelectronics, drug/gene delivery, regenerative medicine, tissue engineering, etc. [100, 107, 108, 111–117].

One of the most common uses of PEM films in biotechnology, is as drug delivery systems. Usually, the drug molecules are loaded on a sacrificial template which is then coated with LbL and dissolved, leaving intact the drug molecules. This leads to the creation of a hollow shell made of a PEM entrapping the drug molecules. The shell can be destroyed under a specific stimulus, when the target is reached in the body. This fabrication strategy is advantageous because it allows an easy incorporation of functional components (*e.g.*, surface antibody modification for specific uptake) or sensor molecules in different positions of the multilayer composing the hollow shell [116, 117]. Besides drugs, magnetic nanoparticles (used for inducted release or carrier tracking), enzymes and cells can also be loaded in the hollow shell and it is also possible to load them after the PEM formation, adopting more complex strategies [115, 117].

1.7 Magnetic microcarriers

The magnetic feature of magnetic MCs is usually obtained by the incorporation of magnetic nanoparticles (NPs) made of iron oxide (Fe_3O_4) in the MC material. Due to to their low toxicity and biocompatibility, iron oxide NPs have been used for *in vivo* biomedical applications for many years [118, 119]. For example, superparamagnetic NPs are used for treating cancer by magnetic hyperthermia therapy, thanks to their property of producing localized heat when submitted to an alternate magnetic field [120]. Their eventual toxicity in the body depends on the chosen dose and on physical, chemical and structural properties

of the magnetic NP itself [120].

Magnetic MCs are currently used for several applications in the biomedical field and in biotechnology. Magnetic MCs can be surface functionalized to be used as a substrate for the culture of bacteria or to act as biosensors, for example to perform *in vitro* immunoassay [120]. Several models of magnetic MCs for these scopes are already on the market [120]. The feature of being magnetic, makes this kind of MCs interesting for *in vivo* applications, because their position in the body can be tracked by magnetic resonance imaging (MRI) or magnetic resonance imaging navigator (MRI navigator) [121, 122].
MCs are used for genes and drug delivery, by loading the biomolecules in the core and, then, implanting them *in vivo* [120]. They are also used for cell delivery [121]. Two main strategies are possible: cell-laden magnetic MCs are directly implanted *in vivo* or cell-laden MCs are incorporated in a macro-sized construct and, then, implanted. This macro-sized construct is usually made of hydrogel or polymer and has magnetic NPs incorporated [47].

The use of magnetic MCs for dynamic or static cell culture could bring many technical advantages. For instance, it could be useful to separate the MCs from the cells after cell detachment or to isolate the cell-laden MCs from the medium solution during the culture. Nevertheless, only a few studies focused on performing dynamic or static cell culture on magnetic MCs [41, 121, 123, 124]. One example is the study of Xu *et al.* in which the influence of cell growth enhancement of MSCs when cocoltured with rabbit ACs (rACs) was investigated [125]. In order to do so, they created a coculture of the two kinds of cells on MCs in dynamic conditions. The used MCs were composed of alginate, but the ones used to culture rACs were loaded with magnetic NPs. This strategy allowed the authors to selectively separate the rACs-laden MCs from the culture by applying a magnetic field. A schematic drawing of the strategy is shown in Figure 1.14.

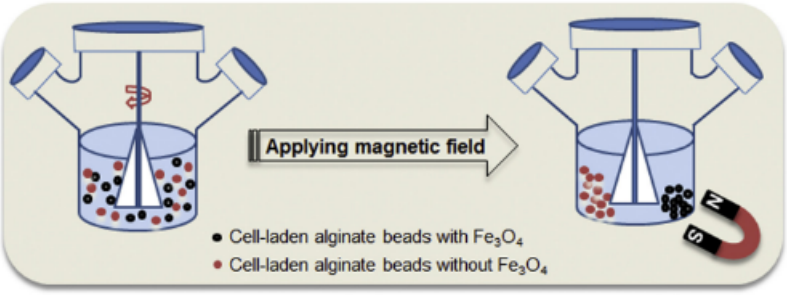

Figure 1.14: Selective separation of rACs-laden MCs from the coculture by applying a magnetic field [125].

Chapter 2

Scope of the thesis and strategy

2.1 Scope of the thesis

The relevance of the use of MCs in the expansion of stem cells and the currently used fabrication and coating techniques for the production of MCs have been introduced in Chapter 1. These elements constitute the framework of this master thesis project.

The scope of this project is to produce magnetic MCs for stem cell expansion. The cellular response to these MCs is evaluated in semistatic culture conditions. However, the optimization of their properties is performed in view of a final use as cell-culture substrate in dynamic culture conditions, as for instance in spinner flasks. The magnetic feature of these MCs would allow a simplified separation of the MCs from the culture medium and sampling during the culture. This is explained in detail in Chapter 4. Nevertheless, the evaluation of the performance of these MCs in dynamic culture conditions is beyond the scope of this project.

As well as magnetic MCs, non-magnetic MCs are produced and tested in semistatic culture conditions. These are intended to serve as a comparison group for the study of the properties of magnetic MCs. The novelty and scientific relevance of this project stands, first of all, in the production of magnetic MCs, but also in the solvent-free production method of the MCs and in the coating of the MCs which is entirely free of animal derived components.
The novelty and scientific relevance of this project stands, first of all, in the production of magnetic MCs. However, two additional major contributions are the solvent-free production method and the chemical nature of the coating, which is entirely free of animal derived components.

2.2 Strategy

The first step is the production of MCs. MCs are made of poly(L-lactic acid) (PLLA), a biocompatible and biodegradable polymer, and are produced by spherulitic crystallization using an organic-solvent-free method. The magnetic properties of the MCs are achieved by incorporating Fe_3O_4 superparamagnetic NPs in the PLLA spherulites. Together with magnetic MCs, non-magnetic MCs are prepared as well, by avoiding the NPs incorporation step. Both kinds of MCs are coated in order to enhance cell attachment on their surface. In order to do so, a polyelectrolyte multilayer (PEM) is deposited in the surface by

Layer-by-Layer (LbL) deposition, then it is functionalized with RGD peptide sequences. A highlight of the coating procedure is that it is free of any animal-derived component, which could possibly transmit xenogeneic infectious agents.

Both kinds of MCs are characterized prior to their evaluation as suitable cell-culture substrates. An important possible limitation of the use magnetic MCs as cell-culture substrate is their eventual iron release, which might render them toxic to cells or influence cell differentiation. Therefore, it was considered fundamental to evaluate their stability, *i.e.* their iron release in solution. Moreover, the incorporation of NPs and the magnetic properties of magnetic MCs are characterized, two factors influencing their response to a magnetic field. The morphology of both kinds of MCs is also evaluated, as it is an important factor influencing cell attachment and differentiation.

Finally, the MCs are tested in vitro for expansion of human adipose derived mesenchymal stromal/stem cells (hASCs). The culture is performed in semistatic conditions and cell attachment and proliferation are evaluated for time periods of 5-6 days. Additionally, the cytotoxic effect of both kinds of MCs to cells is evaluated, to assess if the iron release from magnetic MCs has any dangerous effect in the cell growth. The cytotoxicity was planned to be evaluated in direct and indirect contact condition, as the two tests could provide different information.
Unluckily, due to the lockdown measures adopted in spring 2020, it was only possible to evaluate the cytotoxicity in direct contact conditions and not in indirect contact.

Chapter 3

Experimental methods

3.1 Materials

Microcarrier production

- Poly(L-lactide) (PLLA) Mn 40000-70000 g/mol (Polysciences, USA)
- Polyethylene glycol (PEG) Mn 3500 g/mol (Sigma Aldrich, USA)
- Polyethylene glycol methyl ether (PEG-M) Mn 5000 (Sigma Aldrich, USA)
- Fe_3O_4 Magnetic Nanoparticles (MNPs): Dextran coated iron oxide magnetic nanoparticles (MNPs) suspension (10 mg Fe /mL), (Ocean Nanotech, USA)
- Poly(L-ornithine) (PLO), MW 78 000 g/mol, purity 90-100 %, (Alamanda Polymers, USA)
- Hyaluronic Acid (HA), MW 360 000 g/mol, Research grade, (Lifecore Biomedical, USA)
- Poly(ethyleneimine) (PEI) solution, MW 750,000 g/mol, 50 wt. % in H2O, (Sigma Aldrich, USA)
- Sodium chloride (NaCl), purity 99.5 %, (Sigma Aldrich, USA)
- N-Hydroxysulfosuccinimide sodium salt (Sulfo-NHS), purity 98 %, (Sigma Aldrich, USA)
- N-(3-dimethylaminopropyl)-N'-ethylcarbodiimide hydrochloride (EDC), purity 98 %, (Sigma Aldrich, USA)
- 4-(2-hydroxyethyl)piperazine-1-ethanesulfonic acid (HEPES), purity 99.5 %, (Sigma Aldrich, USA)
- 2-(N-morpholino)ethanesulfonic acid (MES), purity 99 %, (Acros, Belgium)
- GRGDS peptide (RGD peptide), purity 98 %, (Genecust, France)
- Absolute ethanol, purity 95 %, (Acros, Belgium)
- Milli-Q grade water (resistivity of 18.2 mΩ), produced by a Milli-Q^{TM}Reference system of Merck Millipore, USA.

Cell culture

- Human adipose derived mesenchymal stromal/stem cells (hASCs), provided by the research unit Regenerative medicine and Skeleton (University of Nantes, France)
- Mesenchymal stem cell growth medium (basal medium and supplement mix), (Promocell, Germany)
- Bovine serum albumin (BSA), purity 96 %, (Sigma-Aldrich, USA)
- Penicillin/streptomycin (PEST), (Life Technologies, USA)
- Dimethylsulfoxide (DMSO), purity 98 %, (Sigma-Aldrich, USA)
- Fetal bovine serum (FBS), (Sigma-Aldrich, USA)
- Dulbecco's phosphate-buffered saline (devoid of calcium and magnesium) (DPBS), (ThermoFisher Scientific, USA)
- StemPro^{TM} Accutase Cell Dissociation Reagent, (ThermoFisher Scientific, USA)
- PrestoBlue^{TM} Cell Viability reagent, (ThermoFisher Scientific, USA)
- CyQUANT^{TM} Cell Proliferation Assay Kit, (ThermoFisher Scientific, USA)
- Calcein AM (Invitrogen, ThermoFisher Scientific, USA)
- UltraPure^{TM} Ethidium Bromide (Invitrogen, ThermoFisher Scientific, USA)
- Triton TM X-100, (Sigma-Aldrich, USA)

3.2 Overall strategy of production of microcarriers

A scheme of the overall strategy of production of MCs is shown in Figure 3.1. The microcarriers (MCs) consist of spherulites of poly-L-lactic acid (PLLA). PLLA was melt-mixed with poly(ethylene glycol) (PEG) and the spherulites were obtained by isothermal spherulitic crystallization in poly(ethylene glycol) (PEG) medium. Specifically, to obtain magnetic MCs, NPs were incorporated in PEG by freeze-drying prior to the melting step. A biofunctionalized coating was deposited on the surface of the MCs. In order to do so, the MCs were coated with a polyelectrolyte multilayer (PEM) through Layer-by-Layer (LbL) deposition using cationic poly(L-ornithine) (PLO) and anionic hyaluronic acid (HA) as polyelectrolytes. The PEM was postcrosslinked, then, biofunctionalized by grafting RGD peptide sequences.

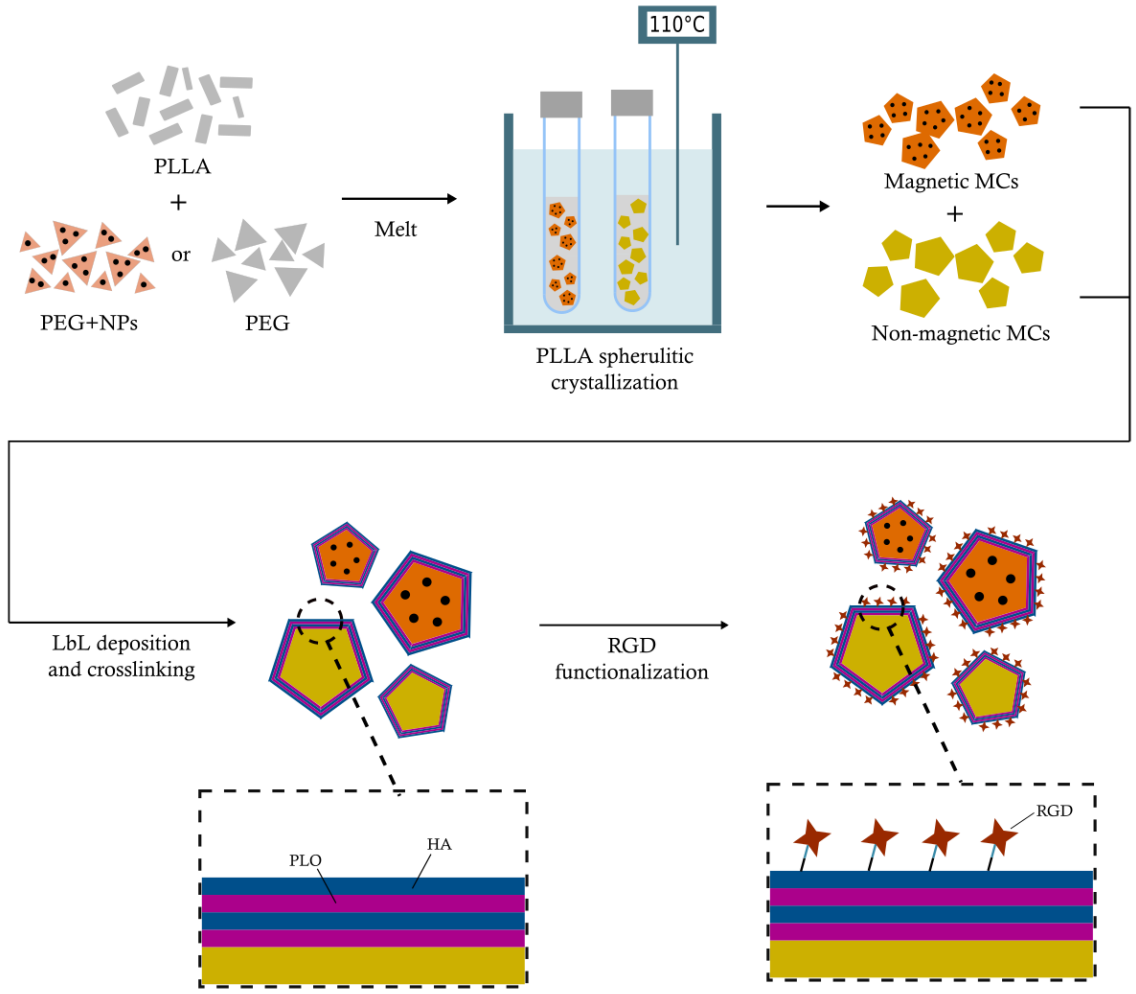

Figure 3.1: Scheme of the overall production strategy of magnetic and non-magnetic MCs.

3.2.1 Fabrication of microcarriers

The fabrication procedures of magnetic and non-magnetic MCs are depicted in Figure 3.2 path A) and B), respectively. A protocol optimized by Kuterbekov in a previous study was followed to produce non-magnetic MCs [59]. Equal quantities of PLLA and PEG were introduced in a glass tube. The tube was, then, hermetically closed with a septum and degassed through two argon-vacuum cycles (1h30 of vacuum, 30 min of argon). The tube was placed in a 230°C oil bath for 5 minutes in order to melt the the two polymers. Then, it was placed in a 110°C oil bath overnight. At this temperature, PLLA crystallizes forming spherulites while PEG stays liquid. The following day, the tube was removed from the 110°C oil bath and cooled down to room temperature. The blend was finally repeatedly washed with MilliQ water to dissolve the PEG and retrieve individual PLLA spherulites. Those spherulites were then sieved to select spherulites with a size range of 150 - 300 μm. The obtained particles were stored in MilliQ Water at room temperature.

To fabricate magnetic microcarriers, magnetic nanoparticles (MNPs) were incorporated in the PEG powder. In order to do so, 3 mg of MNPs per gram of PEG were added in a PEG solution (0.66 g/mL, in MilliQ water). The solution was freeze-dried to obtain a

solid PEG reagent with homogeneously incorporated MNPs. The rest of the fabrication procedure was performed as described above.

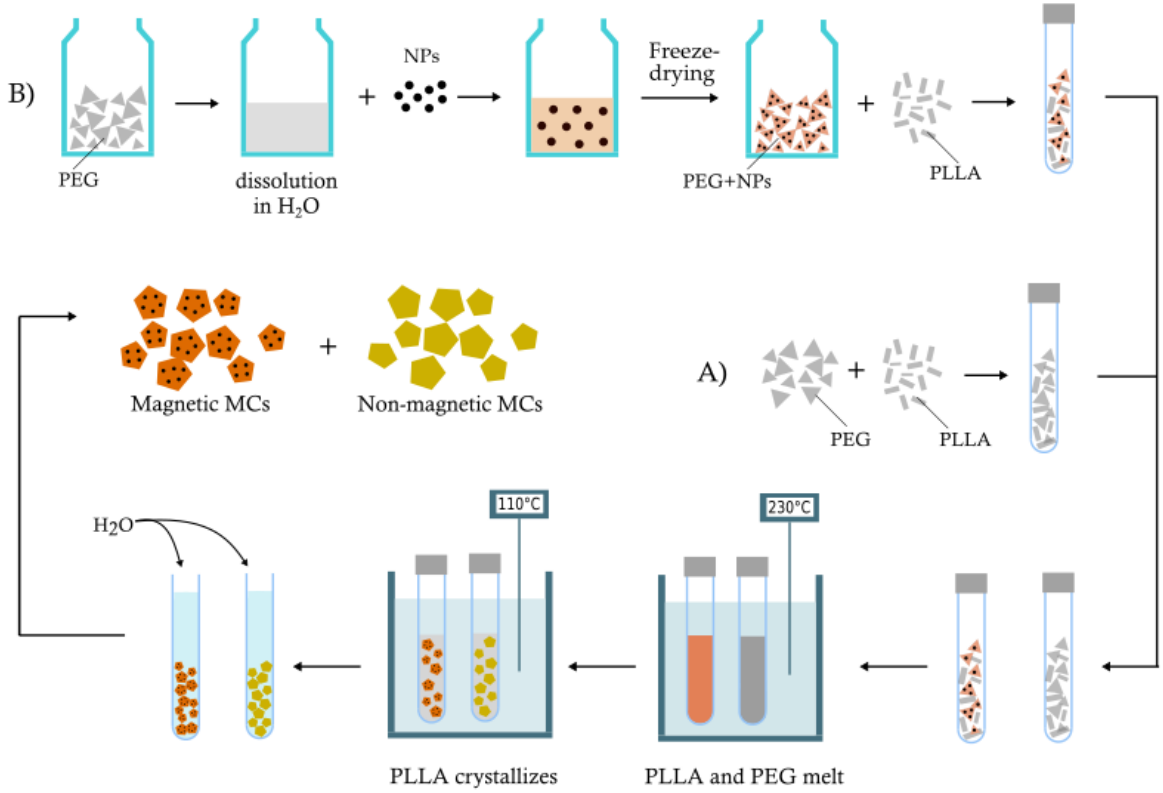

Figure 3.2: Scheme of the fabrication procedure of non-magnetic MCs (A) and magnetic MCS (B).

3.2.2 Deposition of a biofunctionalized coating on microcarriers

A LbL polyelectrolyte coating was first deposited onto the surface of the MCs. Afterwards, the polyelectrolyte coating was functionalized with RGD peptide sequences.

Polyelectrolyte coating

The coating of the MCs was performed with a ROBO-DIPP machine, a machine that is programmed to execute a cyclic dipping procedure in an automatized way. In order to coat the MCs, they were placed in specific inserts having a permeable bottom, which allowed the immersion of the MCs in the polyelectrolytes solutions avoiding their dispersion in the solutions. The inserts containing the MCs were installed on a specifically designed support that was attached to the dipping arm of the ROBO-DIPP machine. A scheme of the support is showed in Figure 3.3.

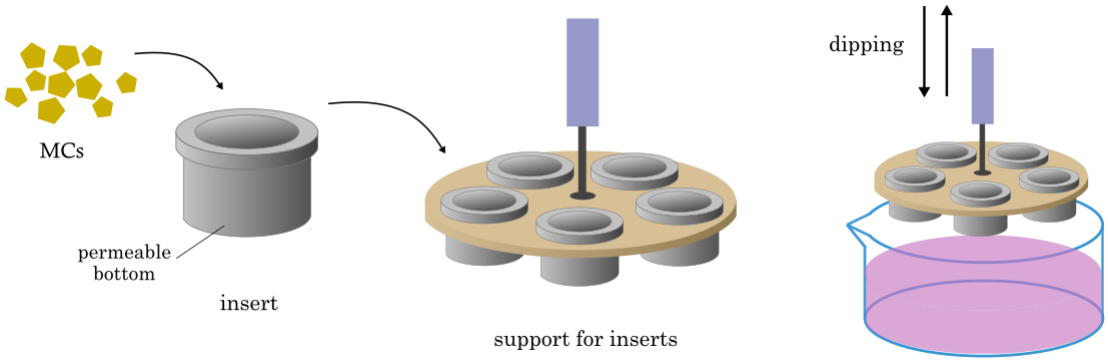

Figure 3.3: Scheme of the support used in the coating procedure, specifically designed to contain the inserts. From left to right: MCs are placed in an insert with permeable bottom, the insert is placed in the support attached to the ROBO-DIPP machine arm and, thanks to the automatized movement of the machine, the support is dipped in solution.

The two employed polyelectrolytes were HA (polyanion) and PLO (polycation). Additionally, PEI (polycation) substituted PLO exclusively for the 1st cycle, as it acts as an anchorage layer for the following polyelectrolyte depositions. The chemical structures of the three polyelectrolytes are shown in Figure 3.4.

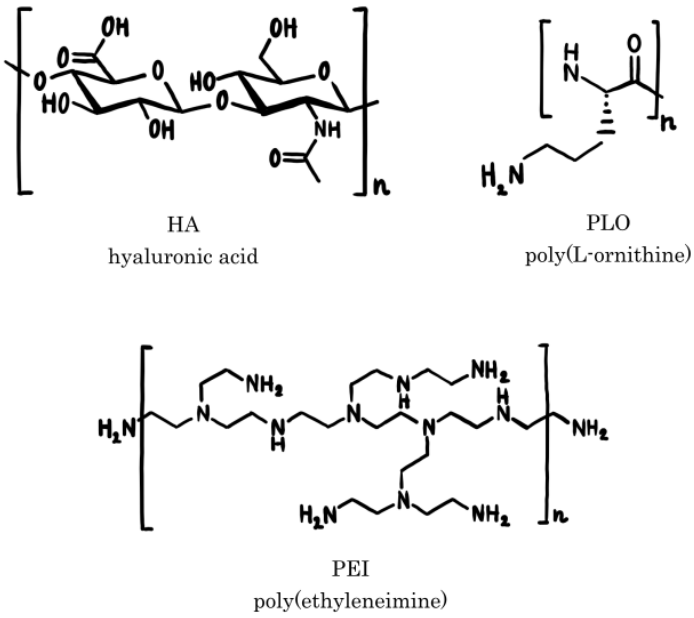

Figure 3.4: Chemical structures of the three polyelectrolytes employed in the LbL coating procedure.

HA, PLO and PEI were dissolved in 0.15 M NaCl, pH 7.4, in concentrations 1 mg/mL, 0.5 mg/mL and 1 mg/mL, respectively. The coating procedure consisted in a cyclic immersion of the MCs in the HA and PLO solutions, for a total of 8 cycles. Each cycle consisted in: immersion in PEO solution (5min) (PEI for the 1st cycle); three rinsings with 0.15 M NaCl (pH 7.4) of 1 sec for 10 times, 5 sec for 5 times and 30 sec for 1 time; immersion in HA

solution (5min) and three rinsings with 0.15 M NaCl (pH 7.4) of 1 sec for 10 times, 5 sec for 5 times and 30 sec for 1 time. A scheme of the dipping procedure is shown in Figure 3.5.

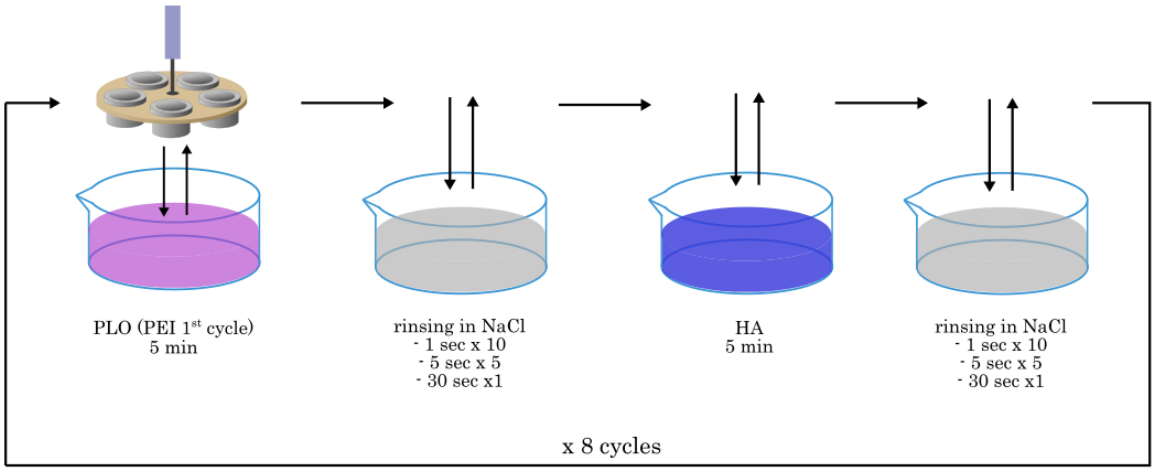

Figure 3.5: LbL dipping procedure. From left to right: immersion in PLO (PEI for the 1st cycle), three rinsings with NaCl, immersion in HA solution and three rinsings with NaCl.

Once the PLO/HA coating was achieved, a post-crosslinking reaction was performed in order to improve the mechanical properties of the coating. For this, the protocol developed by Picart *et al.* was used [126]. The chemical reaction occurring during the crosslinking and schematic drawing showing the effect of the crosslinking on the PEM are shown in Figure 3.6 A and B, respectively. The crosslinking consists in the formation of amide bonds between the carboxyl groups (COOH) of HA and the amino groups (NH_2) of PLO thanks to the combined action of EDC and sulfo-NHS. Initially, the carboxyl group (COOH) of HA reacts with EDC (1st step in Figure 3.6 A). Then, the hydroxyl group (OH) of sulfo-NHS substitutes EDC (2nd step in Figure 3.6 A). Finally, the amino group (NH_2) of PLO reacts with the activated ester to form the amide bond (3rd step in Figure 3.6 A). The amide bond could form only thanks to the action of EDC, but the presence of sulfo-NHS enhances the reaction yields and avoids possible rearrangement of the intermediate species to undesired products [126].

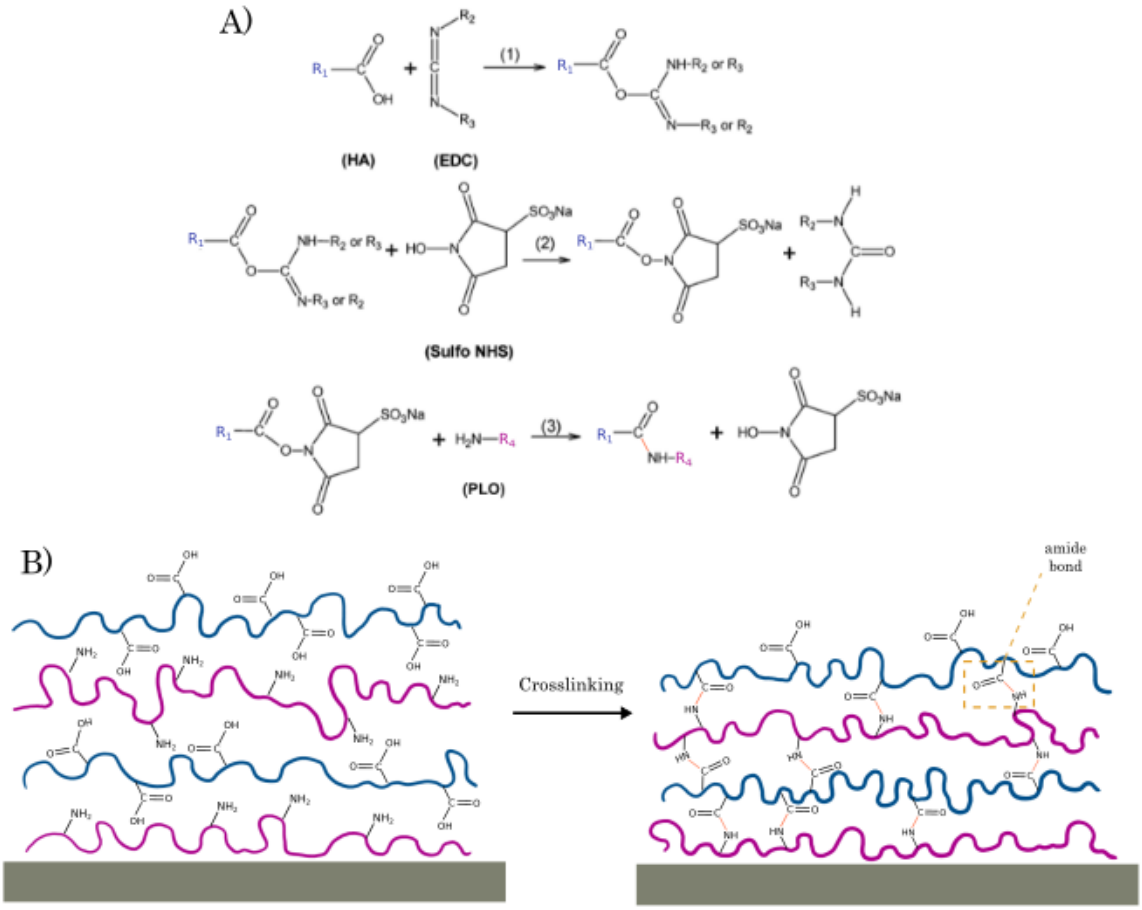

Figure 3.6: A) Formation of the amide bond between the two polyelectrolytes chains by action of the reagents sulfo-NHS and EDC, adapted from [126]. B) Crosslinking of the PEM by formation of amide bonds between the HA chains and PLO chains.

To achieve the crosslinking of the coating, the MCs were incubated in a EDC/sulfo-NHS solution (concentration: EDC 70 mg/mL and NHS 11 mg/mL in 0.15 M NaCl, pH 5.5) overnight at 4°C. The reaction was stopped by 5 rinsings of 20 min each with HEPES solution (20 mM in NaCl 0.15 M, pH 7.4).

RGD grafting

The functionalization of the PEM consists in the grafting RGD peptide sequences to the carboxyl (COOH) ending groups of HA, through the same reaction as for the crosslinking (Figure 3.6A). The employed peptide sequence is Gly-Arg-Gly-Asp-Ser (GRGDS) and the presence of the additional Gly amino acid provides an amino group (NH_2) employed to react with the COOH groups of HA. Therfore, the NH_2 ending group of GRGDS acts as the NH_2 group of PLO in the reaction shown in Figure 3.6A. Figure 3.7 shows a scheme of the RGD grafting to the PEM.

Practically, in order to graft the RGD group on the PEM, the MCs were immersed in a EDC-NHS solution (concentration: EDC 70 mg/mL and NHS 11 mg/mL in MES 0.1 M, pH 6.5) for 15 min at 4°C and then, abundantly rinsed with MES 0.1 M pH 6.5.

This caused the activation of the COOH groups of HA by reacting with EDC and, then, sulfo-NHS. Then, the MCs were immersed in a RGD solution (concentration: 10^{-3} M in MES 0.1 M, pH 6.5) for at least 18 h at 4°C, so that the RGD sequences reacted with the COOH groups of HA.
To stop the reaction, the samples were rinsed 8 times in HEPES 20 mM for 20 min. The samples were placed overnight in HEPES 20 mM solution to completely remove the non-grafted peptide. The following day, additional rinsing were performed: 3 rinsings of 20 min in a solution MilliQ/Ethanol (1:1 v/v), one fast rinsing with MilliQ/Ethanol solution and three rinsings with MilliQ.

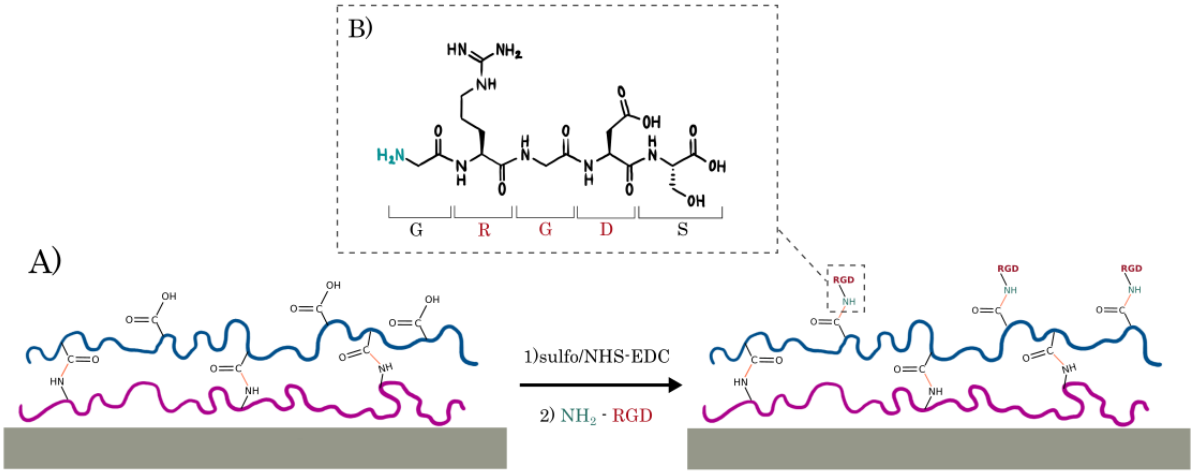

Figure 3.7: A) Functionalization of the PEM with RGD sequences by action of the reagents sulfo-NHS and EDC. B) Chemical structure of the peptide sequence GRGDS employed in the functionalization.

3.3 Characterization of microcarriers

3.3.1 Magnetic nanoparticle incorporation and iron release

Two aspects related to the use of MNPs were evaluated: the amount of MNPs incorporated in the magnetic MCs and the release of MNPs from the magnetic MCs. To evaluate both this aspects, inductively coupled plasma atomic emission spectroscopy (ICP-AES) analyses were performed.

During ICP-AES, a liquid sample is exposed to inductively coupled plasma, which causes the excitation of the atoms and ions contained in the sample. Consequently, the excited atoms or ions emit electromagnetic radiations with wavelength characteristic of the chemical species. The radiations are detected by the instrument and their wavelengths and intensities provide information on the chemical species contained in the sample and on their concentrations, respectively.

Concerning the MNPs incorporation yield, dry samples of MCs were crushed, calcinated at 500°C, dissolved in 1 mL of HCl and 9 mL of water, diluted 10 times in water and, finally, analyzed. Two samples of MCs coming from the same batch were prepared. Concerning the release, instead, the analyses were conducted on the supernatant of MCs incubated

for 12 days in DPBS. MCs samples were placed in a glass vial containing 2 mL of DPBS (concentration 5mg/mL). The vial was incubated for 12 days in a shaking incubator (VWR, USA). The samples were submitted to constant agitation at 100 rpm and to a constant temperature of 37°C. A scheme representing the experimental set-up is shown in Figure 3.8. At specific time points (D1, D5, D8 and D12), 1 mL of supernatant was retrieved from the vial to be analysed by ICP-AES. The samples of supernatant were diluted in 5 mL of water prior analysis. The remaining supernatant was carefully removed and the initial volume of supernatant was restored adding 2 mL of DPBS. As two glass vials containing magnetic MCs were prepared for this assay, for each time point two samples of supernatant were analyzed by ICP-AES, one for each vial.

Figure 3.8: Scheme of the set-up used to assess the iron release from magnetic MCs.

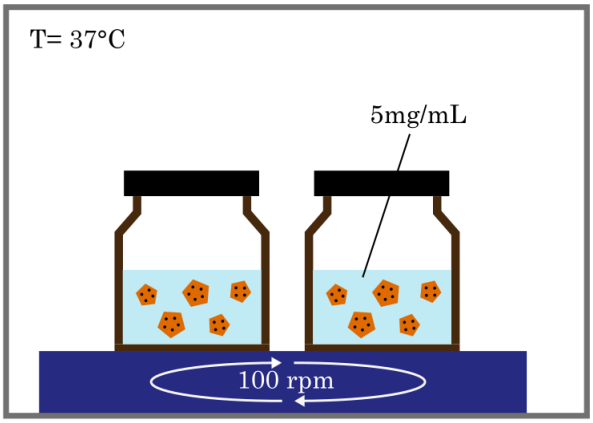

3.3.2 Morphology

To evaluate the morphology of the magnetic and non magnetic microcarriers, Scanning Electron Microscopy (SEM) observations were performed with a JEOL 7600F scanning electron microscope operating at an acceleration voltage of 2 kV. The observed samples were prepared by retrieving small volumes of milliQ water containing MCs in suspension, which were, then, placed on conductive tape. The water was let evaporate to obtain samples of dry MCs. Then, the samples were metallized with a thin layer of gold to make them conductive (coating of 10 - 15 nm).

3.3.3 Magnetic properties

The magnetic properties of the samples were evaluated through micromagnetic analysis with a MicroMag 2900 Alternating Gradient Magnetometer (AGM) [127]. This instrument allows to test the magnetic properties of small amounts of material. The AGM instrument measures the oscillation of the sample produced as a response to the submission of the sample to magnetic fields generated by the instrument.

Two samples of approximately 1 mg of MCs, coming from the same batch of MCs, were analyzed. The samples were prepared as follows. As the MCs are usually stored in milliQ water suspension, the MCs were initially retrieved as a volume of water containing MCs in suspension. To prepare each sample, 100 μL of water containing approximately 1 mg of MCs were retrieved from a of milliQ water suspension of MCs of 10 mg/mL. Then, these MCs suspended in water were placed on adhesive tape and the water was let evaporate

to obtain only dry MCs. When the water was totally evaporated, the adhesive tape was folded, in order to obtain a sample of MCs of the adequate size to be analyzed by the AGM instrument and to fix the MCs in the inner part of the produced sample. Because the MCs were fixed onto tape, the micromagnetic analysis of the adhesive tape by itself was recorded as a control. As the samples were prepared with this method, it was impossible to assess the exact mass of the MCs collected in the samples. Indeed, the mass and the number of MCs collected from the suspension could vary due to non-homogeneity of the water suspension and the retrieving method. We did not try to weight the dry powder (MCs) constituting the samples because this would have probably caused the loss of some MCs in the weighting process.

3.4 In vitro evaluation using human adipose derived mesenchymal stromal/stem cells (hASCs)

3.4.1 Revival of hASCs

Human adipose derived mesenchymal stem cells (hASCs) were cryopreserved in freezing mixture (FBS:DMSO, 9:1) at -80°C. In order to revive them, they were thawed and suspended in pre-warmed complete Mesenchymal Stem Cell Growth Medium 2 in a Falcon tube. The tube was centrifuged at 300 g for 5 min and the supernatant was removed. The cell pellets were suspended in 10 mL of pre-warmed complete medium and, then, transferred in a T75 Cell Culture Flask (Corning, USA). The cells were incubated in a CO_2 Incubator (CB 170, BINDER GmbH, Germany) at 37°C and in a 5% CO_2 atmosphere. The medium was changed every two days and the cells were passaged whenever they reached confluency.

3.4.2 Subculture and maintenance of hASCs

In order to subculture the cells, the conditioned medium in the flask was removed and the cells were washed with sterile DPBS (devoid of calcium and magnesium) to remove all traces of serum. Cells were detached from the T75 flask by 10 min of incubation in 3 mL of pre-warmed StemPro^{TM} Accutase Cell Dissociation Reagent. Cells were inspected by observation with an optical microscope (OLYMPUS epifluorescence IX71 microscope, OLYMPUS, Japan) to ensure the complete cell detachment and dispersion of cell layers. 10 mL of fresh medium were added to interrupt the action of accutase. The supernatant was removed after centrifugation at 300 g for 5 min. The cells pellets were re-suspended in pre-warmed complete medium. A cell counting procedure was performed using a Bürker chamber (VWR, USA). The Bürker chamber consists of a glass support which displays an array of squares (3x3) covered by a glass coverslip. 20 μL of cell pellets suspension were retrieved and mixed with 20 μL of Trypan Blue solution. 10 μL of this solution were introduced between the glass support and the coverslip of the Burker chamber. The cells present in each square were counted and, knowing the total volume of the cell pellets suspension, it was possible to calculate the total cell number. Once the number of cells in solution was known, cells were inoculated in two new T75 flasks in concentration 350,000 cells per T75 flask. Cells were not passaged more than 10 times.

In the case it was necessary to freeze cells for future use, after the detachment, cells were re-suspended in freezing mixture (FBS:DMSO, 9:1) and the cryovials were stored at -80°C.

3.4.3 hASCs seeding and culture on microcarriers in semi-static conditions

1 mg of magnetic or non magnetic MCs were placed in each well of ultra-low attachment Costar 24-Well-Plates (Corning, USA). The MCs in the well plates were sterilized by UV light exposure for 20 min, then, conditioned by addition of 400 μL of complete medium in each well for 20 min.
hASCs were detached from a near confluent T75 flask and counted according to the procedure described in the previous section.
The conditioned medium was removed and 300 μL of cell suspension were added, resulting in a final concentration of 3,500 cells/well. A gentle circular agitation of the well plates was performed for 2 min at an interval of 30 min for 4 h, to ensure an uniform attachment of cells on all the MCs. At the end of the adhesion period, the medium containing the unattached cells was removed and 500 μL of fresh pre-warmed complete medium were added in each well.
In order to evaluate the attachment and proliferation of hASCs on MCs, cell growth was monitored over a period of 5 days. At predetermined time points, assays were performed to assess cell viability and proliferation. Viability of cells was assessed by Live/Dead assay, cell metabolic activity was assessed by PrestoBlue assay and DNA quantification was assessed by CyQUANT assay. The principles of these assays are further explained in section 3.4.4.
At each predetermined time points, quadruplicates (four wells) were analyzed for each tested group, *i.e.* cells growing on magnetic MCs and cells growing on non-magnetic MCs. One well was employed for Live/Dead staining and three wells were employed for PrestoBlue assay. Once the PrestoBlue assay was concluded the cells in the three wells were stored for DNA quantification, as explained in Section 3.4.4. The PrestoBlue assay was performed by incubating cells growing on MCs for 4 h with 400 μL of PrestoBlue solution per well. The supernatants were analyzed by fluorescence spectroscopy with a microplate reader using a gain value of 70. The supernatant of each well was analyzed in triplicates (three volumes of 100 μL were analyzed for each well). The metabolic activity value of the cell growing on MCs in a specific well was computed as average of the values of the triplicate. The error on this value corresponds to the standard deviation. The metabolic activity of a group (for instance, cells growing on magnetic MCs on D2), was computed as average of the metabolic activity values of the three wells. The error on this value corresponds to the standard deviation.

Cytotoxicity of microcarriers by direct contact

Cells were inoculated on sterile 24-Well-Plates at a seeding density of 25,000 cells/well. Additional pre-warmed complete medium was added, in order to have 400 μL of complete medium per well. The well plates were incubated at 37 °C and 5% of CO_2.
When cells reached 60% confluency, 1 mg or 2 mg of magnetic or non magnetic MCs were added in each well. In the wells intended as negative control, pre-warmed complete medium was added (400 μL). In the wells intended as positive control, Triton X in 0.1% in pre-warmed complete medium was added (400 μL). The well plates were incubated at

37 °C and 5% of CO_2.
After 24h and 48h of incubation, the cells incubated with the MCs and with the controls were imaged by optical microscopy (in contrast phase or bright field), in order to evaluate their morphology, and the metabolic activity of the cells was evaluated by PrestoBlue assay. The PrestoBlue assay was performed by incubating the cells for 4 h with 600 μL of PrestoBlue solution per well and analyzing the supernatants by fluorescence spectroscopy with a microplate reader using a gain value of 74.
For both incubation periods, triplicates (three wells) were analyzed for each tested group, *i.e.* cells growing alone, cells in contact with Triton X, cells in contact with magnetic and non magnetic MCs, in concentrations 1 mg/well and 2 mg/well. In the evaluation of the cell morphology, the cells contained in one of the three wells were imaged and in the evaluation of the cell metabolic activity by PrestoBlue assay, the cells contained in three wells were analyzed. The metabolic activity value of cells in a specific well, the metabolic activity of a specific group (for instance, cells growing alone after 24h of incubation) and the errors correlated to these values were computed as performed during the culture of hASCs on MCs in semi-static conditions, described in section 3.4.3. The metabolic activity of cells expressed as a percentage with respect to the emission intensity measured for the negative control (cells alone) after the same incubation times, was computed by calculating the ratio between the metabolic activity of each evaluated group and the metabolic activity of cells growing alone (after the same incubation times) and multiplying by one hundred. The errors on these values were obtained by error propagation.

It should be noticed that in ISO standard of the test for *in vitro* cytotoxicity it is suggested to add the materials to the cells at 80% confluency and to evaluate the cytotoxicity after 24h and/or 72h of incubation [128]. However, different time points and confluency values can be used if properly justified. For the single cytotoxicity test performed, which is presented in Section 5.2, different parameters than the suggested ones were chosen in order to not reach a too high cell confluency by the end of the test.

3.4.4 Evaluation of hASCs characteristics

Cell viability evaluation by Live-Dead assay

The Live-Dead assay is a qualitative assay giving information on the viability of cells. The cells are stained with two fluorescent dyes: calcein AM, binding to living cells, and ethidium bromide, binding to dead cells. The calcein AM produces an intense green fluorescence in live cells while the ethidium bromide dye interacts with the dead cells binding with the nucleic acids of cells having a damaged membrane.

The hASCs growing on MCs were removed from the wells and transferred in a new well plate. The medium was removed and the samples were washed twice with DPBS. The samples were stained with calcein (2 μL per mL of DPBS) and ethidium bromide (2 μL per mL of DPBS), and incubated for 20 min, in dark at room temperature.

The stained cells were observed and imaged by fluorescence microscopy with an OLYMPUS epifluorescence IX71 microscope equipped with a green filter U-MWIBA3 (excitation 460 - 495 nm, emission 510 - 550 nm) and a red filter U-MNIGA3 (excitation 540 - 550 nm,

emission 575 - 625 nm).

Metabolic activity evaluation by PrestoBlue assay

The PrestoBlue assay is a quantitative assay based on the evaluation of the metabolic activity of the cells. It is based on the action of resazurin, which, when entering in contact with cells, is reduced to resorufin, a pink-colored and highly fluorescent compound. The fluorescence emission intensity of the solution is a quantitative indicator of cell metabolic activity. The cell metabolic activity itself acts as a qualitative indicator of cell proliferation and viability [129].

The conditioned medium was removed from the wells containing hASCs growing on MCs. PrestoBlue solution (10% PrestoBlue in pre-warmed complete medium) was added in each well. The plate was, then, incubated in the dark for 1-4 hours. At the end of the incubation period, 100 μL of supernatant were retrieved from each well in triplicates and transferred in a black 96-Well-Plate. The supernatant was analyzed by fluorescence spectroscopy (excitation wavelength 560 nm, emission wavelength 590 nm) using a microplate reader (Infinite M Nano, TECAN, Switzerland).

DNA quantification by CyQUANT assay

CyQUANT® Cell Proliferation assay is based on the use of a dye, which exhibits a strong fluorescence enhancement when bound to cellular nucleic acids. This method allows to evaluate the amount of DNA and consequently the number of cells contained in the samples [130].

hASCs growing on MCs suspended in medium were transferred from the wells to eppendorf tubes. The medium was removed and the hASCs growing on MCs were rinsed twice with DPBS by centrifugation for 3 min at 300 *g*. The supernatant was removed and the tubes were stored at -80°C until analysis.
CyQUANT assay was performed on the cell growing on MCs as per manufacturer's instructions. The frozen samples conserved at -80°C in eppendorf tubes or well plates, were thawed. 200 μL of freshly prepared CyQUANT working solution (5% volume Cell-lysis buffer and 0.5% volume CyQUANT® GR dye in MilliQ water) were added in each tube or well. Each sample was agitated by vortexing and incubated 5 min at room temperature. After the incubation period, 100 μL of supernatant were retrieved from each sample and transferred in a black 96-Well Plate. The supernatant was analyzed with a microplate reader by fluorescence spectroscopy (excitation wavelength 480 nm, emission wavelength 520 nm).

T-test

T-tests were performed to evaluate the statistical difference between different values of metabolic activity of cells growing on MCs and/or in adhesion well plates, during both the cytotoxicity assay and the evaluation of cell attachment and proliferation of MCs. One-tailed and two-tailed tests were performed. The working principles of the t-test are

presented in the following.

A t-test is a statistical test which aims to assess if two groups are statistically equivalent by evaluating their means and variances. It has a significance value (α), which is usually 0.05. A two-tailed, or non-directional, t-test consists in the formulation of two hypotheses: H_0 (null hypothesis), stating that the two data sets are statistically equivalent, and H_1 (alternative hypothesis), stating that the two data sets are statistically different. A one-tailed or directional t-test has the same null hypothesis of a two-tailed test but has a H_1 which states that one data set is significantly bigger than the other. A one-tailed test is more accurate than a two-tailed test. In both cases, the t-test provides a probability value (P value). If $P < \alpha$, H_0 is rejected and the two groups are considered statistically different (or one group statistically bigger than the other). While, if $P > \alpha$, H_1 is rejected and the two groups are considered statistically equivalent.

Chapter 4

Characterization of the microcarriers

As mentioned in Chapter 2, the aim of this thesis is to produce magnetic MCs and test them for semistatic culture of stem cells in view of a possible use in dynamic cell culture. In dynamic culture, magnetic MCs, thanks to their property of being easily magnetized by an applied magnetic field, would be easily retrieved from the culture medium by using a magnetic field. Firstly, this would enable an easy sampling of MCs during the culture for inline characterization of cells growing on MCs without affecting or perturbing the rest of the culture. Secondly, it would allow an easier harvesting of cells once the culture ends. Indeed, cells growing on magnetic MCs could be easily retrieved, transferred in a new recipient and detached from the surface by enzymatic treatment (by using trypsin, collagenase or accutase) combined to agitation. Then, the magnetic MCs would be retrieved from the solution, leaving exclusively the cell pellets. This strategy is less invasive for the cells, leads to a reduction of the manipulation steps for the operator and renders the downstream process, *i.e* the process of harvesting cells, more efficient and simple.

As already mentioned in Section 1.7, the use of magnetic MCs for cell culture has been already tested by several research groups [121, 123] and the possibility of selectively retrieving magnetic MCs from a dynamic culture has been performed by the group of Xu *et al.* [125].

In the next Section 4.1, the methods employed to fabricate magnetic and non magnetic MCs are presented and justified. Particularly, the procedure of fabrication of magnetic MCs is deepened, taking into account the requirements just mentioned concerning their magnetic properties. Moreover, the approach adopted to characterize magnetic and non magnetic MCs is explained.
Afterwards, the performed characterizations and the obtained results are presented in Sections 4.2, 4.3, 4.4 and 4.5.

4.1 Strategy of production of microcarriers and introduction to their characterization

The MCs were fabricated following a protocol developed by Kuterbekov *et al.* in a previous study [59]. According to this protocol, the MCs were produced by isothermal spherulitic crystallization of PLLA in PEG medium.
Initially, the two polymers were melted together at 230°C, then, PLLA selectively crystal-

lized in spherulites at a temperature between 140 and 110°C.
The highlights of this fabrication method are that it is organic-solvent-free, differently than most fabrication methods currently used, and that the size, mechanical properties and density of the obtained MCs are easily tunable. Indeed, the study from Kuterbekov *et al.* demonstrates that these features are depending on PLLA molar mass, PLLA:PEG ratio and crystallization temperature [54–57, 59]. For this project, a mass ratio of 50:50, a molar mass of PLLA of 40000-70000 g/mol (Mn) and temperature of spherulitic crystallization of 110°C, were chosen as they were demonstrated to be the optimal to produce MCs with size, density and mechanical properties appropriate for cell culture in dynamic condition.

The magnetic MCs were desired to exhibit superparamagnetic behaviour. This implies that they would be easily magnetized when a magnetic field is applied, for instance, when it is desired to retrieve them from a solution. In addition, a superparamagnetic behaviour implies a fast recovery of the non-magnetized state when no magnetic field is applied. Contrarily, if the magnetic MCs would remain magnetized even when no magnetic field is applied, their magnetization could cause their aggregation or an undesired cellular response. In order to obtain MCs displaying superparamagnetic features, Fe_3O_4 superparamagnetic NPs were incorporated in the polymeric matrix of the MCs.

Fe_3O_4 NPs were chosen among the several available superparamagnetic NPs for their biocompatibility and low toxicity. Indeed, these NPs are approved for biomedical applications and are one of the most used type of NPs for biomedical application *in vivo* [119].

In order to incorporate magnetic NPs in the polymeric matrix of the MCs, the fabrication procedure proposed by Kuterbekov *et al.* was slightly adjusted.

As a first step, the magnetic NPs in water suspension were added to a solution of PEG in water. Afterwards, in order to remove the water, the solution was freeze-dried leading to a dry PEG powder with homogeneously incorporated magnetic NPs. At this point, the obtained PEG powder was used to fabricate the magnetic MCs, following the same procedure employed for non-magnetic MCs. Thus, the PEG powder was mixed with PLLA, the mixture was melted and PLLA was selectively crystallized in spherulites. As a consequence of the melting of the two polymers, the NPs were released by PEG and incorporated in PLLA with a yield of at least 50%, as the mass ratio is 50:50.

The NPs were incorporated in PEG with a concentration of 3 mg of iron per gram of PEG. This concentration was demonstrated to be the optimal one for the fabrication of magnetic MCs for dynamic culture in a previous optimization study. In fact, magnetic MCs prepared with higher NPs concentrations were not suitable for dynamic cell culture, as they would tend to stick to the magnetic stirring arm of the spinner flask instead of being suspended in solution. On the other hand, magnetic MCs prepared with lower NPs concentrations had too weak magnetic properties, leading to the impossibility of being retrieved from the culture medium.

Finally, it was desired to characterize different properties of the magnetic MCs to assess their suitability as cell-culture substrate for semistatic and dynamic cell culture.

First of all, the incorporation of NPs in the magnetic MCs was investigated. This influences

both the stability and the magnetic properties of the magnetic MCs. Then, the stability of magnetic MCs, *i.e.* their iron release in solution, was investigated. This is a fundamental parameter because a high iron release could be harmful for cell growth and influence cell differentiation [131, 132]. Finally, the magnetic properties of the magnetic MCs were evaluated to assess if they exhibited the expected superparamagnetic behaviour.
Moreover, the morphology and the surface porosity of the magnetic MCs were evaluated and compared with the one of non-magnetic MCs. Indeed, these two parameters influence cell attachment and proliferation as mentioned in Chapter 1.

4.2 Magnetic nanoparticles incorporation in magnetic microcarriers

Two samples of magnetic MCs were analyzed by ICP-AES in order to assess the content in iron, which is connected to the content in magnetic NPs. The magnetic MCs were prepared by incorporating magnetic NPs at a concentration of 3 mg of iron per gram of PEG. This amount of iron is considered as a theoretical iron content as it is the iron contained in PEG and PLLA during the fabrication process of MCs.

The results of the ICP-AES analysis showed that the content in iron in the magnetic MCs was 1.70±0.06 mg per g of MCs. This value is the average of the content of the two analyzed sample which were collected from the same batch of MCs. The error on this value corresponds to the standard deviation. Knowing the content in iron in the magnetic MCs, it is possible to calculate the yield of iron incorporation. The obtained values are summarized in the following table. The error on the yield is computed by propagation of the error on the iron incorporated in the MCs.

Theoretical iron content (mg of iron/g of PEG)	Measured iron content (mg of iron/g of MCs)	Incorporation yield %
3	1.70± 0.06	57±2

Table 4.1: Summary of the obtained results concerning the incorporation of iron in the magnetic MCs.

First, it can be stated that the iron-incorporation yield corresponds to the NP incorporation yield in the magnetic MCs. Additionally, a comment on the fabrication procedure can be made. The fabrication method of MCs consists in mixing PLLA and freeze dried powder of PEG containing magnetic NPs in equal quantities, melting them and, then, letting PLLA crystallize in spherulites at 110°C. During the melting step, the NPs contained in PEG are released and they mix with PLLA. Then, when PLLA crystallizes, 57% of NPs are incorporated in the spherulites instead of staying in the molten PEG.

4.3 Stability of magnetic microcarriers

Fe_3O_4 magnetic nanoparticles are frequently used for *in vivo* and *in vitro* applications, implying a close contact with cells. However, these nanoparticles can release iron in the

culture environment. Several studies investigated the effects on cells of iron in solution and showed that the presence of iron can inhibit cell growth, influence cell differentiation and, at higher concentrations, cause a cytotoxic effect on cells [131, 132]. Therefore, the magnetic MCs are desired to be stable, meaning that they they do not release amount of iron which can be detrimental for cell behavior.

In order to assess the stability of magnetic MCs, the microparticles coated with the RGD-grafted LbL film were stored in buffer solution (DPBS) at 37°C, under stirring at 100 rpm, for 12 days. Samples of supernatant were retrieved at specific time points (D1, D5, D8 and D12) and analyzed by ICP-AES in order to measure the amount of iron released in the supernatant. At every time point, the remaining supernatant was retrieved and thrown. Then, the initial amount of supernatant was restored with fresh buffer solution.

The release of iron measured at given time points over the chosen time period is shown in Figure 4.1, as daily and cumulative release. The iron release is expressed as μg of iron released per gram of magnetic MCs. This assay was performed in duplicate, thus, for each time point two samples of supernatant were analyzed. Consequently, each daily value of iron release is an average of the values of iron release of the two duplicates. The errors on these values correspond to standard deviations. The cumulative iron release was computed by adding the daily iron release of the specific time point to the ones of the precedent time points. The errors on the cumulative iron release were computed by propagation of the errors on the daily release.

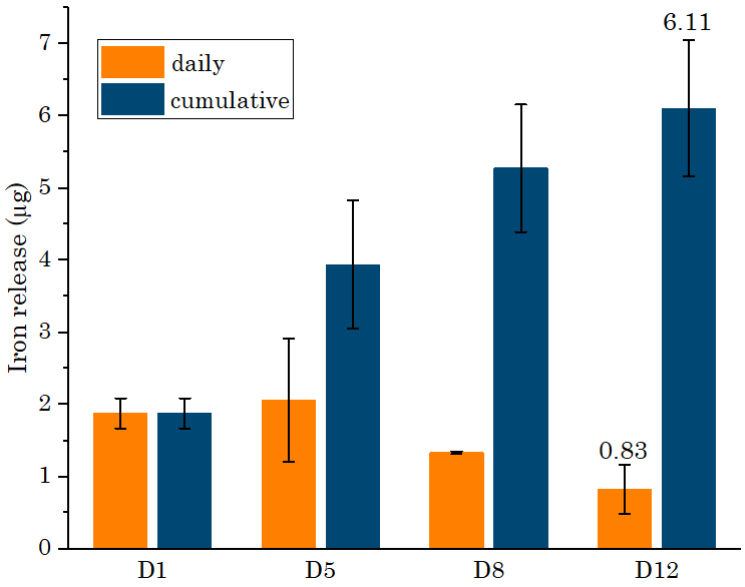

Figure 4.1: Iron release expressed in μg of iron released per gram of magnetic MCs over a period of 12 days. The error bars correspond to standard deviations (two samples were taken at every time point).

First, it can be noticed that the daily iron release decreases progressively with the storage time, until it reaches less than 1 μg per g of magnetic MCs after 12 days in buffer solution (0.8 ± 0.3 μg/g, as can be noticed in Figure 4.1). Consequently, the cumulative release increases progressively, but its daily increase decreases day by day.
The cumulative release on day 12 corresponds to 6.1 ± 0.9 μg/g of MCs, Figure 4.1. This

result can be compared to the iron content initially measured in MCs (1.70±0.06 mg/g of MCs). The percentage of the incorporated iron that is released after 12 days can be expressed as:

$$\%\,\text{iron released} = \frac{(6.1 \pm 0.9) \cdot 10^{-3}\,\text{mg iron/g MCs}}{1.70 \pm 0.06\,\text{mg iron/g MCs}} \cdot 100 = 0.36 \pm 0.06\%$$

Thus, it can be affirmed that less than the 0.4% of the contained iron was released by the magnetic MCs after 12 days.
The observed iron release, cumulative and daily at all the time points, is significantly lower than the iron concentration observed to be detrimental for cell behavior reported in the literature [131, 132]. This suggests that the assessed iron release from the magnetic MCs should not be a factor influencing cell proliferation, differentiation and, more generally, behaviour.
However, to asses this with certitude and evaluate the cellular response to magnetic MCs a cytotoxicity test is performed. This test is explained in Section 5.2.

4.4 Morphology of microcarriers

The morphology of the MCs influences the cell behaviour. As was mentioned in Section 1.5, roughness and porosity of the surface of the MCs can strongly influence cell attachment and proliferation. Additionally, these features can influence the differentiation of the cells towards different lineages [41]. Moreover, the size and the surface curvature are relevant. Indeed, as a general trend, cells proliferate better on MCs having lower surface curvature, thus, larger size [41].

Accordingly, it was in our interest to investigate the morphology of magnetic and non-magnetic MCs. The two kinds of MCs were prepared following slightly different fabrication procedures and they mainly differ for the incorporation of magnetic NPs in the magnetic MCs. The aim of this characterization is, thus, to investigate the morphology and surface porosity of both kinds of MCs and to assess if the NP incorporation caused any difference in the magnetic group.
Moreover, the MCs were coated to enhance the cell-material interaction. The coating, consisting of a PEM functionalized with RGD sequences, is supposed to modify the surface roughness and porosity. Therefore, this characterization aims also to evaluate how the features of the original surface were modified by the coating.

In order to evaluate the morphology of magnetic and non magnetic MCs, they were observed by SEM. Initially, non-coated samples were observed for both groups. As a reminder, these samples were prepared by letting dry MCs, retrieved from a water suspension, on conductive tape, then metallizing them with gold to make them conductive.

The general morphology and shape of the MCs with and without magnetic NPs are visible in Figure 4.2 A and 4.2 B, respectively. Overall, it can be noticed that the size distribution and the shape of the carriers from the two groups are really similar.

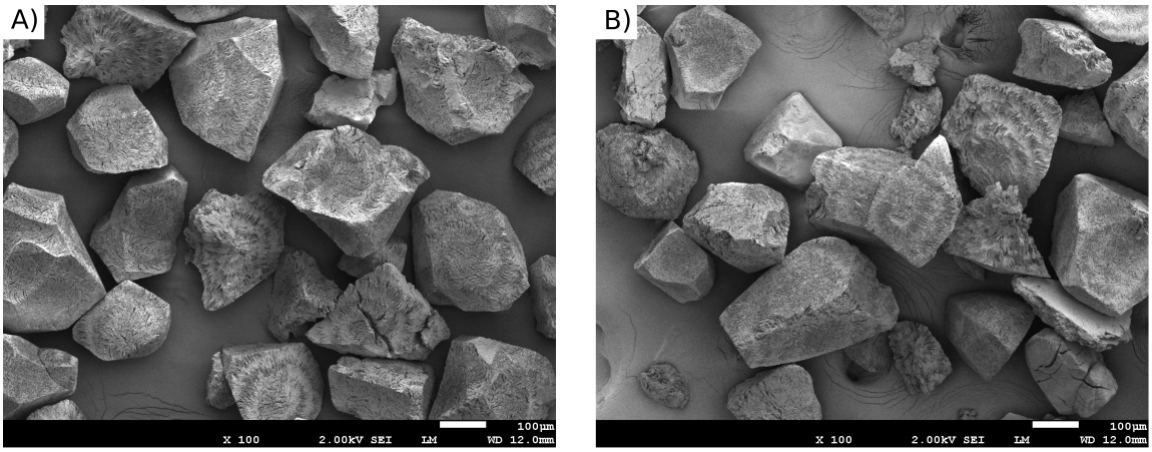

Figure 4.2: SEM images of: A) MCs with magnetic NPs and B) MCs without magnetic NPs.

The size distribution of the two groups (magnetic and non magnetic MCs) was assessed from 2D observations of MCs by optical microscopy in phase contrast. The obtained images are not reported in this thesis. This method was chosen over assessing the size distribution from the SEM images because is a more accurate and less complicated method. We measured an average size of 206.4±56.8 μm and 220.3±56.0 μm for magnetic and non-magnetic MCs, respectively. The measurement of the size of each MC was performed by taking the root square of the product of longest axis of the MC and the length of the MC perpendicularly to the longest axis. The average size of the MCs correspond to the mean value of these measurements and the error on the average size correspond to the standard deviation.
It can be stated that the size distribution of the two kids of MCs is comparable.

SEM observations at higher magnification were performed in order to study the porosity of both kinds of MCs. It was possible to observe the surface of the MCs and to evaluate the top surface porosity. The higher-magnification images of the magnetic and non magnetic MCs are shown in Figure 4.3 and 4.4, respectively. Overall, it can be observed that the pores of both groups have a slightly elongated shape. The pores of the magnetic MCs are characterized by a length around 2-5 μm and a width around 1-2 μm, while the pores of the non-magnetic ones are characterized by a length around 1-2 μm and a width around 0.5-1.5 μm. It can be observed that pores of these sizes cannot allocate cells (cell diameter $\approx$ 10 μm), therefore, cells are expected to grow exclusively on the surface of these MCs and not to enter in the pores. There might be a slight tendency to a higher porosity for magnetic MCs. However, this cannot be assessed with certitude only from these isolated observations: the slightly higher porosity of the magnetic MCs could be an occasional feature.

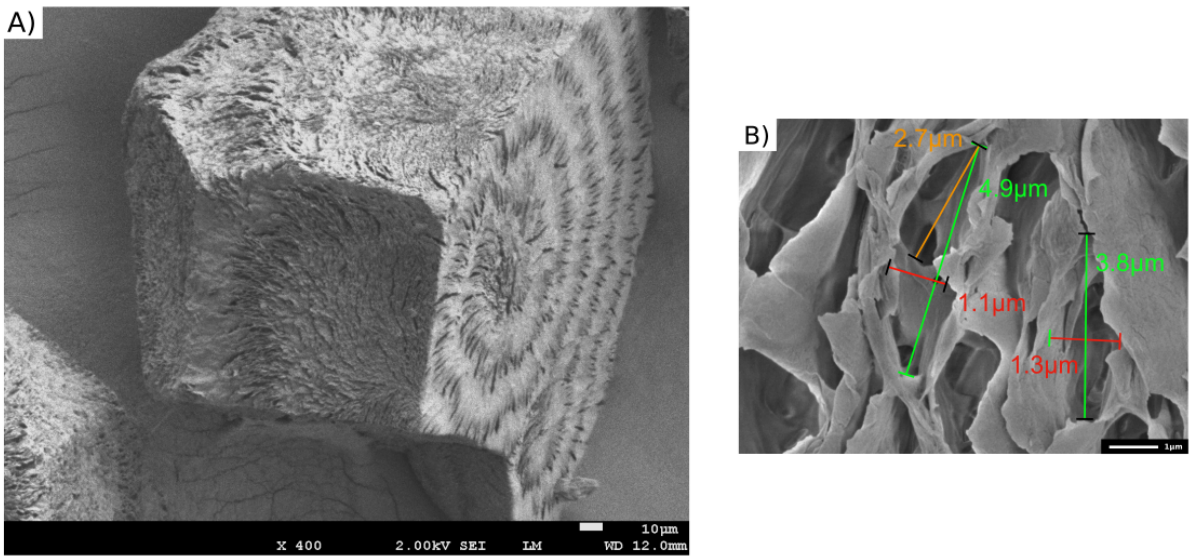

Figure 4.3: A) SEM observation at high magnification of the surface of magnetic MCs. B) Characterization and measurements of the pores present on the surface of magnetic MCs.

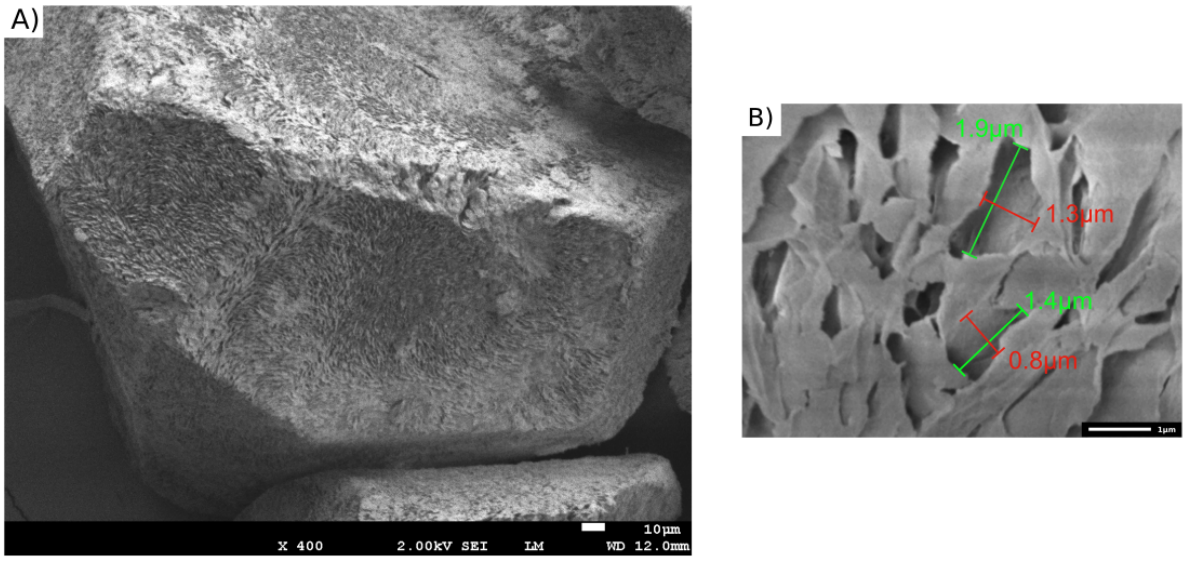

Figure 4.4: A) SEM observation at high magnification of the surface of non-magnetic MCs. B) Characterization and measurements of the pores present on the surface of non-magnetic MCs.

Overall, it can be concluded that shape, size distribution and surface porosity of the two groups are similar apart from some negligible and occasional differences caused by batch to batch variability.

In order to assess an eventual influence of the coating on the porosity and roughness of the MCs, some coated carriers have been observed. Nevertheless these observations were not successful and this evaluation was impossible. Indeed, these samples were prepared following the same procedure used for the non-coated MCs: the coated MCs were retrieved from a water suspension, let dry on conductive tape, then, metallized with

gold to make them conductive. However, during the drying step, the coating shrieked and dried, becoming impossible to properly characterize. The obtained images of coated MCs are reported in Appendix A.
As the evaluation of surface properties of coated magnetic and non-magnetic MCs is particularly important, this investigation could be improved, in the future, by using a different sample preparation procedure.

4.5 Magnetic properties of magnetic microcarriers

4.5.1 Superparamagnetic properties of magnetic microcarriers

This characterization aimed to study the magnetic properties of the magnetic MCs and verify their superparamagnetic behaviour. In order to better present the obtained results, some additional pieces of information are provided. First, some general concepts on magnetism and, second, a description of the working principle of the employed instrument.

Among the several classes of magnetic materials, the focus is here restricted on ferromagnetic and superparamagnetic materials. The hysteresis curves displaying the variation of the magnetization (M) versus the applied magnetic field (H) of these two classes of materials are shown in Figure 4.5 A and 4.5 B, respectively.

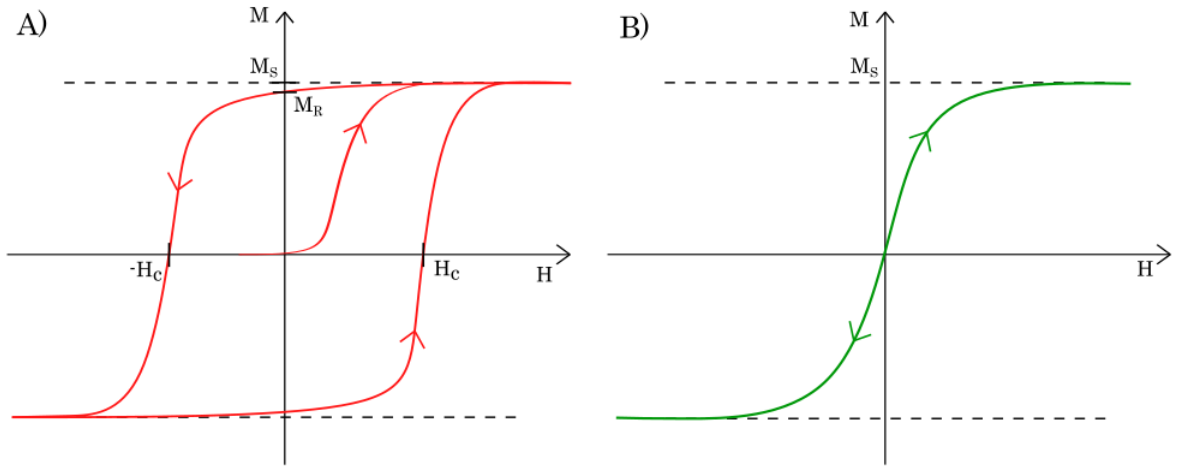

Figure 4.5: Hysteresis curves displaying the variation of the magnetization (M) versus the applied magnetic field (H) of A) a ferromagnetic material and B) a superparamagnetic material.

Ferromagnetic materials are known for displaying a spontaneous overall magnetization, called remanent magnetization (M_R), when they are not submitted to any applied magnetic field, thus, when H=0. In order to reverse the orientation of the magnetization, a magnetic field equal to the coercive field (H_c) has to be applied. In addition, when an strong magnetic field of positive or negative magnitude is applied, all the magnetic domains of the material orient in the same direction, and the magnetization of the material is called saturation magnetization (M_s) [133]. The mentioned parameters can be identified in Figure 4.5 A.

Attention should be drawn to the the difference between magnetization (M) and magnetic moment (m). The magnetization is a local property of a magnetic domain in the material.

The sum of the magnetization vectors of all the magnetic domains gives the magnetic moment, which is an extensive property of the entire sample. The magnetic moment (m) is expressed as the magnetization (M) integrated on the volume (V) of the sample:

$$m = \iiint M dV$$

Nevertheless, in the discussion concerning ferromagnetic materials, these two concepts are often confused or mixed.

When the size of a ferromagnetic material is decreased to the nanoscale, the material loses its ferromagnetic features and acquires superparamagnetic properties.

Because the size of the material is so small, it is not energetically favourable for the material do divide itself in different magnetic domains, thus, each particle consists of a single magnetic domain. The magnetization vector of the particles is not stable and it switches randomly due to thermal energy [134]. It can be noticed that, in this case, magnetization and magnetic moment of the material correspond. As a consequence, when a superparamagnetic material is submitted to an applied magnetic field, its magnetization simply follows the direction of the applied field, as it can be seen in the hysteresis curve reported in Figure 4.5 B [119]. Therefore, parameters such as remanent magnetization (M_R) and coercive field (H_c) do not apply to these materials. However, the saturation magnetization (M_s) is still a relevant parameter.

The magnetic properties of the MCs incorporating magnetic NPs were evaluated through micromagnetic analysis with a MicroMag 2900 Alternating Gradient Magnetometer (AGM). This instrument is designed to test the magnetic properties of particularly small amount of material (on the order of 1 mm^3) [127, 135]. The basic working principles of an AGM are mentioned in the following.

The aim of an AGM measurement is to measure the magnetic moment (m) of the sample versus the applied field (H). In order to perform this measurement, the sample is placed between two electromagnets, on a support free to oscillate. A schematic drawing representing the main components of an AGM is shown in Figure 4.7.

First, an uniform magnetic field (H) is generated by the electromagnets of the AGM and applied to the sample. This generates a magnetic moment (m) in the sample, which induces the production of its own magnetic field. Secondly, two gradient coils produce an alternating field ($h(t)$), or alternating current (AC) field, which causes magnetic excitation in the sample. The overall field perceived by the sample is [136]:

$$H_{tot} = H + h(t) = H + G\,\Delta x\,\cos\,\omega t$$

where Δx is the displacement and $G = \mathrm{d}H/\mathrm{d}x$ is the applied field gradient.
The interaction between the own field of the sample and the alternating external field causes the displacement of the sample between the electromagnets. Because the alternating field changes magnitude quickly, the fast variation of the sample displacement leads to the vibration of the sample. The vibrating force applied to the sample is detected by a

piezoelectric displacement detector connected to the sample support and is transduced to an AC voltage. This vibrating force (F) is given by [136]:

$$F = m\,G\,\cos\,\omega t$$

After some mathematical manipulations, an equation to express the dependence of $m_{measured}$ on H can be obtained, where $m_{measured}$ is the moment measured by the instrument [136],

$$m_{measured}(H) = k\left[m(H) + \frac{3}{8}\frac{\mathrm{d}^2 m}{\mathrm{d}H^2}(G\Delta x)^2\right]G$$

with k a constant.
The measurement consists in performing a hysteresis. The applied field (H) is variated between negative and positive magnitude, while the magnetic moment (m) value is measured by detecting the vibrating force acting on the sample. The software returns a plot of magnetic moment *vs* applied field.

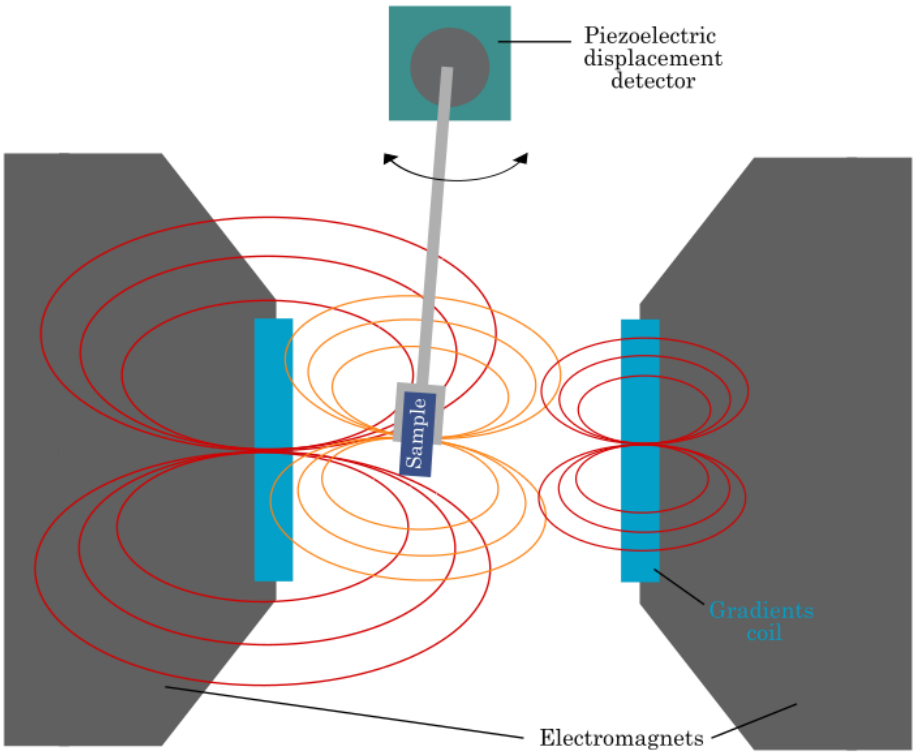

Figure 4.6: AGM schematic [127].

Now the obtained results can be commented. As mentioned previously, a superparamagnetic behaviour was expected from the magnetic MCs. This behaviour should be caused by the presence of superparamagnetic NPs incorporated in the matrix. The matrix (PLLA) is not expected to exhibit magnetic properties. As a reminder, two samples of approximately 1 mg of dry magnetic MCs coming from the same batch were prepared. It was impossible to assess the exact mass of MCs collected in these two samples due to the method of preparation of the samples, as already explained in Section 3.3.3. Briefly, the MCs constituting the two samples came from a water suspension of MCs. As the MCs were retrieved as a volume of water containing MCs, the mass and the number of MCs

collected from the suspension varied due to non-homogeneity of the water suspension and the retrieving method, even if the suspension concentration and the retrieved amount of water were known with certitude.
The dry samples were fixed onto adhesive tape in order to be able to place them on the support of the AGM, then were analyzed. Since the MCs composing the samples came from the same batch, the two samples were expected to have the same concentration in contained iron, thus, the same magnetic properties. For the analysis of both samples, the diamagnetic contributions were cancelled. These contributions might have come from the adhesive tape used to prepare the samples and other sources. This signal subtraction is reasonable because the aim of the analysis is to evaluate the paramagnetism of the sample and not the diamagnetism.

The plots of the magnetic moment (m), measured in electromagnetic unit (emu), versus the applied field (H), measured in oersted (Oe) are reported for the two samples in Figure 4.7 A. Both samples exhibited the typical superparamagnetic hysteresis curve, confirming the expectations [119]. However, the two samples exhibited two different maximal magnetic moment in saturation condition (m_S) (when the applied field is maximal), which are shown in Figure 4.7 as $m_{S,1}$ and $m_{S,2}$. The magnetic moment at saturation of sample 2 ($m_{S,2}$) is higher than the one of sample 1 ($m_{S,1}$). The magnetic moment at saturation depends directly on the saturation magnetization (M_S) of the kind of material, equal for the two samples, and the volume of the sample, slightly different between the two samples, as the two masses were different. From this observation, it can be concluded that sample 1 has a smaller volume than sample 2.

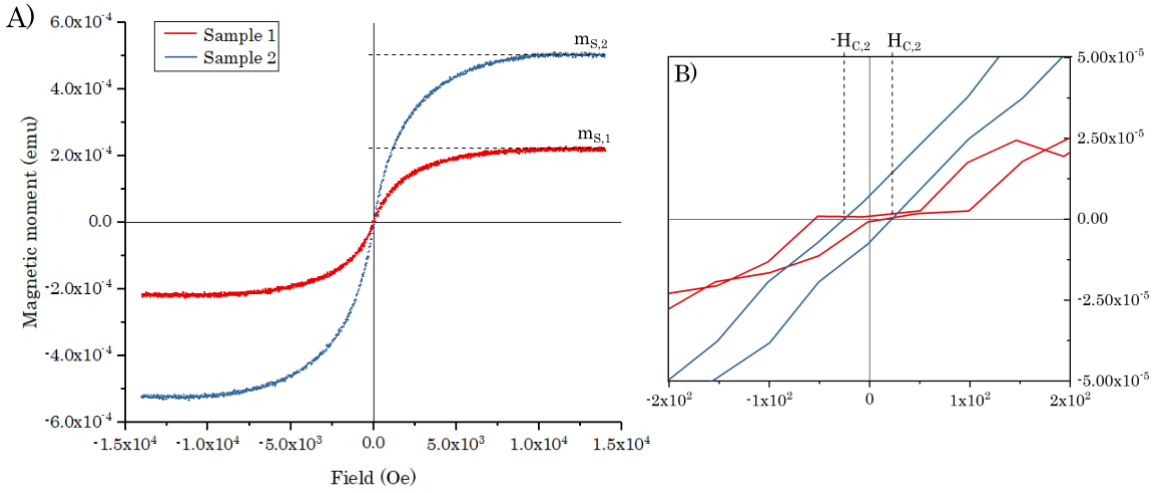

Figure 4.7: A) Hysteresis curves of two samples of magnetic MCs obtained from the AGM measurements. The two samples are made of magnetic MCs coming from the same batch. They have slightly different mass and their mass is approximately 1 mg. B) Close-up of the two plots at values of H close to 0 Oe. The coercive field (H_c) of sample 2 is shown as $H_{C,2}$.

In order to assess if there was any ferromagnetic (or paramagnetic) contribution, the behaviour of the plots close to H=0 is evaluated. Sample 1 shows no detectable coercive field (H_c) while sample 2 shows a coercive field on the order of 20-30 Oe, which is shown in Figure 4.7 B as $H_{C,2}$. A ferromagnetic behaviour of the samples could be caused by

the presence of particularly big magnetic NPs or agglomerates of NPs in the MCs. The agglomeration of NPs could occur, for example, during the fabrication process. In these cases, the size of the magnetic objects, or groups of objects, incorporated in the MCs would exceed the nanoscale, leading to the loss of superparamagnetic properties and the acquisition of ferromagnetic ones.

However, considering that value of coercive field (H_c) measured is really small compared to the interval of magnetic field evaluated or, in the case of sample one, not measurable, they can be considered negligible and the ferromagnetic component of the samples as well.

From Figure 4.7 it can be noticed that the signal of sample 1 is less defined and more variable than the signal of sample 2. This can be justified considering that sample 1 has a small volume and accordingly a small magnetic moment signal. This low signal is particularly subjected to the influence of the alternating magnetic field used for the measurement and this causes the variability of the signal.

Several research groups investigated the magnetic properties of superparamagnetic NPs of different chemical nature with AGM [135, 137, 138]. Specifically, the group of Yang *et al.* characterized Fe_3O_4 superparamagnetic NPs and reported a M_s of 56.4 emu/g. Usually the hysteresis plots are expressed as magnetization (emu/g) vs applied field (Oe) and the magnetization is obtained by normalizing the magnetic moment (emu) by the mass of the sample. This was not possible in this case because the masses of the samples were not known with certitude.

4.5.2 Qualitative evaluation of the magnetic properties of magnetic microcarriers

Another characterization of the magnetic properties of magnetic MCs was performed with the aim of showing qualitatively the behaviour of magnetic MCs when submitted to an applied magnetic field.

For this, a small amount of magnetic MCs suspended in aqueous solution was placed in petri dish. Then, a magnet was slowly approached to the petri dish in order to observe the motion of MCs under the action of a magnetic field. The employed magnet generated a magnetic flux density (B) of 1.4 Tesla (T). The motion of the MCs was recorded using optical microscopy in bright field mode. Some frames of the obtained video are shown in Figure 4.8 in order to show the progressive displacement of the MCs, which occurs really fast.

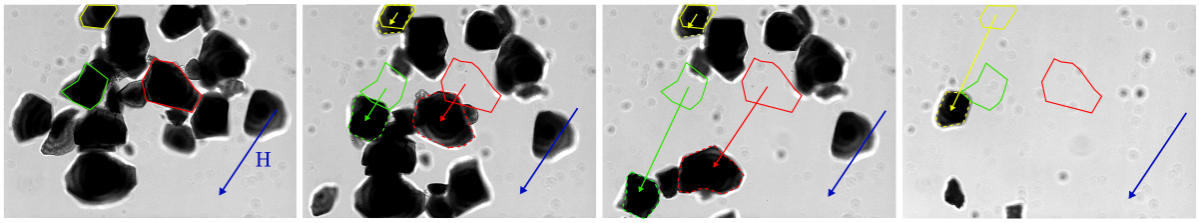

Figure 4.8: Frames of a video showing the movement of magnetic MCs when submitted to a magnetic flux density of 1.4 T (1 frame every ≈ 3 sec). The trajectory of three MCs is highlighted using three different colors. The initial positions of the three MCs are shown by solid-line shapes in all the frames. The positions of the MCs after being subjected to the magnetic field are shown by dashed-line shapes, in the second, third and fourth frames. The direction of the applied magnetic field is represented by a blue arrow.

Additionally, a similar video was recorded using cell-laden MCs after 2 days of culture. Before recording the video, the cell-laden MCs were stained with Calcein-AM to highlight the presence of alive cells. The video was recorded with a fluorescence microscope equipped with a green filter. Some frames of the video are shown in Figure 4.9.

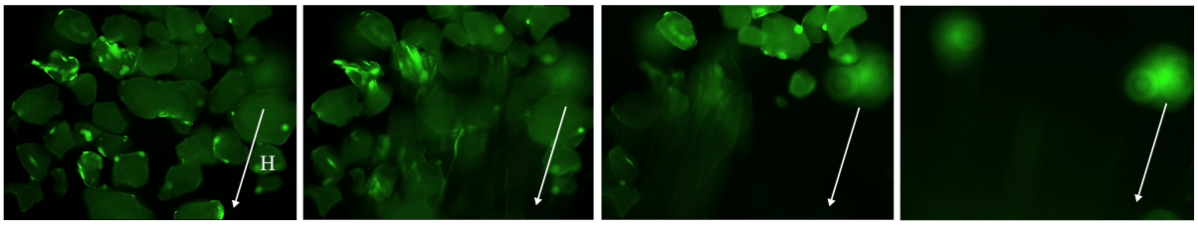

Figure 4.9: Frames of a video showing the movement of magnetic cell-laden MCs when submitted to a magnetic flux density of 1.4 T (1 frame every ≈ 3 sec). The direction of the applied magnetic field is represented by a white arrow.

It can be observed that the magnetic MCs and the magnetic MCs with cells growing on their surface moved when submitted to the magnetic field (Figures 4.8 and 4.9). This movement was caused by the partial or complete magnetization of the magnetic NPs incorporated in the MCs. Especially, from the frames reported in Figure 4.8 it can be noticed that the MCs moved following a trajectory parallel approximately to the direction of the applied magnetic field. The same observation can be deducted from the frames reported in Figure 4.9. However, due to the lower quality of these frames recorded with a fluorescence microscope, it is more difficult to determine the trajectory of the MCs.

It is possible to calculate the magnitude of the magnetic field (H) that was applied to the MCs. The dependence of the magnetic field (H) from the magnetic flux density (B) is described by the relation [139]:

$$H(\mathrm{Oe}) = \frac{1}{\mu_r} \cdot B(\mathrm{G})$$

where is G is Gauss and μ_r is the relative magnetic permeability of the medium, which is adimensional. 1 T corresponds to 10^4 G and the value of μ_r can be approximated to 1 considering that μ_r of air and water are equal to ≈ 1 and ≈ 0.99, respectively [139]. The magnetic field (H) applied to the magnetic MCs can be calculated as:

$$H(\text{Oe}) = \frac{1}{1} \cdot (1.4 \cdot 10^4) = 1.4 \cdot 10^4 \text{Oe}$$

Thus, a magnetic field (H) of $1.4 \cdot 10^4$ Oe successfully magnetizes the magnetic MCs and, additionally, applies a magnetic force to the MCs strong enough to attract them and cause their motion.

Considering again the hysteresis curves obtained by the micromagnetic analysis of the two samples reported in Figure 4.7A, it can be noticed that both samples reached the saturation of the magnetic moment (m_s) when a magnetic fields weaker than $1.4 \cdot 10^4$Oe was applied. Indeed, the saturation of the magnetic moment (m_s) of was reached at $H \approx 7 \cdot 10^3$ Oe, for sample one, and at $H \approx 1 \cdot 10^4$ Oe, for sample two. Therefore, a magnetic field (H) of $1.4 \cdot 10^4$ Oe is significantly larger than the minimum magnetic field (H) required to saturate the magnetization of both the analyzed samples.

Thus, it can be stated that the results obtained with this qualitative evaluation of the magnetic properties of the magnetic MCs are consistent with the results obtained from the micromagnetic analysis presented in the previous section.

A similar qualitative evaluation of magnetic properties was performed by Qu *et al.* in order to characterize the magnetic properties of nanofibrous PLLA MCs with γ-Fe_2O_3 magnetic NPs immobilized on their surface. They demonstrated that the magnetic MCs fabricated moved when subjected to a magnetic field, following the direction of the field, as it was demonstrated in our study. Moreover, they tested the behaviour of the magnetic MCs when submitted to a magnetic field of which direction was varying with time. They showed that the magnetic MCs had an immediate response to the variation of the direction of the applied magnetic field. However they did not report the magnitude of the magnetic field employed, therefore their results are not quantitatively comparable to the ones we obtained.

In conclusion, the characterization of the magnetic properties was successful. It was possible to verify the superparamagnetic nature of the samples and no significant ferromagnetic component was detected. Moreover, it was possible to qualitatively characterize the magnetic properties of the magnetic MCs by showing their response to an applied magnetic field. The two characterization approaches produced comparable results.

Chapter 5

Study of the cellular response to magnetic microcarriers

5.1 Cell adhesion and proliferation on microcarriers

Adhesion and proliferation of hASCs were tested on MCs by performing cell cultures in semi-static conditions on MCs for a time period of 5-6 days. The aim of these experiments is to evaluate if there is any difference between magnetic and non-magnetic MCs used as cell-culture substrates concerning cell attachment and proliferation.

Among the several cell attachment and proliferation experiments that were performed, one representative and successful example was chosen and is presented in the following. hASCss were seeded on MCs with a concentration of 3,500 cells/well in low adhesion well plates, in order to allow cell adhesion and proliferation only on MCs and not on the wall of the well. At specific time points, various tests were performed to check the cellular behavior: cell viability was investigated by Live/Dead staining, metabolic activity was measured by PrestoBlue assay and the number of cells was quantified by CyQUANT tests. However, we found that the results obtained for DNA quantification were not relevant due to a strong interaction between MCs and the dye used for this test. This interaction resulted in wrong value of DNA amount and consequently estimated number of cells in the sample. For this reason, results obtained for DNA quantification are not presented in this thesis.
As a reminder, the Life/Dead assay consists in staining the cells with two fluorescent dyes: Calcein AM, which emits a green light when it binds to living cells, and ethidium bromide, which emits a red light when it binds to nucleic acids contained in cells having a damaged membrane. The Live/Dead images recorded for of magnetic and non-magnetic cell-laden MCs at time points D0, D1, D2 and D5 are shown, in Figures 5.1, 5.2, 5.3 and 5.4, respectively.

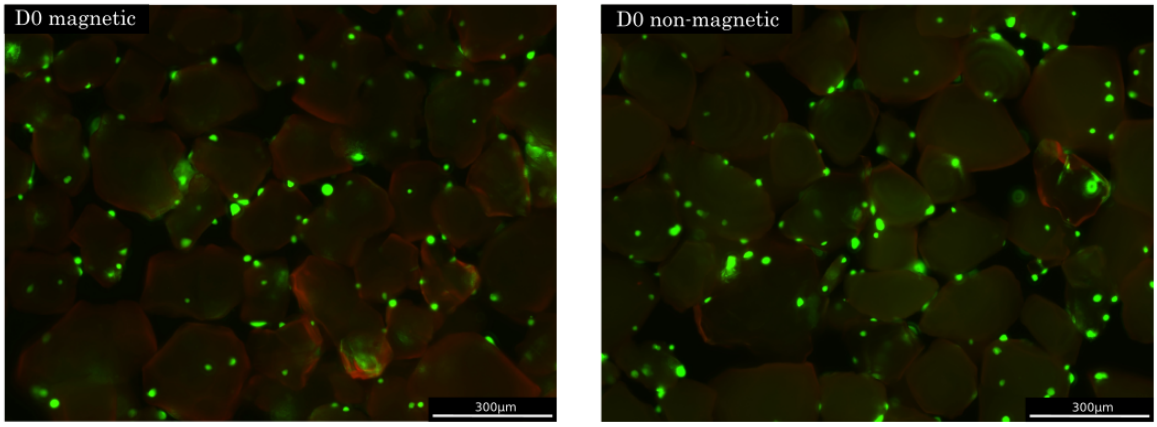

Figure 5.1: Life/Dead images of cell growing on magnetic and non-magnetic MCs on D0.

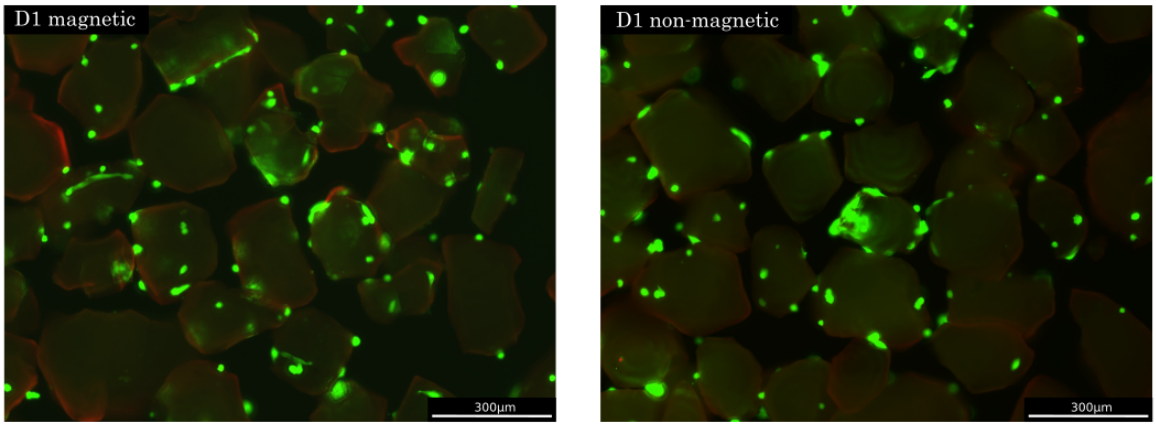

Figure 5.2: Life/Dead images of cell growing on magnetic and non-magnetic MCs on D1.

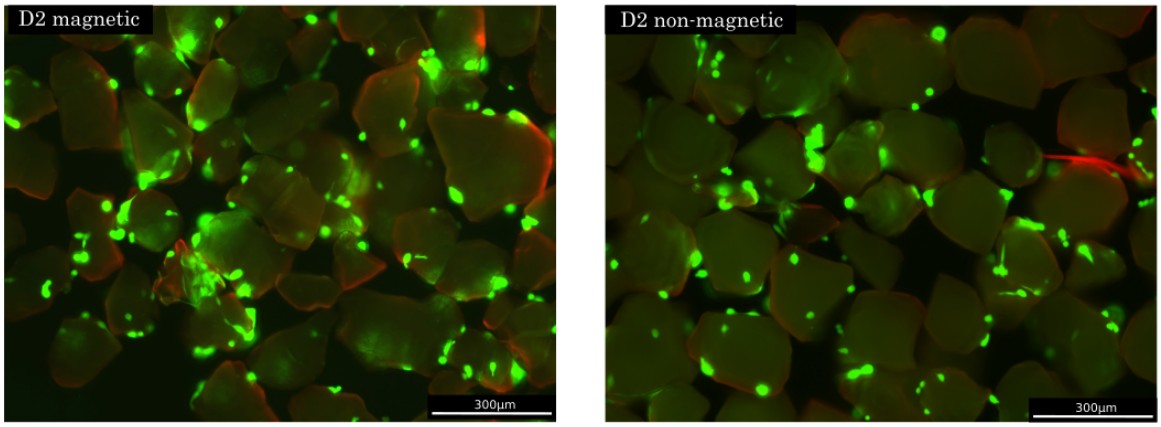

Figure 5.3: Life/Dead images of cell growing on magnetic and non-magnetic MCs on D2.

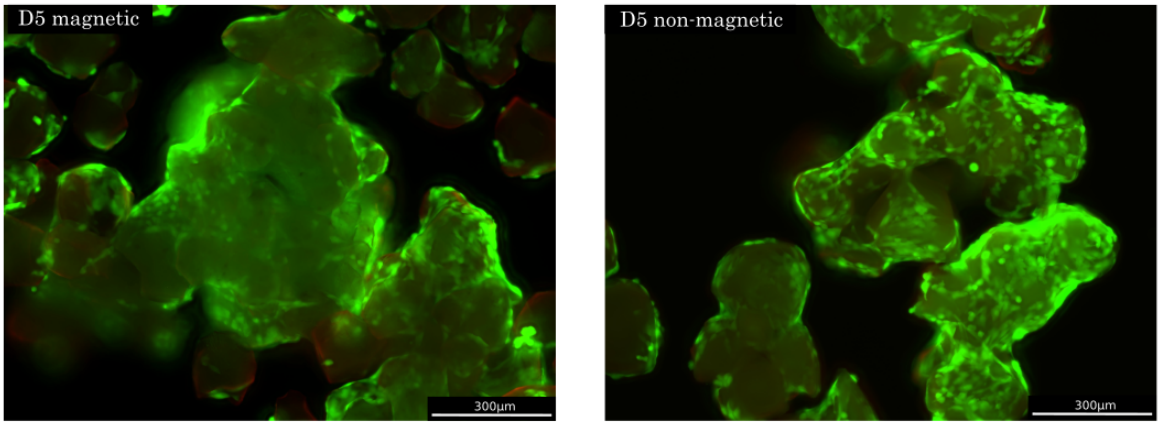

Figure 5.4: Life/Dead images of cell growing on magnetic and non-magnetic MCs on D5.

Overall, it can be observed that in all the images the majority of cells are alive (green stained) and almost no dead cells are present (red stained).
On D0, several cells attached onto the surface of both magnetic and non-magnetic MCs, as can be seen in Figure 5.1.
It can be noticed that, from D0 to D5, increasing numbers of living cells are visible on both kinds of MCs, meaning that cells proliferate through cellular division processes. Furthermore, the fact that fully bare MCs were observed on D0 but not on D5 proves that cells were able to migrate from one MCs to another one, throughout the evaluated period of time. This is observed for both kinds of MCs (Figures 5.1-5.4). On D5, cells reached confluency, *i.e.* they spread on all the available surface on both magnetic and non-magnetic MCs. Due to the confluency, cells started growing between one MC and another by forming bridging aggregates between MCs. Moreover, some cells started growing on top of others, due to the lack of available surface on the MCs. This is observed in Figure 5.4 for both groups.

The metabolic activity of cells growing on magnetic and non-magnetic MCs was measured by PrestoBlue assay, as described in Section 3.4.4. The metabolic activity of cells growing on MCs is expressed as an emission intensity measured in relative fluorescence units (RFU) and is presented in Figure 5.5A. How the metabolic activity values and the errors on these values were computed is described in Section 3.4.3.
Then, the fold increase of the metabolic activity of the two groups is shown in Figure 5.5B. The fold increase was obtained by normalizing each metabolic activity value by the one obtained on the first day (D0). The fold increase is often used in studies on biological systems to express the increase of a measured parameter at any time point of the experiment compared to the value of the parameter at the first time point (or at any other arbitrarily chosen time point). In our case the measured parameter is the metabolic activity of cells. Thus, the fold increase of the metabolic activity expresses how many times the metabolic activity value of cells at a specific time point is the metabolic activity value of cells on the first time point. The errors on the fold increase values were computed by error propagation.

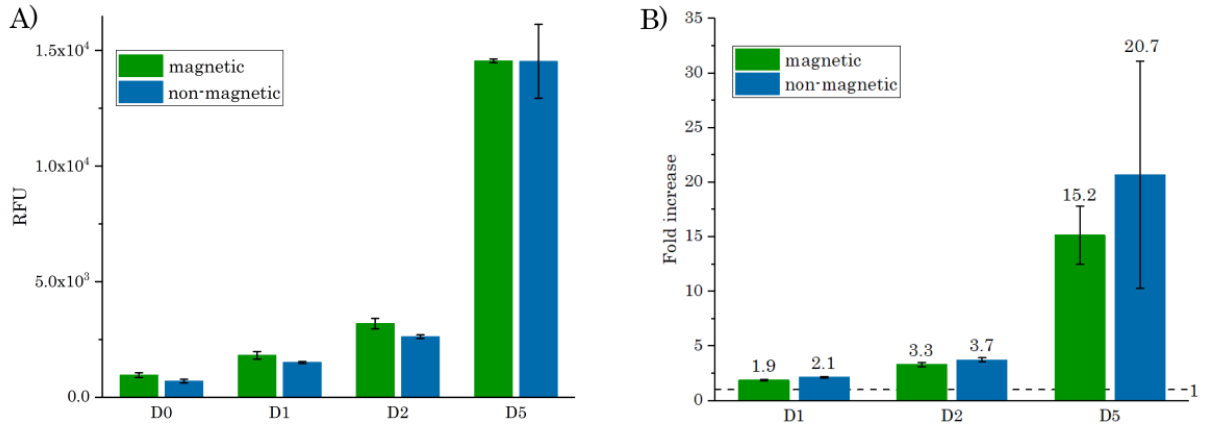

Figure 5.5: Metabolic activity of cells growing on magnetic and non-magnetic MCs at different time points. A) Metabolic activity expressed as fluorescence emission intensity measured in RFU. B) Fold increase of the metabolic activity calculated by normalizing the emission values by the emission value at D0, which is represented by the dashed line.

The metabolic activity of cells growing on both kinds of MCs showed an increasing trend throughout time, as can be seen in Figure 5.5 A and B, suggesting that cells grew and proliferated. For all the evaluated time points, cells growing on magnetic and non-magnetic MCs had similar values of metabolic activity. Specifically on D5, both groups reached a RFU value close to 14,000. Moreover, both groups reached high values of fold increase: 15.2 $\pm$ 2.7 for cells growing on magnetic MCs and 20.7 $\pm$ 10.4 for cells growing on non-magnetic MCs, as can be seen in Figure 5.5 B.

Thanks to the obtained results on cell viability and metabolic activity, some comments on cell attachment can be done. The presence of cells on the MCs on D0 proves that there is a good cell attachment to the MCs surface for both types of MCs. This supports the fact that the biopolymer coating deposited on MCs is efficient to obtain cell adhesion onto MCs. In order to evaluate if the cell attachment on magnetic and non-magnetic MCs is comparable, a one-tailed t-test was performed to compare the metabolic activity of cells at D0 on the two kinds of MCs. The working principle of t-test is explained in Section 3.4.4. This test and all the following ones were performed with an α value of 0.05.

The t-test indicates that the cells on magnetic MCs have a statistically higher metabolic activity than the ones on non-magnetic MCs on D0. This proves that there is a statistical probability that cells adhered onto magnetic MCs more than onto non-magnetic MCs. The results obtained and the relative P value are reported in Table 5.1.

Emission intensities		Accepted hypothesis	P value
Magnetic	Non-magnetic		
959$\pm$103	702$\pm$77	H_1	0.015

Table 5.1: Results of the one-tailed t-test performed to compare cell attachment on magnetic and non-magnetic MCs on D0.

Moreover, some evaluations can be made on cell proliferation. The evolution of the

Life/Dead assay images suggested a good cell proliferation and showed that, on D5, cells growing on both types of MCs reached cell confluency. Also the metabolic activity results suggest a good cell proliferation, as both groups reached a high metabolic activity and high fold increases (15.2 for the magnetic and 20.7 for the non-magnetic) on D5.

A two-tailed t-test was performed to compare the metabolic activity of cells growing on magnetic MCs and cells growing on non-magnetic MCs on the last day of the experiment. The test indicated that the two groups are statistically equivalent and the results are summarized in Table 5.2. This proves that the cell proliferation on magnetic and non-magnetic MCs is statistically equivalent with a confidence level higher than 95%.

Emission intensities		Accepted hypothesis	P value
Magnetic	Non-magnetic		
14551 ± 76	14530 ± 1601	H_0	0.984

Table 5.2: Results of the t-test performed to compare cell proliferation on magnetic and non-magnetic MCs on D5.

In conclusion, it can be stated that both cell attachment and cell proliferation are successful on both kinds of MCs and that the performance of the magnetic MCs regarding these two parameters are comparable to the ones of non-magnetic MCs.

5.2 Cytotoxicity of microcarriers

As mentioned in section 4.3, the magnetic MCs release small amounts of iron in solution. This release might inhibit and/or influence cell growth [131, 140].
The aim of the cytotoxicity assay was to assess whether the magnetic MCs were cytotoxic for the cells. Only one cytotoxicity test was performed. It was impossible to perform this test multiple times, as was planned, due the restricted access to the laboratory according to the lockdown measures adopted by UCLouvain during the COVID-19 pandemic. The cytotoxicity test was conducted in direct contact conditions, *i.e.* the materials were placed directly on the cells. The materials tested were magnetic and non-magnetic MCs at a concentration of 1 or 2 mg/well, and the controls used were cells incubated with Triton X (positive control) and cells alone (negative control). Cell morphology and cell metabolic activity were evaluated, after 24h and 48h of incubation. Section 3.4.3 can be consulted for further details on the procedure.

In order to evaluate cell morphology, cells incubated with materials and controls were imaged with an optical microscope in phase contrast and/or bright field. The obtained images are shown in Figures 5.6-5.10.
No images of the cells intended as positive control (in contact with Triton X) are shown, because they were considered not relevant for the discussion. However, these images are reported in the Appendix A.

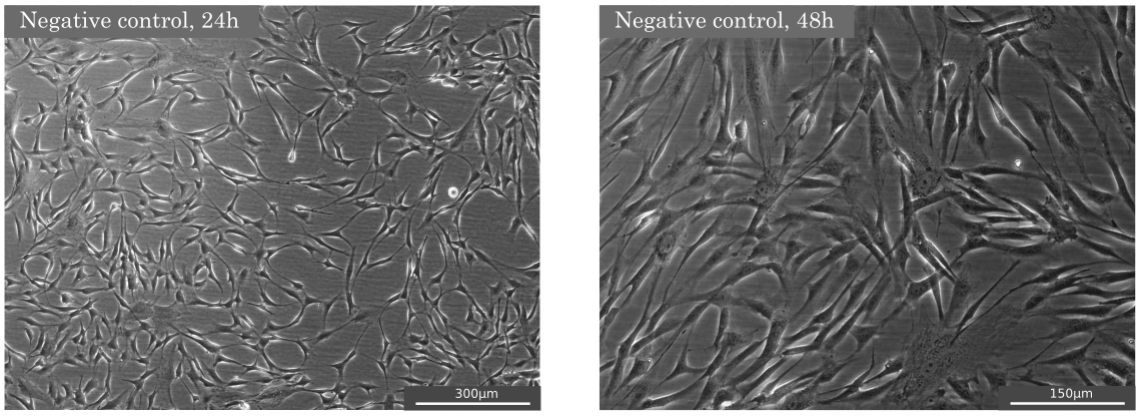

Figure 5.6: Optical microscopy images of cells meant as negative control after 24h (left) and 48h (right) of incubation.

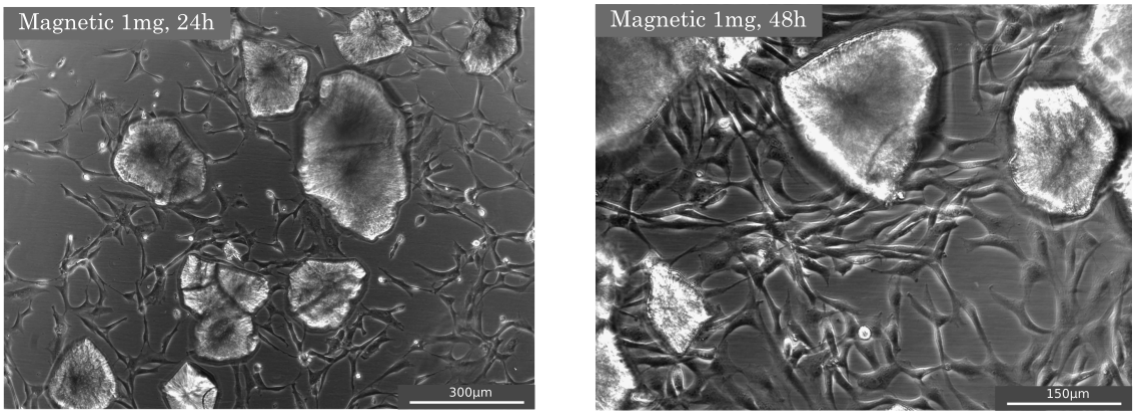

Figure 5.7: Optical microscopy images of cells incubated with 1 mg of magnetic MCs after 24h (left) and 48h (right) of incubation.

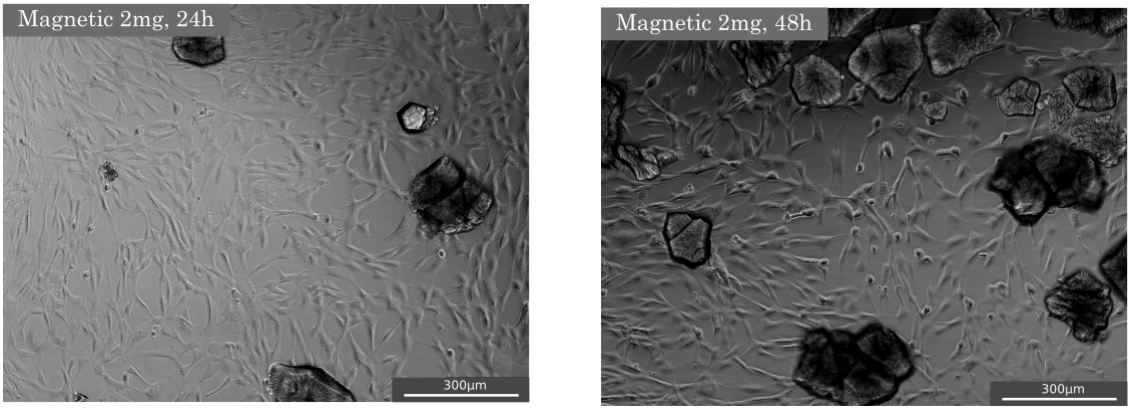

Figure 5.8: Optical microscopy images of cells incubated with 2 mg of magnetic MCs after 24h (left) and 48h (right) of incubation.

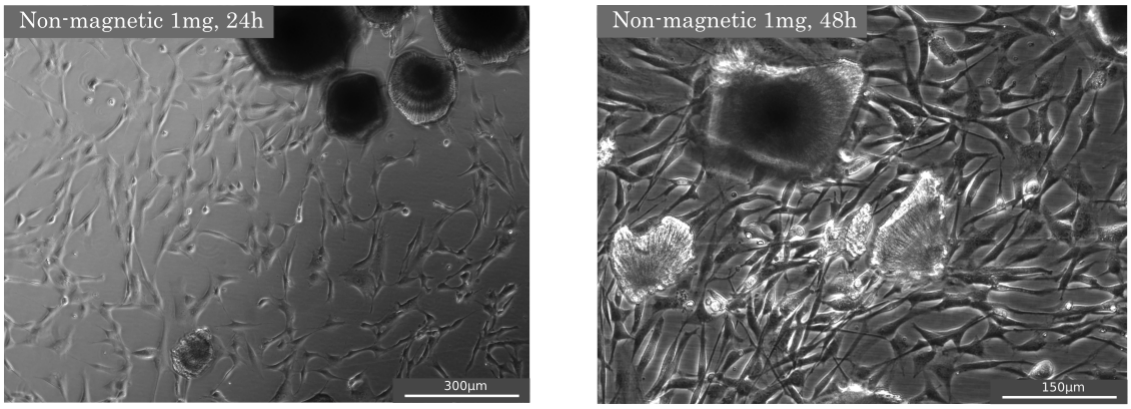

Figure 5.9: Optical microscopy images of cells incubated with 1 mg of non-magnetic MCs after 24h (left) and 48h (right) of incubation.

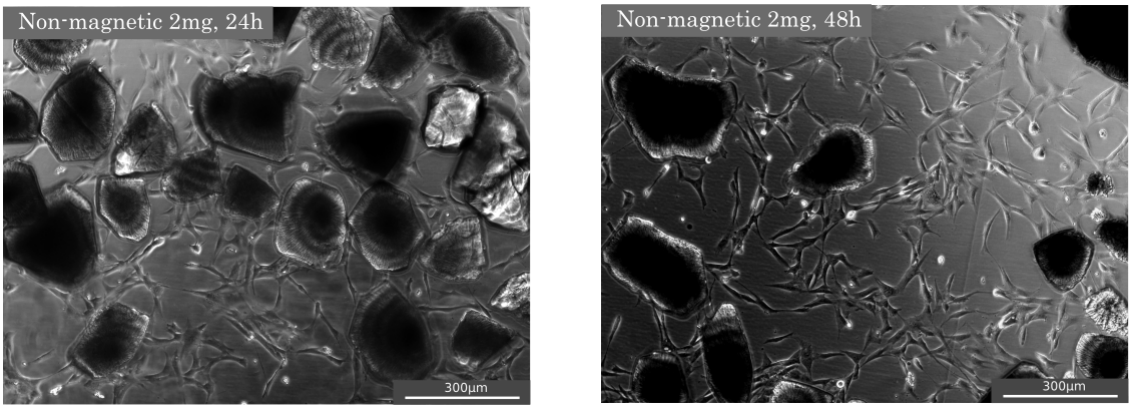

Figure 5.10: Optical microscopy images of cells incubated with 2 mg of non-magnetic MCs after 24h (left) and 48h (right) of incubation.

From Figure 5.6, it can can be noticed that the cells meant as negative control have the elongated morphology that is expected for hASCs growing in 2D conditions, at both incubation periods. From Figures 5.7, 5.8, 5.9 and 5.10, it can be observed that cells in contact with MCs, magnetic and non-magnetic at both incubation periods, overall show a similar morphology to the negative control. Only in a few cases the cells in contact with MCs, magnetic and non-magnetic, exhibit a non-expected rounder shape. This feature can be easily recognized in cells in contact with 1 mg of magnetic MCs (both incubation periods) and 2mg of non-magnetic MCs (both incubation periods) (Figures 5.7 and 5.10). Moreover, sometimes cells in contact with MCs grew non-homogeneously all over the surface. This has been noticed by a more complete observation of the obtained images, some of which are not shown herein, and it was concluded that this phenomenon is happening in all the samples containing MCs. Among the figures shown, this can be noticed in Figures 5.7 (24h incubation), 5.9 (24h incubation) and 5.10 (both incubation periods).
However, generally an increase of the cell number has been noticed from 24h incubation to 48h incubation. This can be seen from all the images previously presented, but it has also been noticed by a more complete observation of all the images obtained. However, it was impossible to count the cells on the recorded images because cells located below MCs

are not visible, thus the obtained results would have been unreliable.

The metabolic activity of cells was evaluated for the different conditions and after different incubation times by PrestoBlue assay.
Cell metabolic activity is expressed as the fluorescence emission intensity measured in RFU. The obtained values are shown in Figure 5.11, for both tested incubation periods. How the metabolic activity values and the errors on these values were computed is described in Section 3.4.3.
Cell metabolic activity is also expressed as percentage with respect to the emission intensity measured for the negative control (cells alone) after the same incubation times. The metabolic activity expressed as percentage is shown in Figure 5.12, for both incubation periods. The errors on cell metabolic activity values expressed as percentages were computed by error propagation.

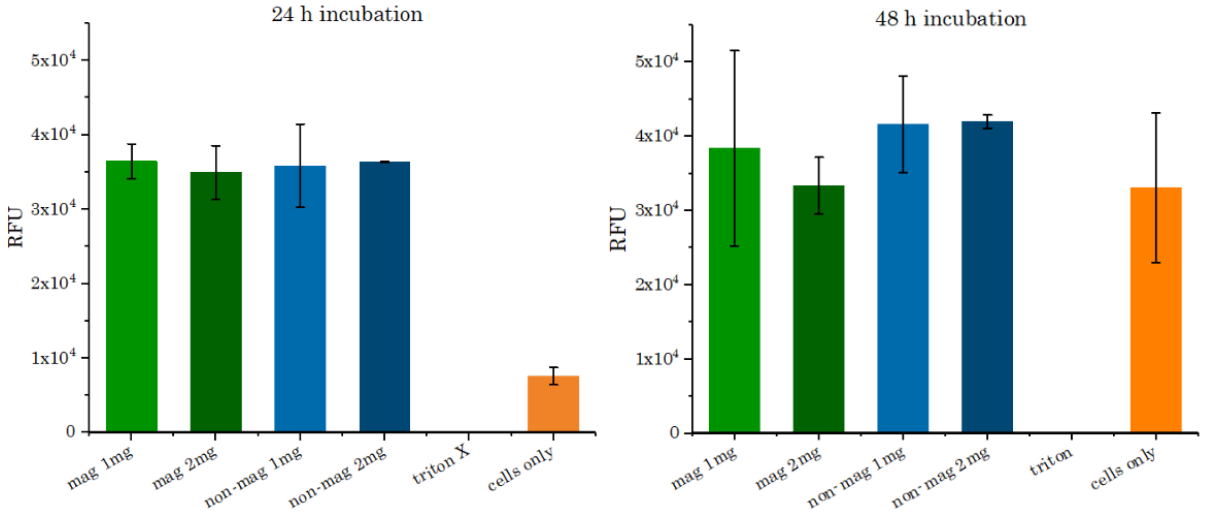

Figure 5.11: Metabolic activity of cells in contact with materials and controls after 24h and 48h of incubation expressed in RFU.

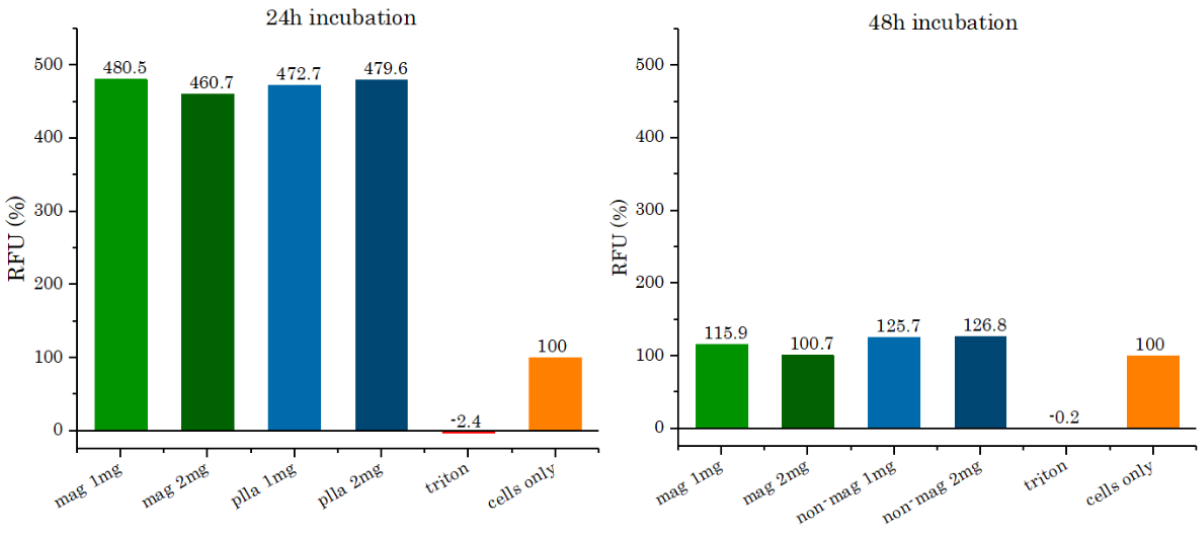

Figure 5.12: Metabolic activity of cells in contact with materials and controls after 24h and 48h of incubation, expressed as percentage of the RFU value of the negative control (cells alone) after the same incubation period.

Throughout the discussion of the results, it should be kept in mind that the metabolic activity is an indicator of the activity of cells: it can be influenced by the environment they have and it cannot be unequivocally correlated to the number of cells.

First, it can be noticed that cells in contact with Triton X show no metabolic activity at both incubation periods, as can be seen in Figure 5.11. On the other hand, cells grown alone, without MCs, show positive metabolic activity at both incubation periods. These observations prove that the chosen controls work. Indeed, the controls are needed to be able to properly evaluate the cytotoxicity of the tested materials. Specifically, a positive control is meant to be a chemical species or material causing a cytotoxic effect on cells, as in the case of reduced cell metabolic activity caused by Triton X. While, on the other hand, a the negative control is meant to be a chemical species or material causing no cytotoxic effect on cells, as in the case of cells growing alone. This conclusion is also supported by the obtained images, in which it can be noticed that cells alone seem healthy and exhibit the expected hASCs morphology (Figure 5.6), while cells in contact with Triton X are dead (Figure reported in the Appendix A).

From both Figures 5.11 and 5.12, it can be clearly noticed that cells in contact with MCs showed a higher metabolic activity than cells alone. For instance, after 24h of incubation, the cells in contact with MCs (magnetic and non-magnetic, in both concentrations) reached values of 460-480% of the metabolic activity of the cells alone (visible in Figure 5.12). After 48h of incubation, this difference between metabolic activity was less visible, but still present: cells in contact with MCs had between 100% and 120% of the metabolic activity of cells alone (in Figure 5.12). One-tailed t-tests confirmed that the metabolic activity of cells in contact with MCs (magnetic and non-magnetic, in both concentration) were statistically larger than the metabolic activity of cells growing alone for both incubation periods. However, the results of these tests are not reported, as these observations can already be clearly recognized as true only by looking at the metabolic activity results shown in Figures 5.11 and 5.12.

Several comments can be done on the evolution of the metabolic activity of the different groups during the two days of experiment. The cells grown without MCs had a metabolic activity of 7,582±1,179 after 24h of incubation and a metabolic activity of 33,128±10,097 after 48h of incubation: a positive trend can be clearly recognized. This can be noticed in Figure 5.11. It can be stated that this increase in the metabolic activity of cells growing alone was probably due to the cell growth, as normally expected.
On the other hand, cells in contact with 1 mg of magnetic MCs had a metabolic activity of 36,434±2,356 after 24h of incubation and a metabolic activity of 38,396 ±13,160 after 48h of incubation. It can be noticed that the metabolic activity of these cells only slightly increased throughout the two days. Similar trends can be recognized in Figure 5.11 for cells growing in contact with 1 and 2 mg of non-magnetic MCs. A particular case is represented by the metabolic activity of cells in contact with 2 mg of magnetic MCs, which slightly decreased over the two days, passing from 34,933±3,632 to 33,370± 3,821.
In general, it can be stated that the metabolic activity of cells in contact with MCs was particularly high at 24h of incubation, but did not significantly increase after 48h of incubation.
The particularly high metabolic activity of cells growing in contact with MCs after 24h incubation, can be explained considering that the addition of MCs to the culture environment could stimulate the metabolic activity of cells. Indeed, the addition of MCs causes an increase in the surface available to cells to migrate and spread. Moreover, the chemical nature and charge of the surface of the MCs are different than the ones of the surface of the well plate. Therefore, these differences can be perceived by cells, which can behave differently in contact with these two surfaces. Overall, these parameters might act as stimulating factors to cells, leading to an increase in their metabolic activity.
The not significantly high values of metabolic activity of cells in contact with MCs after 48h of incubation are probably caused by the cell adjustment to the variation of the environment. It could be affirmed that the presence of the MCs slightly inhibited the cell growth, but this cannot be concluded with certitude as the metabolic activity is not an indicator of the cell number.
Specifically, the metabolic activity of cells in contact with 2 mg of magnetic MCs decreased by 4.5% from 24h to 48h of incubation. This suggests that the presence of such a high concentration of magnetic MCs might have slightly inhibited cell growth. However, this cannot be stated with certitude because the decrease of metabolic activity could be exclusively caused by the adjustment of cells to the addition of the MCs.

The main aim of the cytotoxicity test is to evaluate if the two groups tested (magnetic MCs and non-magnetic MCs) have a statistically equivalent effect on cell behaviour or not. In order to compare the groups, two-tails t-tests with a significance level of 0.05 were performed.
The metabolic activity of cells in contact with 1 mg of magnetic MCs was compared to the one of cells in contact with 1 mg of non-magnetic MCs and the same for the two groups in concentration 2 mg of MCs/well. The results of the performed tests are reported in Tables 5.3 and 5.4, for 24h incubation and 48h incubation, respectively. The tests indicated that the groups are statistically equivalent in all the cases considered.

24 h incubation			
Emission intensities		Accepted hypothesis	P value
Magnetic 1 mg 36434.3± 2355.9	Non-magnetic 1 mg 35843.8 ±5577.8	H_0	0.877
Magnetic 2 mg 34933.1±3632.3	Non-magnetic 2 mg 36368.2±62.2	H_0	0.564

Table 5.3: Emission values of the samples after 24 h incubation and P values related to the comparison between the two groups, *i.e.* magnetic and non-magnetic MCs.

48 h incubation			
Emission intensities		Accepted hypothesis	P value
Magnetic 1 mg 38396.1±13159.7	Non-magnetic 1 mg 41638.5±6449.6	H_0	0.727
Magnetic 2 mg 33369.5±3820.9	Non-magnetic 2 mg 42000.5± 873.4	H_0	0.053

Table 5.4: Emission values of the samples after 48 h incubation and P values related to the comparison between the two groups, *i.e.* magnetic and non-magnetic MCs.

Because a P value of 0.053 was obtained in the comparison between cells in contact with 2 mg of magnetic MCs and 2mg of non-magnetic MCs after 48h of incubation, it has been decided to perform also a one-tailed t-test to compare the groups. The formulated hypotheses are: H_0, stating that the two groups are statistically equivalent, and H_1, stating that the group of 2 mg non-magnetic MCs has a statistically higher metabolic activity than the group 2 mg magnetic. Finally, the one-tailed test rejected H_0. The results are summarized in Table 5.5.

48 h incubation			
Emission intensities		Accepted hypothesis	P value
Magnetic 2 mg 33369.5±3820.9	Non-magnetic 2 mg 42000.5± 873.4	H_1	0.026

Table 5.5: Emission values of the samples after 48 h incubation and P values related to the comparison between the two groups, *i.e.* magnetic and non-magnetic MCs.

To summarize, in all cases evaluated with a two-tailed t-test, the two groups are statisticaly equivalent, stating, thus, the statistical equivalence between the metabolic activity of cells in contact with magnetic and non-magnetic MCs. A particular case is represented by the comparison between cells in contact with magnetic and non-magnetic MCs at a concentration of 2 mg/well after 48h of incubation, for which the one-tailed test rejected the statistical equivalence.

To conclude, it can be stated that the cytotoxicity test was successful. Overall, the cells in contact with MCs showed the expected cell morphology and cell growth measured from metabolic activity was not significantly inhibited by the presence of MCs. Moreover, the metabolic activity of cells growing in contact with magnetic and non-magnetic MCs, at both concentrations, was higher than cells alone for both incubation period. Thus, there is no evidence of cytotoxic effect on cells caused by the presence of the MCs.
The statistical equivalence between the metabolic activity of cells in contact with magnetic and non-magnetic MCs was affirmed by two-tailed t-tests. Therefore, it can be stated that the behaviour of cells in contact with magnetic and non-magnetic MCs is equivalent, at both concentrations of MCs and for both incubation periods. An exception is represented by the behaviour of cells in contact with magnetic and non-magnetic MCs at a concentration of 2 mg/well after 48h of incubation.

In conclusion, this test was the first step of the investigation on the effect of MCs on hACSs behavior. However, this experiment, being the only cytotoxicity test performed in this thesis, is not conclusive. In order to definitely conclude regarding the effect of MCs on cell behavior, the cytotoxicity test has to be repeated multiple times.
Moreover, it would be interesting to perform cytotoxicity tests in indirect contact conditions, in which the materials tested are placed in the wells where cells grow, but not in direct contact. Thanks to the different experimental conditions, these tests could provide additional and different information on the effect of MCs on the cell behaviour.

Conclusions

Summary of the main results

This master thesis aimed to fabricate magnetic MCs, characterize them and study the cellular response of hASCs to these MCs employed as cell culture substrate in semistatic culture conditions. The specifications of these MCs were designed for a future application as culture substrate for dynamic culture.

First, the MCs were fabricated with a biopolymer (PLLA) by an organic-solvent-free strategy. Magnetic and non-magnetic versions of the MCs were produced. The magnetic properties of MCs were achieved by incorporation of superparamagnetic iron oxide NPs in the MC core. The MCs were coated with a biofunctionalized coating consisting in a PEM exposing RGD peptide sequences for enhanced cell adhesion.

The MCs were characterized in order to asses their magnetic properties, stability, morphology and NP incorporation rate. The iron content of the magnetic MCs was evaluated by ICP-AES analysis, concluding on a 56% NP incorporation rate in the MCs. The stability of the MCs was investigated by measuring the amount of iron released in DPBS solution after storage for 12 days under agitation at 37°C. It was concluded that only a minimal percentage of the iron incorporated in the MCs (0.4%) is released after 12 days. The magnetic properties of the magnetic MCs were investigated by analysis with AGM. It was concluded that magnetic MCs exhibit a superparamagnetic behaviour, as expected, and no significant evidence of ferromagnetic behaviour was detected, proving the absence of agglomerates of NPs in the MC matrix. The results obtained from the AGM analysis were coherent with the results obtained from a qualitative evaluation of the magnetic properties of magnetic MCs. This analysis consisted in recording the response of magnetic MCs suspended in water to an applied magnetic field. Both these characterization strategies showed that a magnetic field (H) on the order of magnitude of $1.4 \cdot 10^4$ Oe was sufficient to saturate the magnetization of the MCs and to submit them to a magnetic force which could move them in water solution.
Morphology, size distribution and surface porosity of both kinds of MCs (magnetic and non-magnetic) were studied. It was concluded that the two groups exhibit comparable features concerning these parameters.

The final step of this work consisted in studying the cellular response of hASCs to magnetic MCs in semistatic culture conditions. Cell attachment and proliferation of hASCs on magnetic MCs were investigated conducting a routine cell culture in semistatic conditions for 6 days and using non-magnetic MCs as control. The viability and metabolic activity of cells growing on the surface of MCs were evaluated, indicating that hASCs attachment and proliferation on magnetic and non-magnetic MCs were comparable and statistically

equal with a confidence level of 95%.
Additionally, one test to assess the cytotoxic effect of MCs on hASCs was performed in direct contact conditions by evaluation of the cell morphology and metabolic activity. It was observed that both magnetic and non magnetic MCs do not cause any cytotoxic effect to hASCs. However, before being able to conclude this with certitude, this test should be repeated multiple times.

Overall, the scope of the project was achieved proving that the magnetic MCs produced are suited for cell culture of hASCs in semistatic condition. This represents the first step towards a possible application of these MCs as cell culture substrate in dynamic culture.

Future perspectives

Many positive results were obtained in this project. However, several points regarding the characterization of the MCs and the study of the cellular response to MCs could be deepened or improved.

Regarding the characterization, we did not manage to properly characterize the coating of the MCs by SEM observation. This could be performed in the future by adopting a different sample preparation procedure. Moreover, many strategies could be employed to characterize mechanical properties and porosity (surface and internal) of the MCs.

Regarding cell attachment and proliferation, both kinds of MCs exhibited good performance as cell-culture substrate. Nevertheless, the fold increases reachable with these MCs (15-20 fold increase) are still lower than the fold increase obtained in planar culture conditions (30-35 fold increase). Therefore, the specifications of the MCs such as RGD functionalization, surface coating and mechanical properties of the surface could be improved to reach higher production yields.

Because of the measures adapted to prevent the spreading of Coronavirus and the anticipated closure of the research labs, it was impossible to repeat an adequate number of times the cytotoxicity assay in direct contact conditions. Therefore, it is necessary to repeat this experiment to obtain more accurate results and to better understand the causes of the unexpected results regarding the metabolic activity of cells in contact with MCs. Additionally, a cytotoxicity test in indirect conditions could be performed to investigate whether the direct contact between cells and MCs has any influence on cell behaviour.

Appendix A

Supporting information

A.1 SEM observations of coated microcarriers

As mentioned in Section 4.4, some coated MCs have been observed by SEM with the aim of evaluating the influence of the coating on the porosity and roughness of the MCs. The observed MCs were non-magnetic MCs coated with the biofunctionalized coating, which was fabricated as described in Section 3.2.2. However, the sample preparation procedure, caused the drying and shrinking of the coating deposited on these MCs. Therefore, it was impossible to conclude anything on the properties of the coating. The shrunk coating formed round agglomerates on the surface, which are clearly visible in Figure A.1 A and, at a higher magnification, in Figure A.1B.

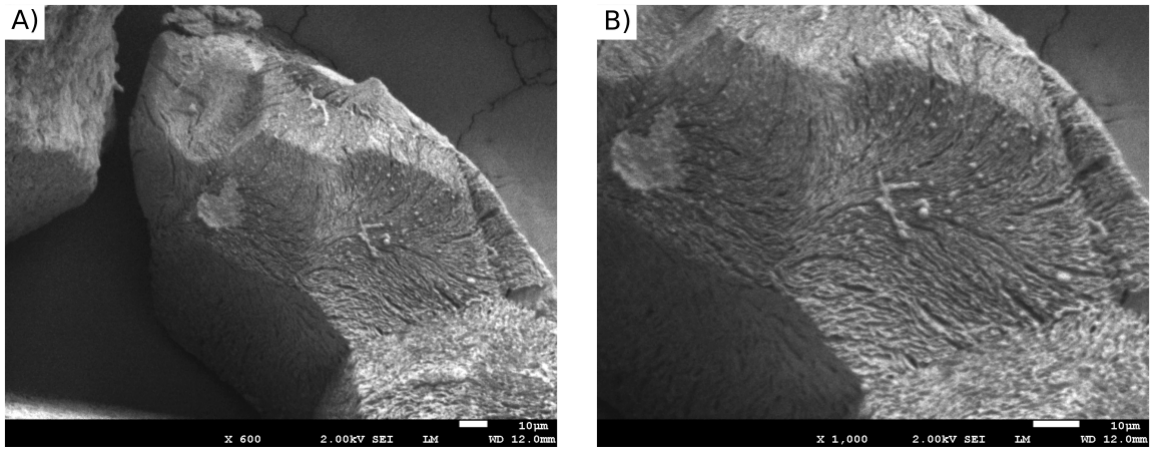

Figure A.1: SEM observation of the surface coating of non-magnetic MCs, showing the coating shrinkage. A) Magnification X 600. B) Magnification X 1,000.

A.2 Cell imaging for cytotoxicity test

In the framework of the study of the cellular response to MCs, a test to evaluate the cytotoxicity effect of MCs on cells in direct contact conditions was performed. In order to evaluate the cell morphology after 24h and 48h of incubation, cells were imaged by optical microscopy in phase contrast and bright field mode, after 24h and 48h of incubation. As a reminder, cells were growing in contact with magnetic and non-magnetic MCs, at two different concentrations (1 and 2 mg/well). Moreover, cells growing alone and cells

incubated with Triton X were used as negative and positive controls, respectively. For simplicity, only a few of the images recorded are reported in Section 5.2. Thus, some additional images are reported herein.
First, in Figure A.2 the cells meant as positive control (in contact with Triton X) are shown, for both incubation periods. It can be noticed that for both incubation periods the cells are death. This proves that Triton X is an adequate chemical species to be employed as positive control, as explained in 5.2.

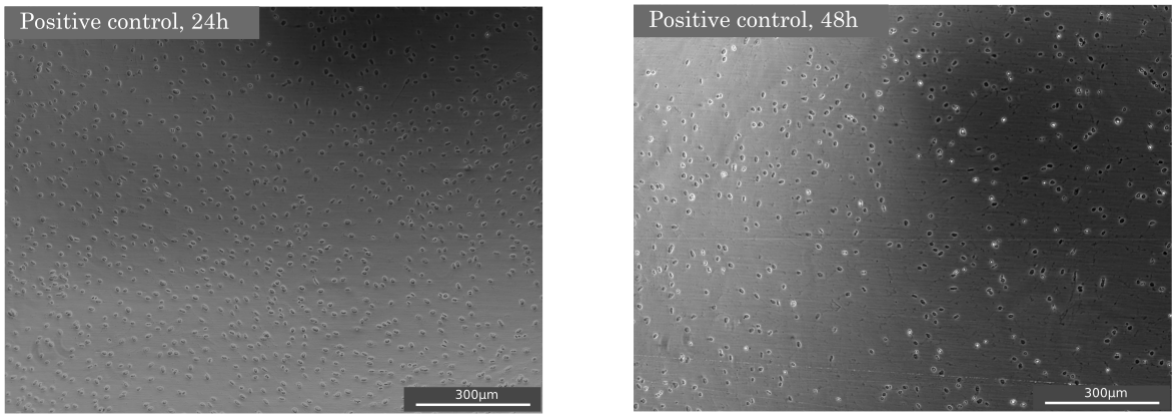

Figure A.2: Optical microscopy images of cells meant as positive control after 24h (left) and 48h (right) of incubation.

Additional images of the cells meant as negative control at both incubation periods are shown in Figure A.3.

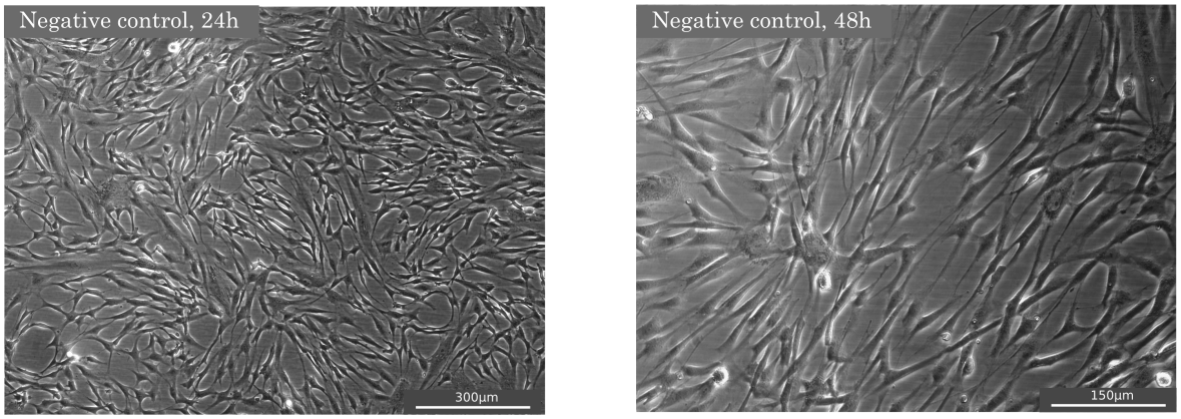

Figure A.3: Optical microscopy images of cells meant as positive control after 24h (left) and 48h (right) of incubation.

The following images show cells in contact with magnetic and non-magnetic MCs at concentrations 1 and 2 mg/well after 24h and 48h of incubation.

In Section 5.2, it was mentioned that cells in contact with MCs sometimes grew non-homogeneously on the surface of the adhesion well plates. In the images reported here, the zones of the substrate less populated by cells are pointed by red arrows. This phenomenon

was observed for both kinds of MCs, at both concentration and after both incubation periods.

Only in one case it was clearly recognizable the presence of cells growing on MCs. This was the case of cells in contact with 1 mg of magnetic MCs after 48h of incubation. The cells growing on the MCs are pointed out by green arrows in Figure A.6A.

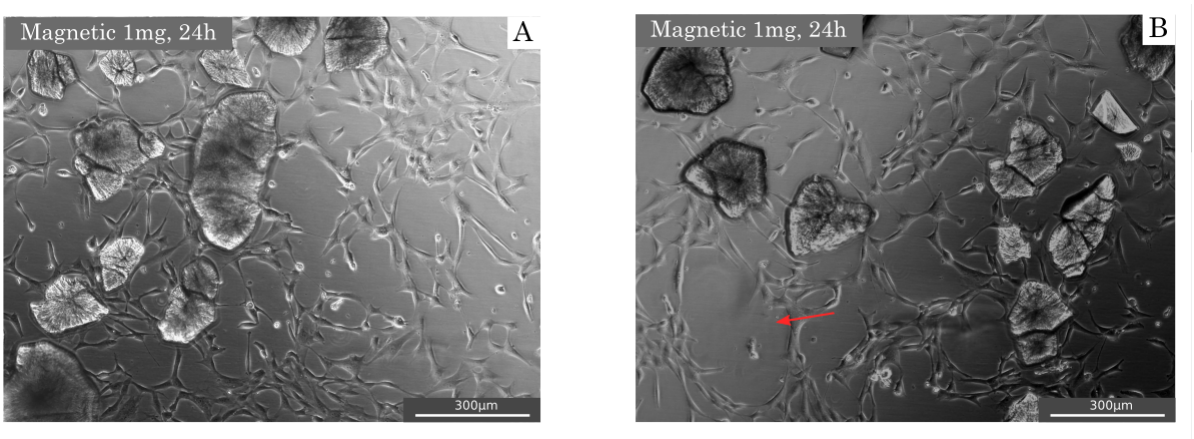

Figure A.4: Optical microscopy images of cells growing in contact with 1 mg of magnetic MCs after 24h of incubation. The red arrow in image (B) points at a zone less populated by cells.

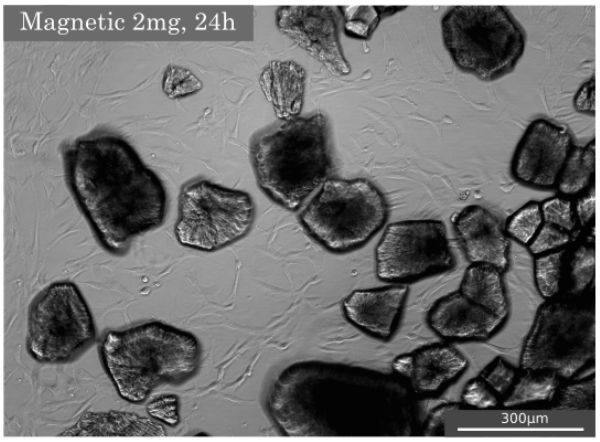

Figure A.5: Optical microscopy image of cells growing in contact with 2 mg of magnetic MCs after 24h of incubation.

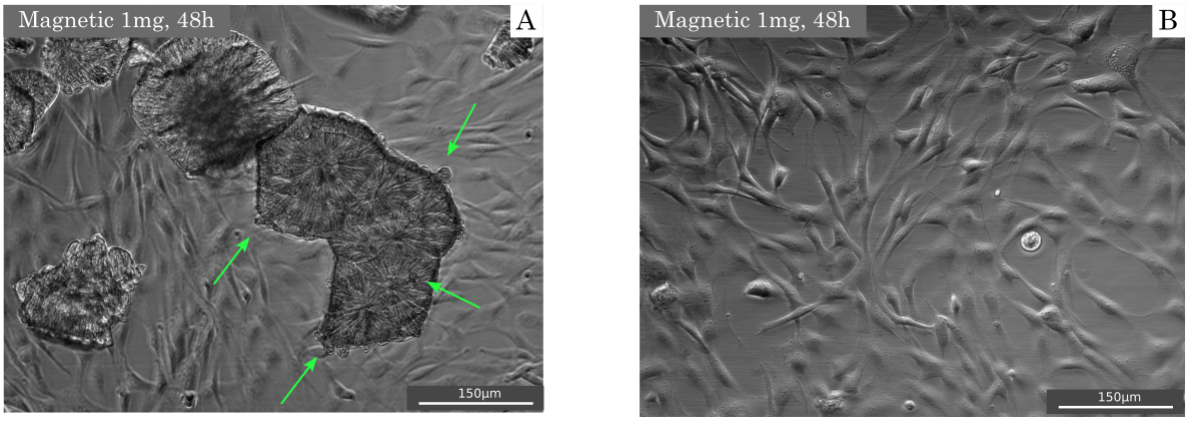

Figure A.6: Optical microscopy images of cells growing in contact with 1 mg of magnetic MCs after 48h of incubation. The green arrows in image (A) point at cells growing on the surface of a MC.

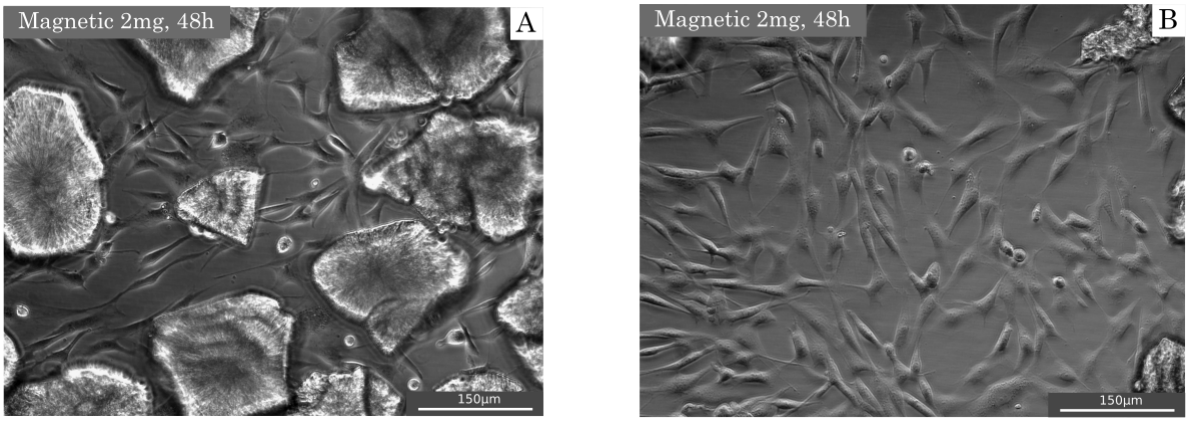

Figure A.7: Optical microscopy images of cells growing in contact with 2 mg of magnetic MCs after 48h of incubation.

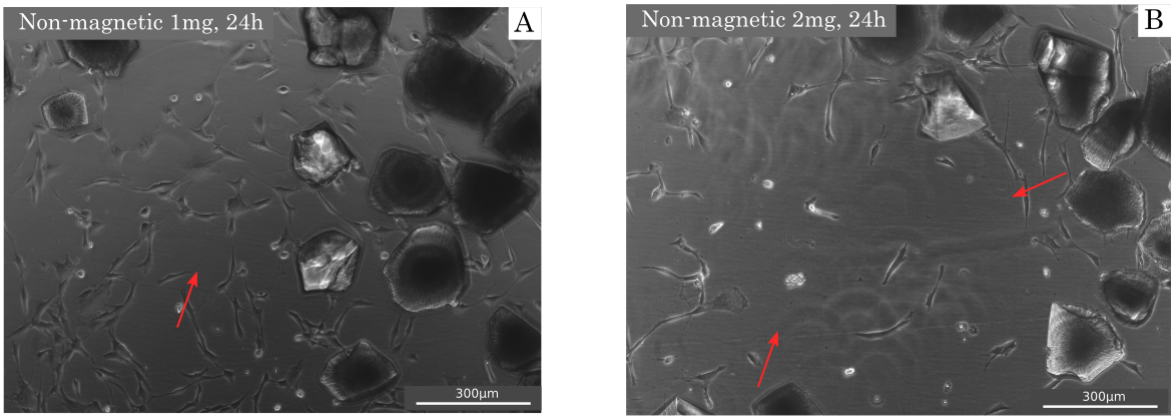

Figure A.8: Optical microscopy images of cells growing in contact with 1 mg of non-magnetic MCs (A) and 2 mg of non-magnetic MCs (B) after 24h of incubation. The red arrows in both images point at zones less populated by cells.

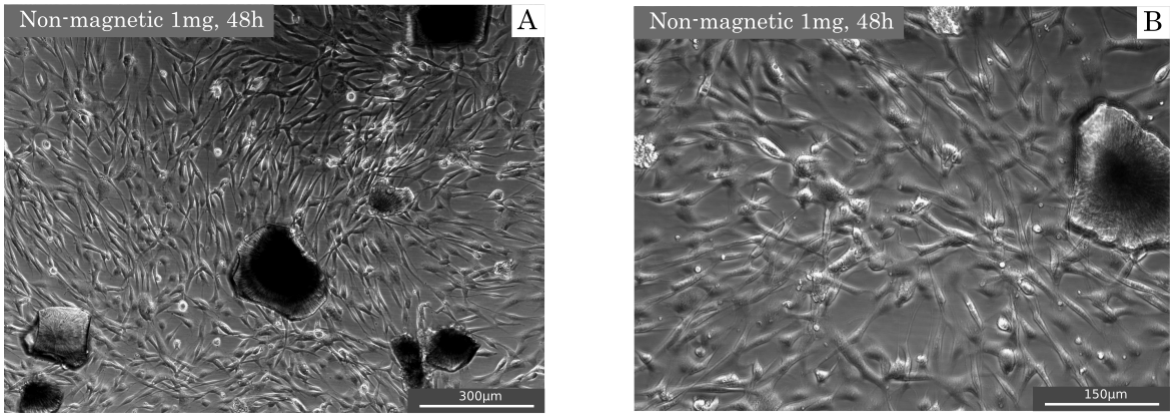

Figure A.9: Optical microscopy images of cells growing in contact with 1 mg of non-magnetic MCs after 48h of incubation.

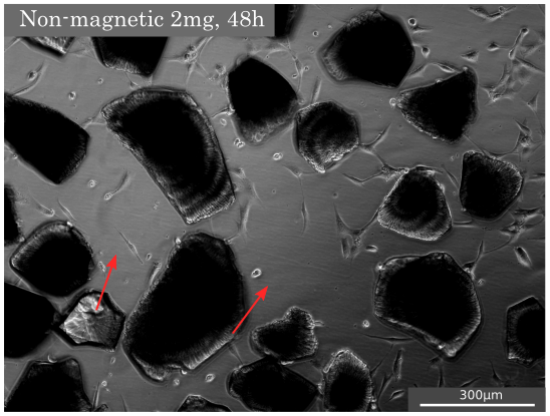

Figure A.10: Optical microscopy images of cells growing in contact with 2 mg of non-magnetic MCs after 48h of incubation. The red arrows point at zones less populated by cells.

Bibliography

[1] Q. A. Rafiq, K. Coopman, and C. J. Hewitt, "Scale-up of human mesenchymal stem cell culture: Current technologies and future challenges", *Current Opinion in Chemical Engineering*, vol. 2, no. 1, pp. 8 –16, 2013, ISSN: 2211-3398. DOI: https://doi.org/10.1016/j.coche.2013.01.005. [Online]. Available: http://www.sciencedirect.com/science/article/pii/S2211339813000063.

[2] C. Argentati, F. Morena, M. Bazzucchi, I. Armentano, C. Emiliani, and S. Martino, "Adipose stem cell translational applications: From bench-to-bedside", *International Journal of Molecular Sciences*, vol. 19, p. 3475, Nov. 2018. DOI: 10.3390/ijms19113475.

[3] K. P. Robb, J. C. Fitzgerald, F. Barry, and S. Visawanathan, "Mesenchymal stromal cell therapy: Progress in manufacturing and assessments of potency", *Cytotherapy*, vol. 21, no. 3, pp. 289 –306, 2019, ISSN: 1465-3249. DOI: https://doi.org/10.1016/j.jcyt.2018.10.014. [Online]. Available: http://www.sciencedirect.com/science/article/pii/S1465324918306753.

[4] D. W. Levine, D. I. C. Wang, and W. G. Thilly, "Optimization of growth surface parameters in microcarrier cell culture", *Biotechnology and Bioengineering*, vol. 21, no. 5, pp. 821–845, 1979. DOI: 10.1002/bit.260210507. [Online]. Available: https://onlinelibrary.wiley.com/doi/abs/10.1002/bit.260210507.

[5] V. Jossen, C. van den Bos, R. Eibl, and D. Eibl, "Manufacturing human mesenchymal stem cells at clinical scale: process and regulatory challenges", *Applied Microbiology and Biotechnology*, vol. 102, no. 9, pp. 3981–3994, 2018, ISSN: 14320614. DOI: 10.1007/s00253-018-8912-x.

[6] X. Y. Chen, J. Y. Chen, X. M. Tong, J. G. Mei, Y. F. Chen, and X. Z. Mou, "Recent advances in the use of microcarriers for cell cultures and their ex vivo and in vivo applications", *Biotechnology Letters*, vol. 42, no. 1, pp. 1–10, 2020, ISSN: 15736776. DOI: 10.1007/s10529-019-02738-7. [Online]. Available: https://doi.org/10.1007/s10529-019-02738-7.

[7] M. Lim, W. Ong, and S. Sugii, "The current landscape of adipose-derived stem cells in clinical applications", *Expert Reviews in Molecular Medicine*, vol. 16, 2014. DOI: 10.1017/erm.2014.8. [Online]. Available: https://www.scopus.com/inward/record.uri?eid=2-s2.0-84906931889&doi=10.1017\%2ferm.2014.8&partnerID=40&md5=0b4c337773e5e7c6b73dbdf91da325ae.

[8] U. Sahin, S. K. Toprak, P. A. Atilla, E. Atilla, and T. Demirer, "An overview of infectious complications after allogeneic hematopoietic stem cell transplantation", *Journal of Infection and Chemotherapy*, vol. 22, no. 8, pp. 505–514, 2016, ISSN: 14377780. DOI: 10.1016/j.jiac.2016.05.006. [Online]. Available: http://dx.doi.org/10.1016/j.jiac.2016.05.006.

[9] G. Pachón-Peña, G. Yu, A. Tucker, X. Wu, J. Vendrell, B. Bunnell, and J. Gimble, "Stromal stem cells from adipose tissue and bone marrow of age-matched female donors display distinct immunophenotypic profiles", *Journal of Cellular Physiology*, vol. 226, no. 3, pp. 843–851, 2011. DOI: 10.1002/jcp.22408. [Online]. Available: https://onlinelibrary.wiley.com/doi/abs/10.1002/jcp.22408.

[10] E. H. Ntege, H. Sunami, and Y. Shimizu, "Advances in regenerative therapy: A review of the literature and future directions", *Regenerative Therapy*, vol. 14, pp. 136–153, 2020, ISSN: 23523204. DOI: 10.1016/j.reth.2020.01.004. [Online]. Available: https://doi.org/10.1016/j.reth.2020.01.004.

[11] G. J. Cabrita, B. S. Ferreira, C. L. da Silvia, R. Gonçalves, G. Almeida-Porada, and J. M. Cabral, "Hematopoietic stem cells: From the bone to the bioreactor", *Trends in Biotechnology*, vol. 21, no. 5, pp. 233 –240, 2003, ISSN: 0167-7799. DOI: https://doi.org/10.1016/S0167-7799(03)00076-3. [Online]. Available: http://www.sciencedirect.com/science/article/pii/S0167779903000763.

[12] A. K.-L. Chen, S. Reuveny, and S. K. W. Oh, "Application of human mesenchymal and pluripotent stem cell microcarrier cultures in cellular therapy: Achievements and future direction", *Biotechnology Advances*, vol. 31, no. 7, pp. 1032 –1046, 2013, ISSN: 0734-9750. DOI: https://doi.org/10.1016/j.biotechadv.2013.03.006. [Online]. Available: http://www.sciencedirect.com/science/article/pii/S0734975013000657.

[13] A. M. de Soure, A. Fernandes-Platzgummer, C. L. da Silvia, and J. M. Cabral, "Scalable microcarrier-based manufacturing of mesenchymal stem/stromal cells", *Journal of Biotechnology*, vol. 236, pp. 88 –109, 2016, ISSN: 0168-1656. DOI: https://doi.org/10.1016/j.jbiotec.2016.08.007. [Online]. Available: http://www.sciencedirect.com/science/article/pii/S0168165616314559.

[14] S. Sart, S. N. Agathos, and Y. Li, "Engineering stem cell fate with biochemical and biomechanical properties of microcarriers", *Biotechnology Progress*, vol. 29, no. 6, pp. 1354–1366, 2013, ISSN: 87567938. DOI: 10.1002/btpr.1825.

[15] S. E. Williams, S. Beronja, H. A. Pasolli, and E. Fuchs, "Asymmetric cell divisions promote Notch-dependent epidermal differentiation", *Nature*, vol. 470, no. 7334, pp. 353–358, 2011, ISSN: 00280836. DOI: 10.1038/nature09793.

[16] National Institutes of Health. (2020). Stem cells basics, [Online]. Available: https://stemcells.nih.gov/info/basics/1.htm (visited on 05/04/2020).

[17] D. Ilic and J. M. Polak, "Stem cells in regenerative medicine: introduction", *British Medical Bulletin*, vol. 98, no. 1, pp. 117–126, May 2011, ISSN: 0007-1420. DOI: 10.1093/bmb/ldr012. [Online]. Available: https://doi.org/10.1093/bmb/ldr012.

[18] K. Takahashi and S. Yamanaka, "Induction of Pluripotent Stem Cells from Mouse Embryonic and Adult Fibroblast Cultures by Defined Factors", *Cell*, vol. 126, no. 4, pp. 663–676, 2006, ISSN: 00928674. DOI: 10.1016/j.cell.2006.07.024.

[19] L. Yiangou, A. D. Ross, K. J. Goh, and L. Vallier, "Human pluripotent stem cell-derived endoderm for modeling development and clinical applications", *Cell Stem Cell*, vol. 22, no. 4, pp. 485 –499, 2018, ISSN: 1934-5909. DOI: https://doi.org/10.1016/j.stem.2018.03.016. [Online]. Available: http://www.sciencedirect.com/science/article/pii/S193459091830122X.

[20] D. Sipp, "Challenges in the clinical application of induced pluripotent stem cells", *Stem Cell Research and Therapy*, vol. 1, no. 1, 2010. DOI: 10.1186/scrt9. [Online]. Available: https://www.scopus.com/inward/record.uri?eid=2-s2.0-79956260690&doi=10.1186\%2fscrt9&partnerID=40&md5=be5b6646c34e4247ead70fcd5529082a.

[21] Stem cells Institute of Los Angeles. (2020). Adult stromatic stem cells, [Online]. Available: https://drstemcell.com/stem-cell-therapy/adult-somatic-stem-cells/ (visited on 05/12/2020).

[22] M. Dominici, K. le, I Mueller, I. Slaper-Cortenbach, F. Marini, D. Krause, R. Deans, A Keating, D. Prockop, and E. Horwitz, "Minimal criteria for defining multipotent mesenchymal stromal cells. the international society for cellular therapy position statement. cytotherapy 8: 315-317", *Cytotherapy*, vol. 8, pp. 315–7, Feb. 2006. DOI: 10.1080/14653240600855905.

[23] A. I. Caplan, "Adult mesenchymal stem cells for tissue engineering versus regenerative medicine", *Journal of Cellular Physiology*, vol. 213, no. 2, pp. 341–347, 2007. DOI: 10.1002/jcp.21200. [Online]. Available: https://onlinelibrary.wiley.com/doi/abs/10.1002/jcp.21200.

[24] A. Bajek, N. Gurtowska, J. Olkowska, L. Kazmierski, M. Maj, and T. Drewa, "Adipose-derived stem cells as a tool in cell-based therapies", *Archivum Immunologiae et Therapiae Experimentalis*, vol. 64, no. 6, pp. 443–454, 2016. DOI: 10.1007/s00005-016-0394-x. [Online]. Available: https://www.scopus.com/inward/record.uri?eid=2-s2.0-84968538165&doi=10.1007\%2fs00005-016-0394-x&partnerID=40&md5=b44e4005970ce753e88ea403df884e2e.

[25] S. Sharath, J. Ramu, S. Nair, S. Iyer, U. Mony, and J. Rangasamy, "Human adipose tissue derivatives as a potent native biomaterial for tissue regenerative therapies", *Tissue Engineering and Regenerative Medicine*, vol. 17, Jan. 2020. DOI: 10.1007/s13770-019-00230-x.

[26] W. Ong and S. Sugii, "Adipose-derived stem cells: Fatty potentials for therapy", *International Journal of Biochemistry and Cell Biology*, vol. 45, no. 6, pp. 1083–1086, 2013. DOI: 10.1016/j.biocel.2013.02.013. [Online]. Available: https://www.scopus.com/inward/record.uri?eid=2-s2.0-84876464760&doi=10.1016\%2fj.biocel.2013.02.013&partnerID=40&md5=99e2777968f615ffc994eebf2571dcb9.

[27] N. Sharpless and R. DePinho, "How stem cells age and why this makes us grow old", *Nature Reviews Molecular Cell Biology*, vol. 8, no. 9, pp. 703–713, 2007. DOI: 10.1038/nrm2241. [Online]. Available: https://www.scopus.com/inward/record.uri?eid=2-s2.0-34548153747&doi=10.1038\%2fnrm2241&partnerID=40&md5=599b5aa9a182de3f2cbf2a123a43ef8a.

[28] V. Van Harmelen, K. Röhrig, and H. Hauner, "Comparison of proliferation and differentiation capacity of human adipocyte precursor cells from the omental and subcutaneous adipose tissue depot of obese subjects", *Metabolism: Clinical and Experimental*, vol. 53, no. 5, pp. 632–637, 2004. DOI: 10.1016/j.metabol.2003.11.012. [Online]. Available: https://www.scopus.com/inward/record.uri?eid=2-s2.0-2342644142&doi=10.1016\%2fj.metabol.2003.11.012&partnerID=40&md5=bfba638a6f0e71079ccbf8370fcd1a4b.

[29] ThermoFisher Scientific. (2020). Adherent cell culture vs. suspension cell culture, [Online]. Available: https://www.thermofisher.com/be/en/home/references/gibco-cell-culture-basics/cell-lines/adherent-vs-suspension-culture.html (visited on 04/28/2020).

[30] P. C. Collins, W. M. Miller, and E. T. Papoutsakis, "Stirred culture of peripheral and cord blood hematopoietic cells offers advantages over traditional static systems for clinically relevant applications", *Biotechnology and Bioengineering*, vol. 59, no. 5, pp. 534–543, 1998. DOI: 10.1002/(SICI)1097-0290(19980905)59:5<534::AID-BIT2>3.0.CO;2-B. [Online]. Available: https://onlinelibrary.wiley.com/doi/abs/10.1002/\%28SICI\%291097-0290\%2819980905\%2959\%3A5\%3C534\%3A\%3AAID-BIT2\%3E3.0.CO\%3B2-B.

[31] J. A. Rowley, E. Abraham, A. Campbell, H. J. Brandwein, and S. Oh, "Meeting lot-size challenges of manufacturing adherent cells for therapy", 2012.

[32] D. W. Levine, J. S. Wong, D. I. C. Wang, and W. G. Thilly, "Microcarrier cell culture: New methods for research-scale application", *Somatic Cell Genetics*, vol. 3, no. 2, pp. 149–155, Mar. 1977, ISSN: 1572-9931. DOI: 10.1007/BF01551811. [Online]. Available: https://doi.org/10.1007/BF01551811.

[33] A. Mizukami, T. D. Pereira Chilima, M. D. Orellana, M. A. Neto, D. T. Covas, S. S. Farid, and K. Swiech, "Technologies for large-scale umbilical cord-derived msc expansion: Experimental performance and cost of goods analysis", *Biochemical Engineering Journal*, vol. 135, pp. 36 –48, 2018, ISSN: 1369-703X. DOI: https://doi.org/10.1016/j.bej.2018.02.018. [Online]. Available: http://www.sciencedirect.com/science/article/pii/S1369703X18300779.

[34] N. Timmins, M. Kiel, M. Günther, C. Heazlewood, M. Doran, G. Brooke, and K. Atkinson, "Closed system isolation and scalable expansion of human placental mesenchymal stem cells", *Biotechnology and Bioengineering*, vol. 109, no. 7, pp. 1817–1826, 2012. DOI: 10.1002/bit.24425. [Online]. Available: https://onlinelibrary.wiley.com/doi/abs/10.1002/bit.24425.

[35] E. Y. Fok and P. W. Zandstra, "Shear-controlled single-step mouse embryonic stem cell expansion and embryoid body–based differentiation", *STEM CELLS*, vol. 23, no. 9, pp. 1333–1342, 2005. DOI: 10.1634/stemcells.2005-0112. [Online]. Available: https://stemcellsjournals.onlinelibrary.wiley.com/doi/abs/10.1634/stemcells.2005-0112.

[36] C. Bauwens, T. Yin, S. Dang, R. Peerani, and P. W. Zandstra, "Development of a perfusion fed bioreactor for embryonic stem cell-derived cardiomyocyte generation: Oxygen-mediated enhancement of cardiomyocyte output", *Biotechnology and Bioengineering*, vol. 90, no. 4, pp. 452–461, 2005. DOI: 10.1002/bit.20445. [Online]. Available: https://onlinelibrary.wiley.com/doi/abs/10.1002/bit.20445.

[37] K. Nilsson, *Microcarrier cell culture principles and methods*. Pharmacia, 1981. [Online]. Available: https://books.google.be/books?id=e1z2lZZ_E_EC.

[38] E. T. Papoutsakis, "Fluid-mechanical damage of animal cells in bioreactors", *Trends in Biotechnology*, vol. 9, no. 1, pp. 427 –437, 1991, ISSN: 0167-7799. DOI: https://doi.org/10.1016/0167-7799(91)90145-8. [Online]. Available: http://www.sciencedirect.com/science/article/pii/0167779991901458.

[39] J. A. King and W. M. Miller, "Bioreactor development for stem cell expansion and controlled differentiation", *Current Opinion in Chemical Biology*, vol. 11, no. 4, pp. 394 –398, 2007, ISSN: 1367-5931. DOI: https://doi.org/10.1016/j.cbpa.2007.05.034. [Online]. Available: http://www.sciencedirect.com/science/article/pii/S1367593107000786.

[40] M. J. Osiecki, T. D. Michl, B. K. Babur, M. Kabiri, K. Atkinson, W. B. Lott, H. J. Griesser, and M. R. Doran, "Packed bed bioreactor for the isolation and expansion of placental-derived mesenchymal stromal cells", *PLoS ONE*, vol. 10, no. 12, pp. 1–18, 2015, ISSN: 19326203. DOI: 10.1371/journal.pone.0144941.

[41] S. Derakhti, S. H. Safiabadi-Tali, G. Amoabediny, and M. Sheikhpoor, "Attachment and detachment strategies in microcarrier-based cell culture technology: A comprehensive review", *Materials Science and Engineering: C*, vol. 103, p. 109 782, May 2019. DOI: 10.1016/j.msec.2019.109782.

[42] C. Weber, D. Freimark, R. Pörtner, P. Pino-Grace, S. Pohl, C. Wallrapp, P. Geigle, and P. Czermak, "Expansion of human mesenchymal stem cells in a fixed-bed bioreactor system based on non-porous glass carrier - part a: Inoculation, cultivation, and cell harvest procedures", *International Journal of Artificial Organs*, vol. 33, no. 8, pp. 512–525, 2010. [Online]. Available: https://www.scopus.com/inward/record.uri?eid=2-s2.0-77955408026&partnerID=40&md5=87cbb70881398c780bd89f7c3be88669.

[43] A. Tsai and T. Ma, "Expansion of human mesenchymal stem cells in a microcarrier bioreactor", in *Bioreactors in Stem Cell Biology: Methods and Protocols*, K. Turksen, Ed. New York, NY: Springer New York, 2016, pp. 77–86, ISBN: 978-1-4939-6478-9. DOI: 10.1007/7651_2016_338. [Online]. Available: https://doi.org/10.1007/7651_2016_338.

[44] T. Tharmalingam, K. Sunley, M. Spearman, and M. Butler, "Enhanced production of human recombinant proteins from cho cells grown to high densities in macroporous microcarriers", *Molecular biotechnology*, vol. 49, pp. 263–76, Apr. 2011. DOI: 10.1007/s12033-011-9401-y.

[45] L. Huang, A. M. Abdalla, L. Xiao, and G. Yang, "Biopolymer-based microcarriers for three-dimensional cell culture and engineered tissue formation", *International Journal of Molecular Sciences*, vol. 21, no. 5, 2020, ISSN: 14220067. DOI: 10.3390/ijms21051895.

[46] A. D. Dias, J. M. Elicson, and W. L. Murphy, "Microcarriers with synthetic hydrogel surfaces for stem cell expansion", *Advanced Healthcare Materials*, vol. 6, no. 16, p. 1 700 072, 2017. DOI: 10.1002/adhm.201700072. [Online]. Available: https://onlinelibrary.wiley.com/doi/abs/10.1002/adhm.201700072.

[47] W. Leong and D. Wang, "Cell-laden polymeric microspheres for biomedical applications", *Trends in Biotechnology*, vol. 33, no. 11, pp. 653 –666, 2015, ISSN: 0167-7799. DOI: https://doi.org/10.1016/j.tibtech.2015.09.003. [Online]. Available: http://www.sciencedirect.com/science/article/pii/S0167779915001894.

[48] A. Fernandes, T. Fernandes, M. Diogo, C. L. da Silva, D. Henrique, and J. Cabral, "Mouse embryonic stem cell expansion in a microcarrier-based stirred culture system", *Journal of Biotechnology*, vol. 132, no. 2, pp. 227 –236, 2007, ISSN: 0168-1656. DOI: https://doi.org/10.1016/j.jbiotec.2007.05.031. [Online]. Available: http://www.sciencedirect.com/science/article/pii/S016816560700380X.

[49] R. Chen, S. J. Curran, J. M. Curran, and J. A. Hunt, "The use of poly(L-lactide) and RGD modified microspheres as cell carriers in a flow intermittency bioreactor for tissue engineering cartilage", *Biomaterials*, vol. 27, no. 25, pp. 4453 –4460, 2006, ISSN: 0142-9612. DOI: https://doi.org/10.1016/j.biomaterials.2006.04.011. [Online]. Available: http://www.sciencedirect.com/science/article/pii/S0142961206003279.

[50] K. W. Chun, H. S. Yoo, J. J. Yoon, and T. G. Park, "Biodegradable PLGA microcarriers for injectable delivery of chondrocytes: Effect of surface modification on cell attachment and function", *Biotechnology Progress*, vol. 20, no. 6, pp. 1797–1801, 2004. DOI: 10.1021/bp0496981. [Online]. Available: https://aiche.onlinelibrary.wiley.com/doi/abs/10.1021/bp0496981.

[51] S. Lin and L. Gu, "Influence of crosslink density and stiffness on mechanical properties of type I collagen gel", *Materials*, vol. 8, no. 2, pp. 551–560, 2015, ISSN: 19961944. DOI: 10.3390/ma8020551.

[52] C. A. Rodrigues, T. G. Fernandes, M. M. Diogo, C. L. da Silva, and J. M. Cabral, "Stem cell cultivation in bioreactors", *Biotechnology Advances*, vol. 29, no. 6, pp. 815 –829, 2011, ISSN: 0734-9750. DOI: https://doi.org/10.1016/j.biotechadv.2011.06.009. [Online]. Available: http://www.sciencedirect.com/science/article/pii/S0734975011000851.

[53] A. Preissmann, R. Wiesmann, R. Buchholz, R. G. Werner, and W. Noé, "Investigations on oxygen limitations of adherent cells growing on macroporous microcarriers", *Cytotechnology*, vol. 24, no. 2, pp. 121–134, 1997, ISSN: 09209069. DOI: 10.1023/A:1007973924865.

[54] G. Nykamp, U. Carstensen, and B. Müller, "Jet milling - a new technique for microparticle preparation", *International Journal of Pharmaceutics*, vol. 242, no. 1-2, pp. 79–86, 2002, cited By 54. DOI: 10.1016/S0378-5173(02)00150-3. [Online]. Available: https://www.scopus.com/inward/record.uri?eid=2-s2.0-0037151474&doi=10.1016\%2fS0378-5173\%2802\%2900150-3&partnerID=40&md5=1b2e39187fd815eaa4ab61a9af1d2013.

[55] R. BODMEIER and H. CHEN, "Preparation of biodegradable poly()lactide microparticles using a spray-drying technique", *Journal of Pharmacy and Pharmacology*, vol. 40, no. 11, pp. 754–757, 1988, cited By 148. DOI: 10.1111/j.2042-7158.1988.tb05166.x. [Online]. Available: https://www.scopus.com/inward/record.uri?eid=2-s2.0-0023698042&doi=10.1111\%2fj.2042-7158.1988.tb05166.x&partnerID=40&md5=8587b5adaa1bd262c82c2a3242a94b77.

[56] T. Tice and R. Gilley, "Preparation of injectable controlled-release microcapsules by a solvent-evaporation process", *Journal of Controlled Release*, vol. 2, no. C, pp. 343–352, 1985, cited By 103. DOI: 10.1016/0168-3659(85)90056-2.

[57] K. K. Taek, J. Y. Jun, S. L. Doo, and T. G. Park, "Gas foamed open porous biodegradable polymeric microspheres", *Biomaterials*, vol. 27, no. 2, pp. 152–159, 2006, ISSN: 01429612. DOI: 10.1016/j.biomaterials.2005.05.081.

[58] X. Shi, L. Sun, J. Jiang, X. Zhang, W. Ding, and Z. Gan, "Biodegradable polymeric microcarriers with controllable porous structure for tissue engineering", *Macromolecular bioscience*, vol. 9, pp. 1211–8, Dec. 2009. DOI: 10.1002/mabi.200900224.

[59] M. Kuterbekov, P. Machillot, P. Lhuissier, C. Picart, A. M. Jonas, and K. Glinel, "Solvent-free preparation of porous poly(L-lactide) microcarriers for cell culture", *Acta Biomaterialia*, vol. 75, pp. 300 –311, 2018, ISSN: 1742-7061. DOI: https://doi.org/10.1016/j.actbio.2018.06.009. [Online]. Available: http://www.sciencedirect.com/science/article/pii/S1742706118303453.

[60] Q. A. Rafiq, K. Coopman, A. W. Nienow, and C. J. Hewitt, "Systematic microcarrier screening and agitated culture conditions improves human mesenchymal stem cell yield in bioreactors", *Biotechnology Journal*, vol. 11, no. 4, pp. 473–486, 2016. DOI: 10.1002/biot.201400862. [Online]. Available: https://onlinelibrary.wiley.com/doi/abs/10.1002/biot.201400862.

[61] J. Hupfeld, I. Gorr, C. Schwald, N. Beaucamp, K. Wiechmann, K. Kuentzer, R. Huss, B. Rieger, M. Neubauer, and H. Wegmeyer, "Modulation of mesenchymal stromal cell characteristics by microcarrier culture in bioreactors", *Biotechnology and Bioengineering*, vol. 111, no. 11, pp. 2290–2302, 2014. DOI: 10.1002/bit.25281. [Online]. Available: https://www.scopus.com/inward/record.uri?eid=2-s2.0-84925268082&doi=10.1002\%2fbit.25281&partnerID=40&md5=f1e032705ba3bbd81f71098261cd3d3e.

[62] P. Li, F. Liu, C. Wu, W. Jiang, G. Zhao, L. Liu, T. Bai, L. Wang, Y. Jiang, L. Guo, X. Qi, J. Kou, R. Fan, D. Hao, S. Lan, Y. Li, and J. Liu, "Feasibility of human hair follicle-derived mesenchymal stem cells/CultiSpher®-G constructs in regenerative medicine", *Cell and Tissue Research*, vol. 362, no. 1, pp. 69–86, 2015. DOI: 10.1007/s00441-015-2182-z. [Online]. Available: https://www.scopus.com/inward/record.uri?eid=2-s2.0-84941881027&doi=10.1007\%2fs00441-015-2182-z&partnerID=40&md5=b7b397d0a8480aba110dbc439e36286d.

[63] D. Schop, R. van Dijkhuizen-Radersma, E. Borgart, F. W. Janssen, H. Rozemuller, H. Prins, and J. D. de Bruijn, "Expansion of human mesenchymal stromal cells on microcarriers: Growth and metabolism", *Journal of Tissue Engineering and Regenerative Medicine*, vol. 4, no. 2, pp. 131–140, 2010. DOI: 10.1002/term.224. [Online]. Available: https://onlinelibrary.wiley.com/doi/abs/10.1002/term.224.

[64] G. Mocanu, M. Nichifor, L. Picton, E. About-Jaudet, and D. Le Cerf, "Preparation and characterization of anionic pullulan thermoassociative nanoparticles for drug delivery", *Carbohydrate Polymers*, vol. 111, pp. 892 –900, 2014, ISSN: 0144-8617. DOI: https://doi.org/10.1016/j.carbpol.2014.05.037. [Online]. Available: http://www.sciencedirect.com/science/article/pii/S0144861714005074.

[65] R. Kankala, J. Zhao, C.-G. Liu, X.-J. Song, D.-Y. Yang, K. Zhu, S.-B. Wang, Y. Zhang, and A.-Z. Chen, "Highly porous microcarriers for minimally invasive in situ skeletal muscle cell delivery", *Small*, vol. 15, no. 25, 2019. DOI: 10.1002/smll.201901397. [Online]. Available: https://www.scopus.com/inward/record.uri?eid=2-s2.0-85065449037&doi=10.1002\%2fsmll.201901397&partnerID=40&md5=a2bebb7d4086d84b39e18e0702bced9f.

[66] GF-HElthcare, *Cytodex surface microcarriers*, Brochure, 2002. [Online]. Available: https://www.cytivalifesciences.co.jp/catalog/pdf/18106061_cytodex.pdf.

[67] L. A. Olivier and G. A. Truskey, "A numerical analysis of forces exerted by laminar flow on spreading cells in a parallel plate flow chamber assay", *Biotechnology and Bioengineering*, vol. 42, no. 8, pp. 963–973, 1993, ISSN: 10970290. DOI: 10.1002/bit.260420807.

[68] F. Grinnell, "Cellular adhesiveness and extracellular substrata", in, ser. International Review of Cytology, G. Bourne and J. Danielli, Eds., vol. 53, Academic Press, 1978, pp. 65 –144. DOI: https://doi.org/10.1016/S0074-7696(08)62241-X. [Online]. Available: http://www.sciencedirect.com/science/article/pii/S007476960862241X.

[69] M. Pierschbacher and E. Ruoslahti, "Cell attachment activity of fibronectin can be duplicated by small synthetic fragments of the molecule", *Nature*, vol. 309, no. 5963, pp. 30–33, 1984. DOI: 10.1038/309030a0. [Online]. Available: https://www.scopus.com/inward/record.uri?eid=2-s2.0-0021271957&doi=10.1038\%2f309030a0&partnerID=40&md5=2c57d870a1ac57d46eee085ff1b0e5da.

[70] E. Ruoslahti, "RGD and other recognition sequences for integrins", *Annual Review of Cell and Developmental Biology*, vol. 12, pp. 697–715, 1996. DOI: 10.1146/annurev.cellbio.12.1.697. [Online]. Available: https://www.scopus.com/inward/record.uri?eid=2-s2.0-0029775681&doi=10.1146\%2fannurev.cellbio.12.1.697&partnerID=40&md5=0c7f780e760d474cd828a31cb41046af.

[71] H. Shin, S. Jo, and A. Mikos, "Biomimetic materials for tissue engineering", *Biomaterials*, vol. 24, no. 24, pp. 4353–4364, 2003. DOI: 10.1016/S0142-9612(03)00339-9. [Online]. Available: https://www.scopus.com/inward/record.uri?eid=2-s2.0-0042562089&doi=10.1016\%2fS0142-9612\%2803\%2900339-9&partnerID=40&md5=bd96a279e51bdee65e830701bddc6fb4.

[72] L. Mabonga and A. P. Kappo, "Peptidomimetics: A Synthetic Tool for Inhibiting Protein–Protein Interactions in Cancer", *International Journal of Peptide Research and Therapeutics*, vol. 26, no. 1, pp. 225–241, 2020, ISSN: 15733904. DOI: 10.1007/s10989-019-09831-5.

[73] J. Samanen, F. Ali, T. Romoff, R. Calvo, E. Sorenson, J. Vasko, B. Storer, M. Strohsacker, D. Powers, J. Stadel, A. Nichols, D. Berry, and D. Bennett, "Development of a small RGD peptide fibrinogen receptor antagonist with potent antiaggregatory activity in vitro", *Journal of Medicinal Chemistry*, vol. 34, no. 10, pp. 3114–3125, 1991. DOI: 10.1021/jm00114a022. [Online]. Available: https://www.scopus.com/inward/record.uri?eid=2-s2.0-0025989573&doi=10.1021\%2fjm00114a022&partnerID=40&md5=803248251abed118202c9cee697213e7.

[74] A. de Mel, G. Jell, M. M. Stevens, and A. M. Seifalian, "Biofunctionalization of biomaterials for accelerated in situ endothelialization: A review", *Biomacromolecules*, vol. 9, no. 11, pp. 2969–2979, 2008, ISSN: 15257797. DOI: 10.1021/bm800681k.

[75] P. Tozetti, S. Caruso, A. Mizukami, T. Fernandes, F. da Silva, F. Traina, D. Covas, M. Orellana, and K. Swiech, "Expansion strategies for human mesenchymal stromal cells culture under xeno-free conditions", *Biotechnology Progress*, vol. 33, no. 5, pp. 1358–1367, 2017. DOI: 10.1002/btpr.2494. [Online]. Available: https://www.scopus.com/inward/record.uri?eid=2-s2.0-85020028429&doi=10.1002\%2fbtpr.2494&partnerID=40&md5=6aacafc78850b906a02206092a9ac999.

[76] S. Badenes, T. Fernandes, C. Rodrigues, M. Diogo, and J. Cabral, "Microcarrier-based platforms for in vitro expansion and differentiation of human pluripotent stem cells in bioreactor culture systems", *Journal of Biotechnology*, vol. 234, pp. 71–82, 2016. DOI: 10.1016/j.jbiotec.2016.07.023. [Online]. Available: https://www.scopus.com/inward/record.uri?eid=2-s2.0-84980371010&doi=10.1016\%2fj.jbiotec.2016.07.023&partnerID=40&md5=897b988a5a797fc18daa30cabbdcaa66.

[77] P. Shetty, K. Bharucha, and V. Tanavde, "Human umbilical cord blood serum can replace fetal bovine serum in the culture of mesenchymal stem cells", *Cell Biology International*, vol. 31, no. 3, pp. 293–298, 2007. DOI: 10.1016/j.cellbi.2006.11.010. [Online]. Available: https://onlinelibrary.wiley.com/doi/abs/10.1016/j.cellbi.2006.11.010.

[78] M. Bernardo, M. Avanzini, C. Perotti, A. Cometa, A. Moretta, E. Lenta, C. Del Fante, F. Novara, A. de Silvestri, G. Amendola, O. Zuffardi, R. Maccario, and F. Locatelli, "Optimization of in vitro expansion of human multipotent mesenchymal stromal cells for cell-therapy approaches: Further insights in the search for a fetal calf serum substitute", *Journal of Cellular Physiology*, vol. 211, no. 1, pp. 121–130, 2007. DOI: 10.1002/jcp.20911. [Online]. Available: https://onlinelibrary.wiley.com/doi/abs/10.1002/jcp.20911.

[79] O. Honmou, K. Houkin, T. Matsunaga, Y. Niitsu, S. Ishiai, R. Onodera, S. G. Waxman, and J. D. Kocsis, "Intravenous administration of auto serum-expanded autologous mesenchymal stem cells in stroke", *Brain*, vol. 134, no. 6, pp. 1790–1807, Apr. 2011, ISSN: 0006-8950. DOI: 10.1093/brain/awr063. [Online]. Available: https://doi.org/10.1093/brain/awr063.

[80] M. Patrikoski, M. Juntunen, S. Boucher, A. Campbell, M. Vemuri, B. Mannerstrom, and S. Miettinen, "Development of fully defined xeno-free culture system for the preparation and propagation of cell therapy-compliant human adipose stem cells", *Stem cell research therapy*, vol. 4, p. 27, Mar. 2013. DOI: 10.1186/scrt175.

[81] F. Santos, P. Andrade, M. Abecasis, J. Gimble, L. Chase, A. Campbell, S. Boucher, M. Vemuri, C. Silva, and J. Cabral, "Toward a clinical-grade expansion of mesenchymal stem cells from human sources: A microcarrier-based culture system under xeno-free conditions", *Tissue Engineering - Part C: Methods*, vol. 17, no. 12, pp. 1201–1210, 2011. DOI: 10.1089/ten.tec.2011.0255. [Online]. Available: https://www.scopus.com/inward/record.uri?eid=2-s2.0-81355134650&doi=10.1089\%2ften.tec.2011.0255&partnerID=40&md5=b9b2991afed8a32d9c5d7a505054420f.

[82] V. B. Himes and W. Hu, "Attachment and growth of mammalian cells on microcarriers with different ion exchange capacities", *Biotechnology and Bioengineering*, vol. 29, no. 9, pp. 1155–1163, 1987. DOI: 10.1002/bit.260290917. [Online]. Available: https://onlinelibrary.wiley.com/doi/abs/10.1002/bit.260290917.

[83] S Reuveny, L Silberstein, A Shahar, E Freeman, and A Mizrahi, "Cell and virus propagation on cylindrical cellulose based microcarriers", *Developments in biological standardization*, vol. 50, 115—123, 1981, ISSN: 0301-5149. [Online]. Available: http://europepmc.org/abstract/MED/7341288.

[84] A. Privalova, E. Markvicheva, C. Sevrin, M. Drozdova, C. Kottgen, B. Gilbert, M. Ortiz, and C. Grandfils, "Biodegradable polyester-based microcarriers with modified surface tailored for tissue engineering", *Journal of Biomedical Materials Research Part A*, vol. 103, no. 3, pp. 939–948, 2015. DOI: 10.1002/jbm.a.35231. [Online]. Available: https://onlinelibrary.wiley.com/doi/abs/10.1002/jbm.a.35231.

[85] S. Patntirapong, W. Singhatanadgit, P. Meesap, T. Theerathanagorn, M. Toso, and W. Janvikul, "Stem cell adhesion and proliferation on hydrolyzed poly(butylene succinate)/-tricalcium phosphate composites", *Journal of Biomedical Materials Research - Part A*, vol. 103, no. 2, pp. 658–670, 2015. DOI: 10.1002/jbm.a.35214. [Online]. Available: https://www.scopus.com/inward/record.uri?eid=2-s2.0-84924348532&doi=10.1002\%2fjbm.a.35214&partnerID=40&md5=f26c56a0e64af957d4d6c1c5ab7be9b3.

[86] M. Rufin and M. Grunlan, *Surface-Grafted Polymer Coatings: Preparation, Characterization, and Antifouling Behavior*. 2015, pp. 218–238. DOI: 10.1002/9781118883051.ch7. [Online]. Available: https://www.scopus.com/inward/record.uri?eid=2-s2.0-85018798105&doi=10.1002\%2f9781118883051.ch7&partnerID=40&md5=c3914740b9204d8059cb52a8f17173d4.

[87] M. Frasconi, F. Mazzei, and T. Ferri, "Protein immobilization at gold-thiol surfaces and potential for biosensing", *Analytical and Bioanalytical Chemistry*, vol. 398, no. 4, pp. 1545–1564, 2010, ISSN: 16182642. DOI: 10.1007/s00216-010-3708-6.

[88] G. Decher, "Fuzzy nanoassemblies: toward layered polymeric multicomposites", *Science*, vol. 277, no. August, pp. 1232–1237, 1997. DOI: 10.1126/science.277.5330.1232.

[89] D. Kato, M. Takeuchi, T. Sakurai, S. Furukawa, H. Mizokami, M. Sakata, C. Hirayama, and M. Kunitake, "The design of polymer microcarrier surfaces for enhanced cell growth", *Biomaterials*, vol. 24, no. 23, pp. 4253 –4264, 2003, ISSN: 0142-9612. DOI: https://doi.org/10.1016/S0142-9612(03)00319-3. [Online]. Available: http://www.sciencedirect.com/science/article/pii/S0142961203003193.

[90] M. A. Arifin, M. Mel, N. Samsudin, Y. Z. H. Hashim, H. M. Salleh, I. Sopyan, and N. Nordin, "Ultraviolet/ozone treated polystyrene microcarriers for animal cell culture", *Journal of Chemical Technology & Biotechnology*, vol. 91, no. 10, pp. 2607–2619, 2016. DOI: 10.1002/jctb.4855. [Online]. Available: https://onlinelibrary.wiley.com/doi/abs/10.1002/jctb.4855.

[91] N. Samsudin, Y. Z. H. Y. Hashim, M. A. Arifin, M. Mel, H. M. Salleh, I. Sopyan, and D. N. Jimat, "Optimization of ultraviolet ozone treatment process for improvement of polycaprolactone (PCL) microcarrier performance", *Cytotechnology*, vol. 69, no. 4, pp. 601–616, 2017, ISSN: 15730778. DOI: 10.1007/s10616-017-0071-x.

[92] S. Yuan, G. Xiong, F. He, W. Jiang, B. Liang, S. Pehkonen, and C. Choong, "PCL microspheres tailored with carboxylated poly(glycidyl methacrylate)–REDV conjugates as conducive microcarriers for endothelial cell expansion", *J. Mater. Chem. B*, vol. 3, pp. 8670–8683, 44 2015. DOI: 10.1039/C5TB01836F. [Online]. Available: http://dx.doi.org/10.1039/C5TB01836F.

[93] G. Eibes, F. dos Santos, P. Z. Andrade, J. S. Boura, M. M. Abecasis, C. L. da Silva, and J. M. Cabral, "Maximizing the ex vivo expansion of human mesenchymal stem cells using a microcarrier-based stirred culture system", *Journal of Biotechnology*, vol. 146, no. 4, pp. 194 –197, 2010, ISSN: 0168-1656. DOI: https://doi.org/10.1016/j.jbiotec.2010.02.015. [Online]. Available: http://www.sciencedirect.com/science/article/pii/S016816561000101X.

[94] J. Varani, D. R. Inman, S. E. Fligiel, and W. J. Hillegas, "Use of recombinant and synthetic peptides as attachment factors for cells on microcarriers", *Cytotechnology*, vol. 13, no. 2, pp. 89–98, 1993, ISSN: 09209069. DOI: 10.1007/BF00749935.

[95] J. Hubbell, S. Massia, N. Desai, and P. Drumheller, "Endothelial cell-selective materials for tissue engineering in the vascular graft via a new receptor", *Bio/Technology*, vol. 9, no. 6, pp. 568–572, 1991. DOI: 10.1038/nbt0691-568. [Online]. Available: https://www.scopus.com/inward/record.uri?eid=2-s2.0-0002766824&doi=10.1038\%2fnbt0691-568&partnerID=40&md5=154741312aa1e745599a18fcfeb6ca23.

[96] J. Ranieri, R. Bellamkonda, E. Bekos, T. Vargo, J. Gardella J.A., and P. Aebischer, "Neuronal cell attachment to fluorinated ethylene propylene films with covalently immobilized laminin oligopeptides YIGSR and IKVAV. II", *Journal of Biomedical Materials Research*, vol. 29, no. 6, pp. 779–785, 1995. DOI: 10.1002/jbm.820290614. [Online]. Available: https://www.scopus.com/inward/record.uri?eid=2-s2.0-0029311157&doi=10.1002\%2fjbm.820290614&partnerID=40&md5=f60d387b1dcf9c7977ae4de990ed7d1a.

[97] D. Hern and J. Hubbell, "Incorporation of adhesion peptides into nonadhesive hydrogels useful for tissue resurfacing", *Journal of Biomedical Materials Research*, vol. 39, no. 2, pp. 266–276, 1998. DOI: 10.1002/(SICI)1097-4636(199802)39:2<266::AID-JBM14>3.0.CO;2-B. [Online]. Available: https://www.scopus.com/inward/record.uri?eid=2-s2.0-0032007690&doi=10.1002\%2f\%28SICI\%291097-4636\%28199802\%2939\%3a2\%3c266\%3a\%3aAID-JBM14\%3e3.0.CO\%3b2-B&partnerID=40&md5=acda7a1dafaadc0b472bf32d529d1fc5.

[98] J. Neff, P. Tresco, and K. Caldwell, "Surface modification for controlled studies of cell-ligand interactions", *Biomaterials*, vol. 20, no. 23-24, pp. 2377–2393, 1999. DOI: 10.1016/S0142-9612(99)00166-0. [Online]. Available: https://www.scopus.com/inward/record.uri?eid=2-s2.0-0032721971&doi=10.1016\%2fS0142-9612\%2899\%2900166-0&partnerID=40&md5=7defa71a41458afc68f944065ba473db.

[99] A. Loebsack, K. Greene, S. Wyatt, C. Culberson, C. Austin, R. Beiler, W. Roland, P. Eiselt, J. Rowley, K. Burg, D. Mooney, W. Holder, and C. Halberstadt, "In vivo characterization of a porous hydrogel material for use as a tissue bulking agent", *Journal of Biomedical Materials Research*, vol. 57, no. 4, pp. 575–581, 2001. DOI: 10.1002/1097-4636(20011215)57:4<575::AID-JBM1204>3.0.CO;2-9. [Online]. Available: https://www.scopus.com/inward/record.uri?eid=2-s2.0-0035892412&doi=10.1002\%2f1097-4636\%2820011215\%2957\%3a4\%3c575\%3a\%3aAID-JBM1204\%3e3.0.CO\%3b2-9&partnerID=40&md5=e4236c8aa3c2e32456b13e90923c3cef.

[100] J. Borges and J. F. Mano, "Molecular interactions driving the Layer-by-Layer assembly of multilayers", *Chemical Reviews*, vol. 114, no. 18, pp. 8883–8942, 2014, ISSN: 15206890. DOI: 10.1021/cr400531v.

[101] S. Amorim, I. Pashkuleva, C. Reis, R. Reis, and R. Pires, "Tunable Layer-by-Layer films containing hyaluronic acid and their interactions with CD44", *Journal of Materials Chemistry B*, vol. 8, no. 17, pp. 3880–3885, 2020. DOI: 10.1039/d0tb00407c. [Online]. Available: https://www.scopus.com/inward/record.uri?eid=2-s2.0-85084271533&doi=10.1039\%2fd0tb00407c&partnerID=40&md5=1558c868c99b82499895eb7e5cfd038e.

[102] S. Jung, S. Park, W. Choi, J. Heo, J. Kwon, S. Choi, and J. Hong, "Organosilicate compound filler to increase the mechanical strength of superhydrophilic Layer-by-Layer assembled film", *Journal of Industrial and Engineering Chemistry*, vol. 84, pp. 332–339, 2020. DOI: 10.1016/j.jiec.2020.01.015. [Online]. Available: https://www.scopus.com/inward/record.uri?eid=2-s2.0-85078260763&doi=10.1016\%2fj.jiec.2020.01.015&partnerID=40&md5=720a204d0709d031128149ad1015ac82.

[103] H. K. Steven W. Keller and T. E. Mallouk, "Layer-by-Layer assembly of intercalation compounds and heterostructures on surfaces: Toward molecular "beaker" epitaxy", *Journal of the American Chemical Society*, vol. 116, no. 19, pp. 8817–8818, 1994. DOI: 10.1021/ja00098a055. [Online]. Available: https://www.scopus.com/inward/record.uri?eid=2-s2.0-0000939174&doi=10.1021\%2fja00098a055&partnerID=40&md5=01d6584cfc7bfa4ea9db05a2c990c436.

[104] D. L. Feldheim, K. C. Grabar, M. J. Natan, and T. E. Mallouk, "Electron transfer in self-assembled inorganic polyelectrolyte/metal nanoparticle heterostructures", *Journal of the American Chemical Society*, vol. 118, no. 32, pp. 7640–7641, 1996, ISSN: 00027863. DOI: 10.1021/ja9612007.

[105] C. Gölander, H. Arwin, J. Eriksson, I. Lundstrom, and R. Larsson, "Heparin surface film formation through adsorption of colloidal particles studied by ellipsometry and scanning electron microscopy", *Colloids and Surfaces*, vol. 5, no. 1, pp. 1–16, 1982. DOI: 10.1016/0166-6622(82)80053-X. [Online]. Available: https://www.scopus.com/inward/record.uri?eid=2-s2.0-24044487902&doi=10.1016\%2f0166-6622\%2882\%2980053-X&partnerID=40&md5=9d8adb4113e158d0ccdb1ffb5eb410a5.

[106] M. F. Rubner, "pH-Controlled Fabrication of Polyelectrolyte Multilayers: Assembly and Applications", *Multilayer Thin Films*, vol. 1, pp. 133–154, 2003. DOI: 10.1002/3527600574.ch5.

[107] K. Kadowaki, M. Matsusaki, and M. Akashi, "Control of cell surface and functions by Layer-by-Layer nanofilms", *Langmuir*, vol. 26, no. 8, pp. 5670–5678, 2010, ISSN: 07437463. DOI: 10.1021/la903738n.

[108] Y. Zhu, C. Gao, T. He, X. Liu, and J. Shen, "Layer-by-Layer assembly to modify poly(L-lactic acid) surface toward improving its cytocompatibility to human endothelial cells", *Biomacromolecules*, vol. 4, no. 2, pp. 446–452, 2003, ISSN: 15257797. DOI: 10.1021/bm025723k.

[109] C. Picart, "Polyelectrolyte Multilayer Films: From Physico-Chemical Properties to the Control of Cellular Processes", *Current Medicinal Chemistry*, vol. 15, no. 7, pp. 685–697, 2008, ISSN: 09298673. DOI: 10.2174/092986708783885219.

[110] A. Schneider, C. Vodouhê, L. Richert, G. Francius, E. Le Guen, P. Schaaf, J.-C. Voegel, B. Frisch, C. Picart, and C. Picart, "Multifunctional polyelectrolyte multilayer films: Combining mechanical resistance, biodegradability, and bioactivity", *Biomacromolecules*, vol. 8, no. 1, 139—145, 2007, ISSN: 1525-7797. DOI: 10.1021/bm060765k. [Online]. Available: https://europepmc.org/articles/PMC2535908.

[111] R. R. Costa, C. A. Custõdio, F. J. Arias, J. C. Rodríguez-Cabello, and J. F. Mano, "Layer-by-Layer assembly of chitosan and recombinant biopolymers into biomimetic coatings with multiple stimuli-responsive properties", *Small*, vol. 7, no. 18, pp. 2640–2649, 2011, ISSN: 16136810. DOI: 10.1002/smll.201100875.

[112] Y. Sun, X. Zhang, C. Sun, B. Wang, and J. Shen, "Fabrication of ultrathin film containing bienzyme of glucose oxidase and glucoamylase based on electrostatic interaction and its potential application as a maltose sensor", *Macromolecular Chemistry and Physics*, vol. 197, no. 1, pp. 147–153, 1996. DOI: 10.1002/macp.1996.021970111. [Online]. Available: https://onlinelibrary.wiley.com/doi/abs/10.1002/macp.1996.021970111.

[113] P. Stroeve, V. Vasquez, M. A. Coelho, and J. F. Rabolt, "Gas transfer in supported films made by molecular self-assembly of ionic polymers", *Thin Solid Films*, vol. 284-285, pp. 708 –712, 1996, ISSN: 0040-6090. DOI: https://doi.org/10.1016/S0040-6090(95)08428-2. [Online]. Available: http://www.sciencedirect.com/science/article/pii/S0040609095084282.

[114] M. Onda, Y. Lvov, K. Ariga, and T. Kunitake, "Sequential actions of glucose oxidase and peroxidase in molecular films assembled by Layer-by-Layer alternate adsorption", *Biotechnology and Bioengineering*, vol. 51, no. 2, pp. 163–167, 1996. DOI: 10.1002/(SICI)1097-0290(19960720)51:2<163::AID-BIT5>3.0.CO;2-H. [Online]. Available: https://onlinelibrary.wiley.com/doi/abs/10.1002/\%28SICI\%291097-0290\%2819960720\%2951\%3A2\%3C163\%3A\%3AAID-BIT5\%3E3.0.CO\%3B2-H.

[115] U. Reibetanz, D. Hübner, M. Jung, U. G. Liebert, and C. Claus, "Influence of Growth Characteristics of Induced Pluripotent Stem Cells on Their Uptake Efficiency for Layer-by-Layer Microcarriers", *ACS Nano*, vol. 10, no. 7, pp. 6563–6573, 2016, ISSN: 1936086X. DOI: 10.1021/acsnano.6b00999.

[116] A. Quarta, M. Rodio, M. Cassani, G. Gigli, T. Pellegrino, and L. Del Mercato, "Multilayered magnetic nanobeads for the delivery of peptides molecules triggered by intracellular proteases", *ACS Applied Materials and Interfaces*, vol. 9, no. 40, pp. 35 095–35 104, 2017. DOI: 10.1021/acsami.7b05709. [Online]. Available: https://www.scopus.com/inward/record.uri?eid=2-s2.0-85031301597&doi=10.1021\%2facsami.7b05709&partnerID=40&md5=7f72c6665e2997d705adf5cb95eb6d1e.

[117] S. De Koker, L. J. De Cock, P. Rivera-Gil, W. J. Parak, R. Auzély Velty, C. Vervaet, J. P. Remon, J. Grooten, and B. G. De Geest, "Polymeric multilayer capsules delivering biotherapeutics", *Advanced Drug Delivery Reviews*, vol. 63, no. 9, pp. 748–761, 2011, ISSN: 0169-409X. DOI: https://doi.org/10.1016/j.addr.2011.03.014. [Online]. Available: http://www.sciencedirect.com/science/article/pii/S0169409X11000652.

[118] E. Biazar, Majdi, M. Zafari, M. Avar, S. Aminifard, D. Zaeifi, Ai, Jafarpour, Montazeri, and Gh, "Nanotoxicology and nanoparticle safety in biomedical designs", *International Journal of Nanomedicine*, p. 1117, 2011, ISSN: 1178-2013. DOI: 10.2147/ijn.s16603.

[119] W. Lu, Y. Shen, A. Xie, and W. Zhang, "Green synthesis and characterization of superparamagnetic Fe3O4 nanoparticles", *Journal of Magnetism and Magnetic Materials*, vol. 322, no. 13, pp. 1828–1833, 2010. DOI: 10.1016/j.jmmm.2009.12.035. [Online]. Available: https://www.scopus.com/inward/record.uri?eid=2-s2.0-77950360414&doi=10.1016\%2fj.jmmm.2009.12.035&partnerID=40&md5=d4f8bbe1d96887b95234d70e3c6355e9.

[120] S.-H. Song, J. Lee, J. Yoon, and W. Park, "Functional microparticle RD for IVD and cell therapeutic technology: Large-scale commercialized products", *Biochip Journal*, vol. 13, no. 1, pp. 95–104, 2019. DOI: 10.1007/s13206-019-3107-9. [Online]. Available: https://www.scopus.com/inward/record.uri?eid=2-s2.0-85063263826&doi=10.1007\%2fs13206-019-3107-9&partnerID=40&md5=12374af1a9a7c2019ce0db702b287b65.

[121] A. Lovati, E. Vianello, G. Talò, C. Recordati, L. Bonizzi, E. Galliera, M. Broggini, and M. Moretti, "Biodegradable microcarriers as cell delivery vehicle for in vivo transplantation and magnetic resonance monitoring.", *Journal of biological regulators and homeostatic agents*, vol. 25, no. 2 Suppl, S63–74, 2011. [Online]. Available: https://www.scopus.com/inward/record.uri?eid=2-s2.0-84855181529&partnerID=40&md5=c5bcd8beee0ab407158bdb94565d7f3a.

[122] P. Pouponneau, J. Leroux, G. Soulez, L. Gaboury, and S. Martel, "Co-encapsulation of magnetic nanoparticles and doxorubicin into biodegradable microcarriers for deep tissue targeting by vascular MRI navigation", *Biomaterials*, vol. 32, no. 13, pp. 3481–3486, 2011, ISSN: 0142-9612. DOI: https://doi.org/10.1016/j.biomaterials.2010.12.059. [Online]. Available: http://www.sciencedirect.com/science/article/pii/S0142961211000780.

[123] L. Kim, S. Choi, J. Kim, H. Kim, and S. Kwon, "Single exposure fabrication and manipulation of 3D hydrogel cell microcarriers", *Lab on a Chip*, vol. 11, no. 1, pp. 48–51, 2011. DOI: 10.1039/c0lc00369g. [Online]. Available: https://www.scopus.com/inward/record.uri?eid=2-s2.0-78650119732&doi=10.1039\%2fc0lc00369g&partnerID=40&md5=f8ef51f6b1583fb981df076706020388.

[124] Y. Yu, J. Guo, Y. Wang, C. Shao, Y. Wang, and Y. Zhao, "Bioinspired Helical Micromotors as Dynamic Cell Microcarriers", *ACS Applied Materials and Interfaces*, vol. 12, no. 14, pp. 16 097–16 103, 2020, ISSN: 19448252. DOI: 10.1021/acsami.0c01264.

[125] F. Xu, L. Xu, Q. Wang, Y. Zhou, Z. Ye, and W. Tan, "A three-dimensional dynamic coculture system enabling facile cell separation for chondrogenesis of mesenchymal stem cells", *Biochemical Engineering Journal*, vol. 103, pp. 68–76, 2015. DOI: 10.1016/j.bej.2015.07.003. [Online]. Available: https://www.scopus.com/inward/record.uri?eid=2-s2.0-84937393406&doi=10.1016\%2fj.bej.2015.07.003&partnerID=40&md5=782769ce4b6d9da40ccf36b5ec5a3dd6.

[126] L. Richert, F. Boulmedais, P. Lavalle, J. Mutterer, E. Ferreux, G. Decher, P. Schaaf, J. C. Voegel, and C. Picart, "Improvement of stability and cell adhesion properties of polyelectrolyte multilayer films by chemical cross-linking", *Biomacromolecules*, vol. 5, no. 2, pp. 284–294, 2004, ISSN: 15257797. DOI: 10.1021/bm0342281.

[127] L. S. Cryotronics. (2020). Pmc micromag 2900 series agm, [Online]. Available: https://www.lakeshore.com/products/categories/overview/discontinued-products/discontinued-products/pmc-micromag-2900-series-agm (visited on 04/18/2020).

[128] "Biological evaluation of medical devices - Part 5: Tests for in vitro cytotoxicity", International Organization for Standardization, Geneva, CH, Standard, Jun. 2009.

[129] ThermoFisher Scientific. (2020). Prestoblue™ cell viability reagent, [Online]. Available: https://www.thermofisher.com/order/catalog/product/A13262#/A13262 (visited on 04/16/2020).

[130] T. Scientific. (2020). CyQUANT™ cell proliferation assay, for cells in culture, [Online]. Available: https://www.thermofisher.com/order/catalog/product/C7026#/C7026 (visited on 04/16/2020).

[131] G. Ge, H. Wu, F. Xiong, Y. Zhang, Z. Guo, Z. Bian, J. Xu, C. Gu, N. Gu, X. Chen, and D. Yang, "The cytotoxicity evaluation of magnetic iron oxide nanoparticles on human aortic endothelial cells", *Nanoscale Research Letters*, vol. 8, no. 1, pp. 1–10, 2013, ISSN: 1556276X. DOI: 10.1186/1556-276X-8-215.

[132] T. R. Pisanic, J. D. Blackwell, V. I. Shubayev, R. R. Fiñones, and S. Jin, "Nanotoxicity of iron oxide nanoparticle internalization in growing neurons", *Biomaterials*, vol. 28, no. 16, pp. 2572–2581, 2007, ISSN: 01429612. DOI: 10.1016/j.biomaterials.2007.01.043.

[133] L. Corbellini, J. Plathier, C. Lacroix, C. Harnagea, D. Ménard, and A. Pignolet, "Hysteresis loops revisited: An efficient method to analyze ferroic materials", *Journal of Applied Physics*, vol. 120, 2016.

[134] J. Sung Lee, J. Myung Cha, H. Young Yoon, J. Lee, and Y. Keun Kim, "Magnetic multi-granule nanoclusters: A model system that exhibits universal size effect of magnetic coercivity", *Scientific Reports*, Jul. 2015. DOI: 10.1038/srep12135.

[135] D. Ağaoğulları, S. J. Madsen, B. Ögüt, A. L. Koh, and R. Sinclair, "Synthesis and characterization of graphite-encapsulated iron nanoparticles from ball milling-assisted low-pressure chemical vapor deposition", *Carbon*, vol. 124, pp. 170–179, 2017, ISSN: 00086223. DOI: 10.1016/j.carbon.2017.08.043.

[136] J. W. Harrell, "Effect of AC gradient field on magnetic measurements with an alternating gradient magnetometer", *Journal of Magnetism and Magnetic Materials*, vol. 205, no. 1, pp. 121–129, 1999, ISSN: 03048853. DOI: 10.1016/S0304-8853(99)00487-4.

[137] J. Tan, W. Zhang, and A. L. Xia, "Facile synthesis of inverse spinel NiFe2O4 nanocrystals and their superparamagnetic properties", *Materials Research*, vol. 16, no. 1, pp. 237–241, 2013, ISSN: 15161439. DOI: 10.1590/S1516-14392012005000157.

[138] S. Sabale, V. Jadhav, S. Mane-Gavade, and X. Y. Yu, "Superparamagnetic CoFe2O4@Au with High Specific Absorption Rate and Intrinsic Loss Power for Magnetic Fluid Hyperthermia Applications", *Acta Metallurgica Sinica (English Letters)*, vol. 32, no. 6, pp. 719–725, 2019, ISSN: 21941289. DOI: 10.1007/s40195-018-0830-5. [Online]. Available: https://doi.org/10.1007/s40195-018-0830-5.

[139] "Definitions and units", in *Introduction to Magnetic Materials*. John Wiley Sons, Ltd, 2008, ch. 1, pp. 1–21, ISBN: 9780470386323. DOI: 10.1002/9780470386323.ch1. [Online]. Available: https://onlinelibrary.wiley.com/doi/abs/10.1002/9780470386323.ch1.

[140] Q. Yang, J. Jian, S. B. Abramson, and X. Huang, "Inhibitory effects of iron on bone morphogenetic protein 2-induced osteoblastogenesis", *Journal of Bone and Mineral Research*, vol. 26, no. 6, pp. 1188–1196, 2011, ISSN: 08840431. DOI: 10.1002/jbmr.337.

UNIVERSITÉ CATHOLIQUE DE LOUVAIN
École polytechnique de Louvain
Rue Archimède, 1 bte L6.11.01, 1348 Louvain-la-Neuve, Belgique | **www.uclouvain.be/epl**